Intracellular pH regulation by sodium-hydrogen exchanger isoforms in preimplantation mouse embryos

Violetta Siyanov

A thesis submitted to the
Faculty of Graduate and Postdoctoral Studies
in partial fulfillment of the requirements
for the Doctor of Philosophy degree in
Cellular and Molecular Medicine

Department of Cellular and Molecular Medicine
Faculty of Medicine
University of Ottawa

Abstract

Intracellular pH (pH_i) impacts many cellular mechanisms including cellular metabolism, gene expression, cell volume regulation, cell survival and proliferation. Most cells use two general pH_i regulatory mechanisms: HCO_3^-/Cl^- antiporters (AE, *Slc4a* family) to reduce internal alkaline load, and Na^+/H^+ exchangers (NHE, *Slc9a* family) that protect cells from acidosis. Previous studies with preimplantation (PI) embryos have shown robust activity of HCO_3^-/Cl^- exchanger in all stages of development. It was also determined that inhibition of this exchange with the stilbene AE inhibitor 4,4'-diisothiocyanostilbene-2,2'-disulfonic acid (DIDS) was detrimental to embryo development from the 2-cell stage to blastocyst when cultured at high external pH. In this study I investigated which of the five known plasma membrane NHE isoforms was present and active within mouse PI embryos and their role as pH_i regulators throughout preimplantation embryo development. In mouse oocytes and preimplantation embryos, mRNAs were detected encoding NHE1 (SLC9A1), NHE3 (SLC9A3), and NHE4 (SLC9A4), with higher mRNA levels for each in fully-grown oocytes through one-cell stage embryos and then generally lower levels after the two-cell stage. No transcripts for NHE2 (SLC9A2) or NHE5 (SLC9A5) were detected. Measurements of intracellular pH during recovery from acidosis, induced by transient ammonium pulse, suggested that recovery occurred and was mediated by NHE activity at all preimplantation stages assessed (one-cell, two-cell, eight-cell and morula). This recovery was inhibited by 1 mM amiloride, a general NHE inhibitor. The observed residual recovery was attributed to passive passage of protons across the membrane, rather than the activity of NHE4 (an amiloride-resistant isoform), since no further decrease in recovery rates from

acidosis was observed upon amiloride increase to 5 mM. Furthermore, recovery from acidosis at each stage was entirely inhibited by cariporide, which is very highly selective for NHE1. In contrast, the moderately NHE3-selective inhibitor S3226 did not preferentially block recovery, nor did adding S3226 increase inhibition over that achieved with cariporide alone, indicating that NHE3 did not play a functional role in pH_i regulation at any stage assessed. Another regulator of intracellular pH against acidosis, previously reported to be active in oocytes and 1-cell embryos, the sodium-dependent bicarbonate/chloride exchanger (NDBCE; SLC4A8), had low or absent activity in two-cell embryos. This indicated that NHE1 is likely the only significant regulator of pH_i in preimplantation mouse embryos, at least after the 1-cell stage. Culturing embryos from the one-cell or two-cell stages in acidotic medium inhibited their development, as assessed by development to the blastocyst stage and cell lineage allocation. However, inhibition of NHE1 with cariporide, NDBCE with DIDS, or both together did not further decrease embryo development to the blastocyst stage more extensively under conditions of chronic acidosis than at normal pH. This suggests that mouse PI embryos have a restricted ability to counteract chronic acidosis by means of pH_i regulatory mechanisms, despite clearly being able to recover from acute acidosis via NHE1 activity.

Table of Contents

Abstract ii

Table of Contents iv

List of Figures ix

List of Tables xi

List of Abbreviations xii

Acknowledgments xiv

Introduction 1

1. Follicular, Oocyte and Early Embryo Development 1

1.1. Follicular and oocyte development 1

1.2. Preimplantation embryo development 8

1.3. Mammalian oviduct: the environment for PI embryo development 8

2. Oocyte Maturation 14

2.1. Oocyte nuclear (meiotic) maturation 14

2.2. Cytoplasmic maturation 16

2.3. Ovulation 20

2.4. Fertilization 20

3. Preimplantation Embryo Development 22

3.1. First cell cycle 22

3.2. Zygotic gene activation (ZGA) 22

3.3. Cleavage and compaction 23

3.4. Blastocyst formation 24

4. pH_i Regulation 26

5. Na^+/H^+ antiporters 29

5.1. Na^+/H^+ exchanger general structure 30
5.2. Inhibitors 31
5.3. Transport Models 35
5.4. Regulation of NHEs 36
5.5. Regulation by pH 42
5.6. Volume regulation 43

6. pH_i Regulation in Preimplantation Embryos 48
6.1. Na^+/H^+ exchanger 48
6.2. HCO_3^-/Cl^- exchanger 51
6.3. Na^+-HCO_3^-/Cl^- exchanger 52

7. Cell Volume Regulation in Oocytes and PI Embryos 54

Objective and Specific Aims 57

Materials and Methods 60

1. Chemicals and Solutions 60
1.1. Oocyte and embryo culture and handling media 60
1.2. Media for pH_i measurements 60

2. Animals, gamete and embryo manipulation 65
2.1. Animals and super-ovulation 65
2.2. Oocyte collection 66
2.3. Egg and embryo collection 66
2.4. Blastocyst diameter 67

3. Molecular Biology Techniques 68
3.1. Nomenclature 68
3.2. Determination of NHE exchanger mRNA in embryos via RT-PCR 68

4. Immunocytochemistry 72
4.1. Embryo fixation and whole-mount indirect immunofluorescence 72
4.2. Blastocyst differential staining 73

5. Measurement of Intracellular pH **74**
5.1. Intracellular pH measurements 74
5.2. Probing Na^+/H^+ exchanger activity in PI embryos 79
5.3. Inhibition of Na^+/H^+ exchangers with pharmacological agents 80
5.4. Effect of changes in external pH 81

6. Embryo Cultures in Varying pH Conditions **85**
6.1. Culture of embryos under varying CO_2 concentrations in the presence and absence of NHE1 inhibitor cariporide 85
6.2. Embryo cultures with various DMO concentrations 85
6.3. Inhibiting NDBCE and NHE1 while culturing embryos with varying CO_2 concentrations 86

7. Statistics **87**

Results **88**

1. Na^+/H^+ Exchanger Expression in Preimplantation Embryo **88**
1.1. Slc9 transcript expression in preimplantation embryos 88
1.2. Expression of NHE isoforms at a protein level 89

2. Presence of Functional Na^+/H^+ Exchange During Embryo Development **96**
2.1. Role of NHE1 in embryo recovery from acidosis 99
2.2. Role of NHE3 in PI embryo recovery from acidosis 105
2.3. Effect of inhibition of NHE4 in 2-cell embryos 106

3. Effect of Chronic Acidosis and NHE Inhibitors on PI Embryos in Culture **114**
3.1. Embryo development in the presence of cariporide at various CO_2 concentrations 114
3.2. Internal pH of 2-cell embryos in various acidic environments 115
3.3. Embryo development in the presence of cariporide and various DMO concentrations 118

4. Role of NDBCE and NHE in Embryo Recovery from Acidosis **121**

4.1. Recovery from acidosis in media containing bicarbonate 121
4.2. Removal of bicarbonate from media prevents the activity of NDBCE 122

5. Effect of Chronic Acidosis and Various Inhibitors on Preimplantation Embryos in Culture 125
5.1. Embryo development in the presence of cariporide and DIDS at various DMO concentrations 125
5.2. Measurement of blastocoel diameters in various treatment groups 126
5.3. Embryo development in the presence of cariporide and DIDS at various CO_2 concentrations 129
5.4. Effect of external pH on internal pH of embryos in the presence of cariporide and H_2DIDS 129
5.5. Cell allocation in cultured blastocysts during prolonged exposures to acidic environments. 132

Discussion 137

1. Na^+/H^+ Exchanger Expression in Preimplantation Embryos 137
1.1. Transcripts encoding SLC9A1, SLC9A3 and SLC9A4 Na^+/H^+ exchanger isoforms were detected in oocytes and PI stage embryos. 137
1.2. NHE protein expression within COCs and blastocysts 139

2. NHE1 is the primary pH_i regulatory mechanism in PI mouse embryos 144

3. NHE's do not regulate against prolonged acidosis in *in-vitro* cultured embryos 148

4. NHE antiporters as pH_i regulatory mechanisms in other mammalian species 153

5. What is the role of NHEs in embryos? 157

6. Health relevance 163

7. Future work 165

8. Conclusions **166**

References **168**

Appendix **189**

List of Figures

Figure 1: Development of oocytes and follicles in the ovary. 2

Figure 2: Images of mouse oocytes at several stages of meiotic maturation. 6

Figure 3: Preimplantation development: the female mouse reproductive tract composed of the ovary, oviduct and the uterus. 11

Figure 4: Photomicrographs of mouse preimplantation embryos. 13

Figure 5: Key molecules controlling the meiotic arrest or the progression through meiotic maturation. 18

Figure 6: pH_i regulation. 27

Figure 7: Molecular structures of Na^+/H^+ exchanger inhibitors. 33

Figure 8: Predicted molecular architecture of the mammalian Na^+/H^+ exchanger and binding partners. 40

Figure 9: Model of mammalian cell volume regulation. 46

Figure 10: SNARF-1 fluorescence. 77

Figure 11: Assay for Na^+/H^+ exchanger (NHE) or Na^+-dependent HCO_3^-/Cl^- exchanger (NDBCE) activity (ammonium pulse assay). 83

Figure 12: Expression of Slc9 NHE family Na^+/H^+ exchanger mRNA. 91

Figure 13: Localization of NHE1 and NHE3 (SLC9A1 and SLC9A3) proteins in freshly collected (A) mouse cumulus-oocyte complexes and (B) blastocyst stage embryos. 93

Figure 14: Recovery from induced acidosis in 2-cell mouse embryos by Na^+/H^+ exchangers. 97

Figure 15: Concentration-response curve for the effect of cariporide (NHE1 inhibitor) on the Na^+-dependent pH_i recovery at the 2-cell stage following an ammonium pulse. 101

Figure 16: Dose dependent inhibition of NHE1 in preimplantation mouse embryos. 103

Figure 17: Concentration-response curve for the effect of S3226. 108

Figure 18: Identification of NHE isoforms that aid in the recovery from acidosis in preimplantation embryos. 110

Figure 19: Effect of increased amiloride on recovery from acidosis in 2-cell embryos. 112

Figure 20: Effect of cariporide on PI embryo development and resting pH_i with chronic acidosis in vitro. 116

Figure 21: Development of 2-cell embryos in the presence of the cell-permeant weak acid DMO. 119

Figure 22: NDBCE activity in GV oocytes and 2-cell embryos. 123

Figure 23: Embryo development in the presence of DIDS and cariporide at various DMO concentrations. 127

Figure 24: Development of 2-cell embryos to blastocysts in the presence of NDBCE and NHE1 inhibitors. 130

Figure 25: The effect of culture in presence of NHE1 and NDBCE inhibitors on blastocyst cell numbers. 134

Figure 26: Summary of gene transcripts for Na^+/H^+ isoforms (Slc9), HCO_3^-/Cl^- exchanger (Slc4a2) and Na^+-HCO_3^-/Cl^- (Slc4a8) within mouse granulosa cells, oocytes, MII eggs and preimplantation embryos. 142

Figure 27: Model summarizing pH regulation in (a) oocytes and (b) preimplantation embryos. 160

List of Tables

Table 1: Inhibitors of Na^+/H^+ Exchangers 34

Table 2: List of media components and their source. 62

Table 3: List of chemicals 63

Table 4: Media for pH_i measurements and pH experiments. 64

Table 5: Primers used for isoform-specific detection of NHE mRNA by RT-PCR 71

List of Abbreviations

AE1	anion exchanger 1-3
AM	acetoxymethyl or acetate esters
AMIL	amiloride
ANOVA	analysis of variance
APC	anaphase promoting complex
ATP	adenosine triphosphate
bp	base pairs
BSA	bovine serum albumin
C-terminal	carboxy terminal
CA	carbonic anhydrase
Ca^{2+}_i	intracellular calcium
CaM	calmodulin
cAMP	adenosine 3-5-cyclic monophosphate
cDNA	complementary deoxyribonucleic acid
CSF	cytostatic factor
dbcAMP	dibutyril adenosine 3,5-cyclic monophosphate
DIDS	4,4'-diisothiocyanostilbene-2,2'-disulfonic acid
DMO	5-5-dimethyl-2-4-oxazolidinedione
DMSO	dimethyl sulfoxide
EIPA	5-(*N*-ethyl-*N*-isopropyl)amiloride, hydrochloride
FSH	follicle stimulating hormone
GV	germinal vesicle
GVBD	germinal vesicle breakdown
h	hour
H_2DIDS	4,4'-diisothiocyanostilbene-2,2'-disulfonic acid, disodium salt
hCG	human chorionic gonadotropin
ICM	inner cell mass
IP_3	inositol triphosphate
IVF	in vitro fertilization
KSOM	K^+ supplemented optimized medium
LH	luteinizing hormone
MAPK	mitogen-activated kinase
MI	metaphase I
MII	metaphase II
min	minute
MPF	maturation-promoting factor or metaphase-promoting factor
mOsM	milliosmole
mRNA	messenger ribonucleic acid
n	number of embryos
N	number of experiments
N-terminal	amino terminal
NDBCE	Na^+-HCO_3^-/Cl^- exchanger
NHE1-5	Na^+/H^+ exchanger isoform 1-5
OF	oviductal fluid

PB	polar body
pH_i	intracellular pH
pH_o	extracellular pH
pHU/min	pH units per minute
PI	preimplantation
PMSG	pregnant mares' serum gonadotropin
PN	pronucleus/pronuclei
RT-PCR	reverse-transcribed polymerize chain reaction
s.e.m.	standard error of the mean
SNARF-1-AM	carboxyseminaphthorhodafluor-1-acetoxymethyl ester
ZGA	zygotic gene activation
ZP2 and ZP3	zona sperm binding receptors

Acknowledgments

Foremost, I would like to thank my supervisor Professor Jay Baltz, for his guidance and mentorship throughout my Ph.D. research project. He has challenged me to ask the right questions and helped me develop the skills to find the answers, both in the literature and in the laboratory. For that I will always be grateful. I would also like to thank the members of my advisory committee, Dr. Barbara Vanderhyden, Dr. Chris Kennedy and Dr. Johne Liu, their encouragement and recommendations concerning the direction and scope of my work were invaluable. I would like to thank the past and present members of the Baltz Laboratory for their friendship and support.

Heartfelt thanks to my family and friends for their love and support. My parents Elena and Anatoli, who through my childhood and academic pursuit had always encouraged me to follow my heart and inquisitive mind in any path it took me and my siblings, Elina and Yanna, for their life long friendship and camaraderie.

Finally, I would like to thank my husband Rubin, whose unconditional love and unwavering belief in me had given me the strength to see this project to fruition. You brought light and laughter into my life, and brightened the dark days that seemed so insurmountable at the time. Words cannot express how much I love you and how grateful I am for your support.

Introduction

1. Follicular, Oocyte and Early Embryo Development

1.1. Follicular and oocyte development

The generation of a female gamete (or oogenesis) begins well before the birth of the fetus. A developing mouse fetus' primordial germ cells (PGCs) are located within the allantois on day 7.2 post coitus (E7.2) (Eppig, 2004; Ginsburg et al., 1990; McLaren and Southee, 1997). On embryonic day 9.5 post coitus the PGCs start to migrate along the hindgut and finally settle in the genital ridge by day 11.5 (Parker and Schimmer, 2006). These PGCs, now residing in the ovary, undergo numerous cycles of mitotic cell division, until millions of precursor cells are formed (Falconer and Avery, 1978; Hogan, 1994). In the subsequent stages of fetal development (E13 in mice), oogonia undergo the initial stages of meiosis and become known as primordial oocytes. Once this is completed, meiosis halts in the dictyate stage (prophase I) where most remain until reproductive cycles begin at puberty (Ginsburg et al., 1990). Soon after, the precursors to the follicular somatic cells surround the oocyte in a single squamous layer to form the *primordial follicles* as shown in Figure 1 (Eppig, 2001). At birth, those oogonia that have not incorporated into a primordial follicle die through cellular apoptosis (Parker and Schimmer, 2006).

Primordial follicles remain in this quiescent phase until recruited into the primary stage for growth at the time of female sexual maturity. Growth of primordial oocytes is initiated by the synchronized and collaborative actions of signals arising from different compartments, such as oocytes, somatic cells and stroma.

Figure 1: Development of oocytes and follicles in the ovary.

Oocyte growth is shown schematically, proceeding from the primary follicle to the ovulated egg counter clockwise. A cohort of non-growing **(1)** primordial follicles is recruited at each menstrual cycle to resume growth and development. FSH stimulates a cohort of primordial follicles to grow and become **(2)** primary oocytes; the surrounding follicle cells proliferate to yield a multilayered structure. **(3)** Preantral follicle, an antrum (cavity) forms in the follicle of a fully-grown oocyte, while the inner granulosa cells remain associated with the oocyte, the outer (mural) granulosa cells differentiate into luteal cells after ovulation. **(4)** The antral (Graafian) follicle contains a fully-grown oocyte arrested in first meiotic prophase (GV), which upon hormonal stimulation (with LH) is prompted to complete the first meiotic cycle. The oocyte is again rearrested, this time in metaphase (of meiosis II) and the egg is ovulated **(5)** awaiting fertilization. **(6)** The egg is surrounded by a cumulus-oocyte-complex. **(7)** Once the oocyte is expelled the remaining follicle develops into the corpus luteum.

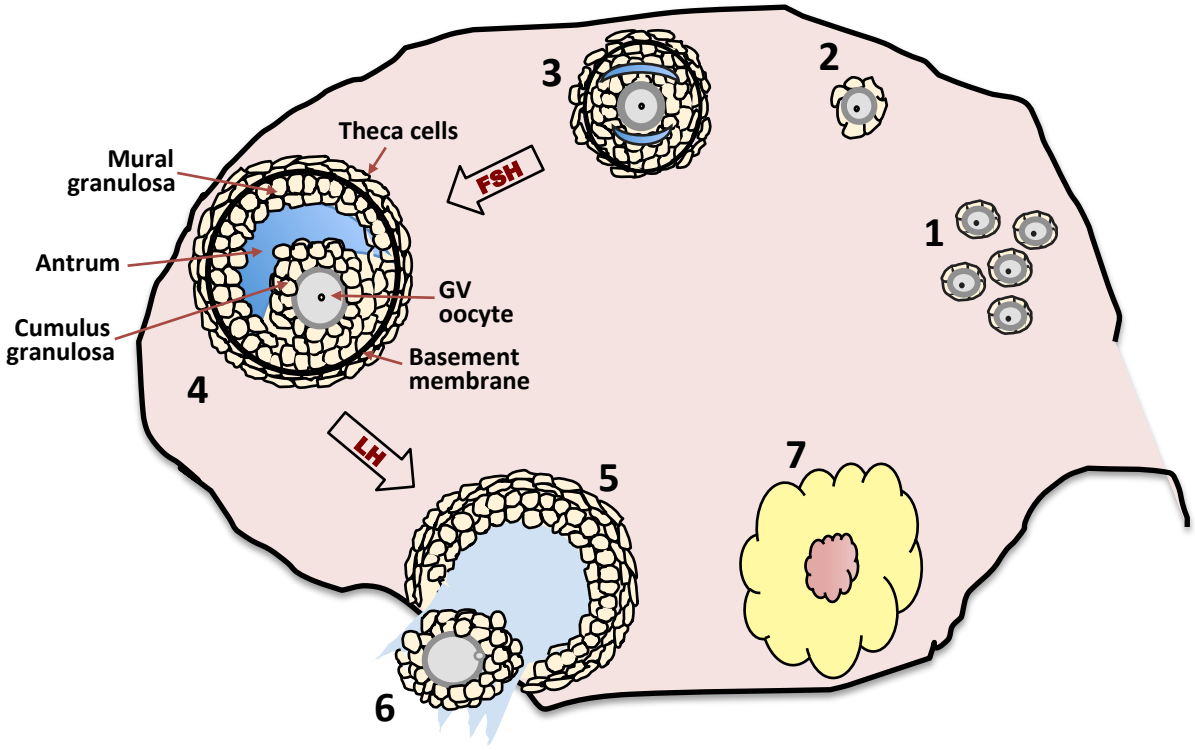
3
2
Theca cells
Mural granulosa
FSH
1
Antrum
GV oocyte
Cumulus granulosa
Basement membrane
4
LH
5
7
6

Figure 1

Follicle Stimulating Hormone (or FSH) is not required for this transition since no FSH receptors are expressed at this stage of development (Oktay et al., 1997; Oktem and Urman, 2010). The enclosed oocyte is stimulated to grow and the surrounding follicular cells now are identified as granulosa cells, which begin to proliferate and change shape from squamous to cuboidal, and the zona pellucida (ZP) begins to develop around the oocyte thus forming the primary follicle (Rankin et al., 1996). The zona pellucida is an outer shell composed of glycoproteins that encircles oocytes and preimplantation embryos. Once the oocyte becomes surrounded by multiple layers of granulosa cells, the follicle is called a pre-antral or secondary follicle (Figure 1) (Eppig, 2001). Mature antral follicles (or Graafian follicles) consist of two divided granulosa cell populations: (1) cumulus cells surrounding the oocyte (forming the cumulus oocyte complex - COC) and (2) mural granulosa cells comprising the inner layer of the follicular wall, in contact with the basement membrane, which is surrounded externally by differentiated ovarian stromal cells, named theca cells (Buccione et al., 1990; Erickson, 1983; Skinner, 2005). Development into a multi-layered secondary follicle from a primary follicle is a lengthy process that takes months in humans. This slow process does not appear to require the actions of gonadotrophins, even though pre-antral follicles may express FSH receptors (Oktay et al., 1997).

Follicle growth after the antral stage is characterized by further proliferation of granulosa cells and, theca cells, oocyte growth and the formation of the antrum, a fluid filled cavity (Eppig and O'Brien, 1996). At this point FSH becomes vital for the recruitment of the dominant follicle from a cohort of growing follicles. An intact nuclear membrane characterizes prophase I-arrested oocytes with the nucleus designated as a germinal vesicle (GV - Figure 2).

Mature oocytes resume meiosis in response to the pre-ovulatory surge of luteinizing hormone (LH) or upon removal of the COC from the ovary, whereby the nuclear envelope is disassembled or broken down (germinal vesicle breakdown, GVBD), and half of the genetic material is expelled into a small cell called the polar body (PB), which degenerates (Figure 2). The oocyte reenters meiotic arrest, this time in the metaphase II stage as a mature egg, and is ovulated, awaiting fertilization (Sorensen and Wassarman, 1976). The second meiotic division and second PB extrusion is triggered by fertilization.

Figure 2: Images of mouse oocytes at several stages of meiotic maturation.

Photomicrographs (top) and confocal sections (bottom) stained for DNA (green) and tubulin (red) of mouse oocytes at the germinal vesicle (GV) stage, metaphase I (MI) and metaphase II (MII) stages. A mature oocyte has a prominent nucleus with a single nucleolus that is clearly visible at their center, which are called germinal vesicles (GV). A surge of luteinizing hormone (LH) initiates oocyte meiotic maturation, which also spontaneously occurs upon release from the follicle *in vitro*. Meiotic maturation is marked by germinal vesicle breakdown (GVBD), followed by progression through meiosis I (MI oocyte). The first meiotic cycle is completed when the oocyte releases its first polar body (PB) and forms the MII spindle, producing a mature MII egg.

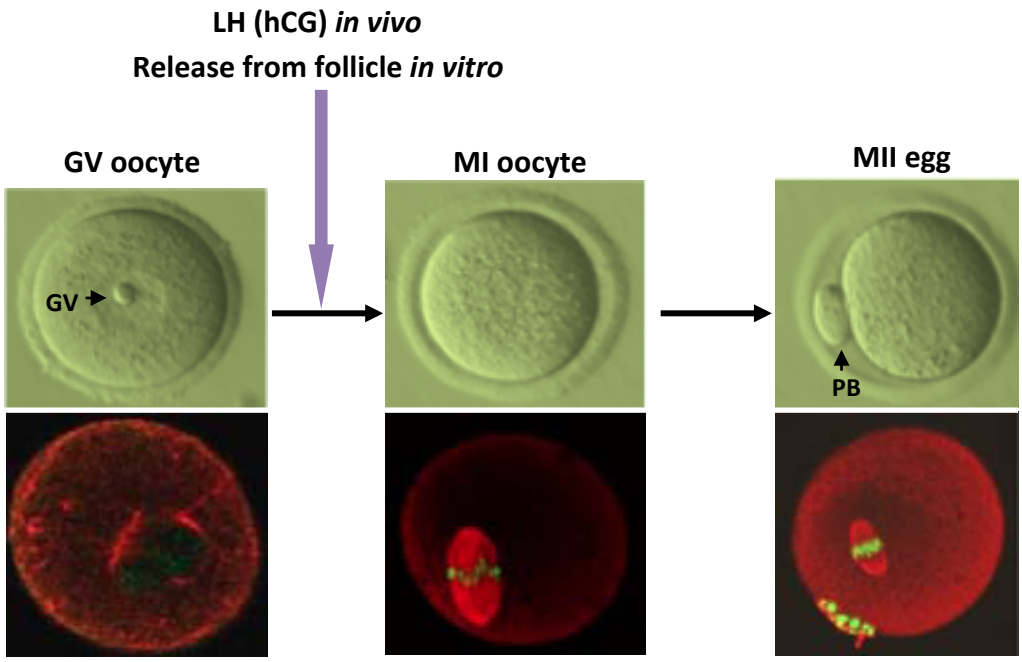
LH (hCG) *in vivo*
Release from follicle *in vitro*
GV oocyte
MI oocyte
MII egg
GV
PB

Figure 2

1.2. Preimplantation embryo development

The development of the mammalian preimplantation (PI) embryo comprises the period from fertilization to implantation. The ovulated MII egg (Figure 2) moves out into the peritoneal space where it is caught by the fimbriae which push it into the oviduct, or Fallopian tube (Figure 3) where it is fertilized and early embryogenesis ensues. As the zygote travels down the oviduct, it undergoes a series of reductive (i.e., reducing cell volume) cleavages producing 2, 4, 8 and 16-cell embryos (Figure 3, 4), followed by the compaction of blastomeres to form a morula. The morula stage is characterized by the expression of cell surface adhesion molecules (E-cadherin) and the formation tight and gap junctions, thus establishing intercellular connection between adjacent blastomeres (Hogan, 1994; Winkel et al., 1990). Late in the morula stage, the embryo undergoes a process of cavitation and forms a fluid-filled cavity called a blastocoel, and segregation of embryo cells into different lineages (Wang and Dey, 2006). The embryo, now a blastocyst, is composed of two cell types: the outer epithelial trophectoderm (TE) and the pluripotent inner cell mass (ICM) (Figure 3, 4). During the fifth day of development, in mice, the mature blastocyst digests its extracellular matrix (the zona pellucida) by use of trypsin-like enzymes, a process called hatching (Hogan, 1994). The ICM generates future cell lineages of the embryo proper and the inner extra-embryonic membranes, while the TE makes the first physical and physiological connection with the luminal epithelium of the maternal uterus for implantation and forms the placenta and outer membranes (MacPhee et al., 2000).

1.3. Mammalian oviduct: the environment for PI embryo development

The oviduct is a muscular tube with a mucosal lining. It is usually conceptually divided into four sections: the infundibulum fringed by fimbriae, ampulla, isthmus and

utero-tubal junction (Figure 3). The fimbriae are finger-like projections with highly ciliated epithelial cells (Hogan, 1994; Leese, 1988). The ampulla is the location of fertilization, while the isthmus is involved in the transport of sperm, eggs, and developing preimplantation embryos (Crow et al., 1994). The oviductal fluid (OF) is an amalgam of components from plasma and some oviduct-specific proteins formed by the oviductal cells (Leese, 1988).

Oviductal fluid composition has been analyzed in several species, including cow, ewe, sow, rabbit, mouse and human. In these species certain amino acids, particularly alanine, glycine, glutamate, hypotaurine and taurine, are present in high concentrations (Guérin et al., 1995), with a reported low concentration of glutamine in the mouse oviductal fluid as compared to plasma (Harris et al., 2005). Amino acids play an important role during cleavage stage embryo development not only as energy substrates and protein building blocks, but as osmoregulators (Dawson et al., 1998), heavy ion chelators (Van Winkle et al., 1990), and antioxidants (Harris et al., 2005; Lane, 2001).

Ion concentrations in tubal fluid are similar to those in serum for the majority of the species. Nevertheless, high concentrations of K^+, HCO_3^- (Borland et al., 1980; Borland et al., 1977), Cl^- and Na^+, were reported across the species, with levels significantly higher than plasma (Collins and Baltz, 1999; Dickens and Leese, 1994). The electrolyte composition of oviductal fluid is important to preserve osmolarity and pH. It has been observed that oviductal fluid pH is much higher than plasma (pH 7.5 - 8.0; Figure 3) as quantified in several mammalian species (Leese, 1988). Maas et al (1977) measured oviduct pH in rhesus monkey and found that, at ovulation, pH was 7.5-7.8, significantly higher than during the follicular phase at 7.1-7.3. During the follicular period HCO_3^- was 35mM and rose to 90mM during ovulation (Maas et al., 1977). pH of rabbit oviductal fluid was

measured to be about 7.6 - 8.0 during ovulation (Iritani et al., 1971), in pigs oviduct pH at this stage was shown to be 7.8 - 8.0 (Nichol et al., 1997), while rat ampullar fluid pH during this period was shown to be 8.0 - 8.2 (Ben-Yosef et al., 1996). It was proposed that high HCO_3^- and K^+ levels in the oviduct assist in the scattering of the cumulus mass and to help control sperm motility and embryo metabolism (Boatman, 1997; Coy et al., 2012). High potassium levels were shown to contribute to capacitation and sperm acrosome reaction, resulting in the release of hyaluronidase, which in turn scatters the cumulus mass surrounding the oocyte, while the elevated bicarbonate concentration increases oviductal pH, which leads to sperm hyperactive motility towards the ovulated oocyte (Reviewed in Coy et al., 2012).

Figure 3: Preimplantation development: the female mouse reproductive tract composed of the ovary, oviduct and the uterus.

The unfertilized MII egg is ovulated from the follicle into the oviduct. The oviduct consists of three segments: fimbriae, ampulla and isthmus. The fimbriae capture the ovulated egg and propel it into the oviduct. The egg is fertilized in the ampulla. The isthmus of the oviduct is the site of preimplantation embryo development and is alkaline compared to the pH of the follicular and uterine fluid. After fertilization, the 1-cell embryo undergoes a series of reductive cleavages (2-cell, 4-cell, 8-cell), followed by compaction to form a morula. The compacted embryo enters the uterus, where the morula cavitates, forming a fluid-filled cavity surrounded by trophectoderm (TE) cells. The blastocyst hatches out of the zona pellucida and implants in the uterine wall. The trophectoderm will form the extra-embryonic tissues such as the placenta while the inner cell mass (ICM) will develop into the fetus.

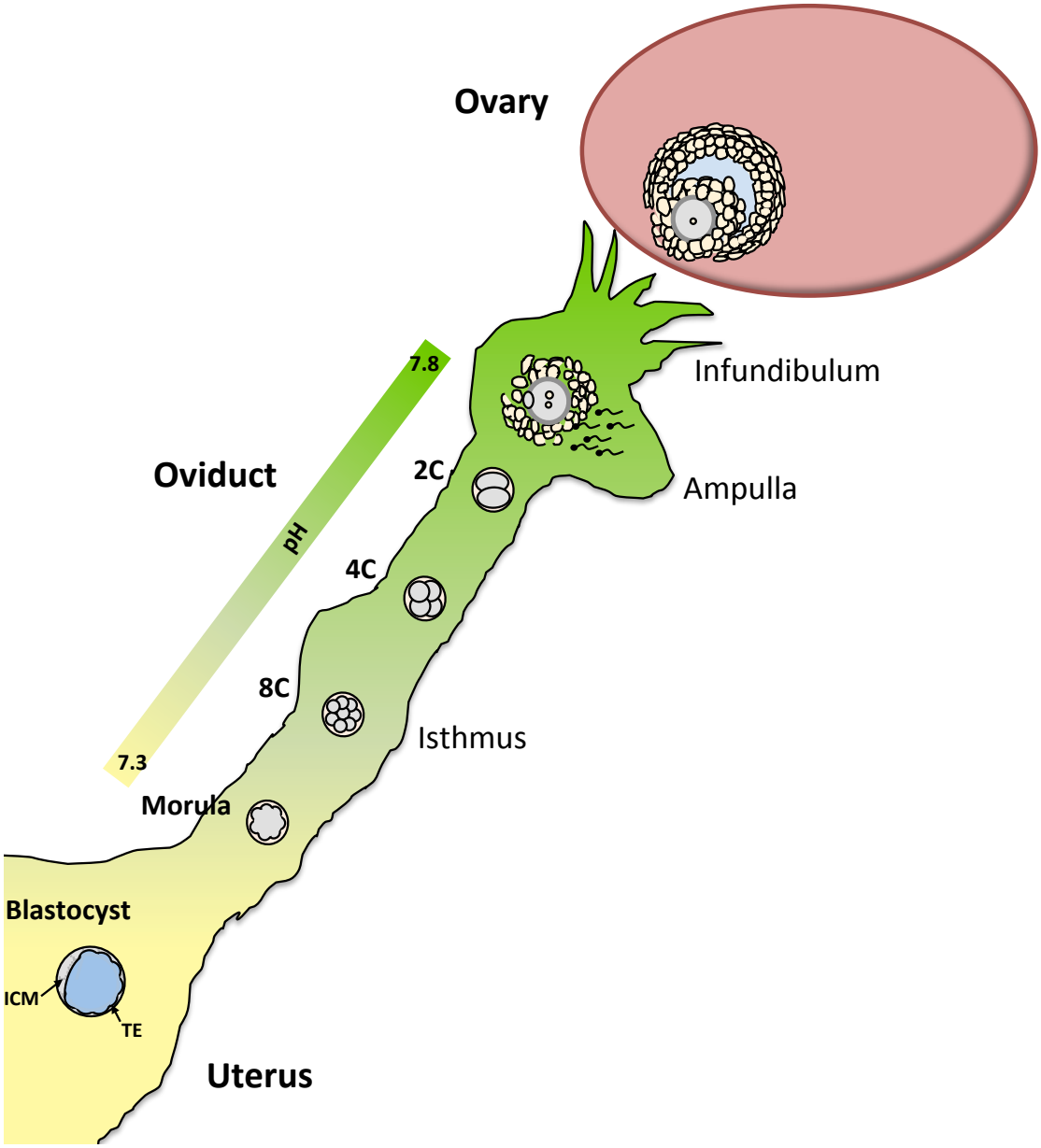
Ovary
Infundibulum
Ampulla
Oviduct
7.8
pH
7.3
2C
4C
8C
Isthmus
Morula
Blastocyst
ICM
TE
Uterus

Figure 3

Figure 4: Photomicrographs of mouse preimplantation embryos.

Embryos were derived from mating of CF-1 females and BDF males, and were collected from oviducts as 1-cell embryos and then cultured *in vitro* for up to 5 days. Shown: 1-cell, 2-cell, 4-cell, 8-cell, morula and blastocyst-stage embryos. PN = pronuclei, PB = polar body, ICM = inner cell mass, T = trophectoderm, B = blastocoel.

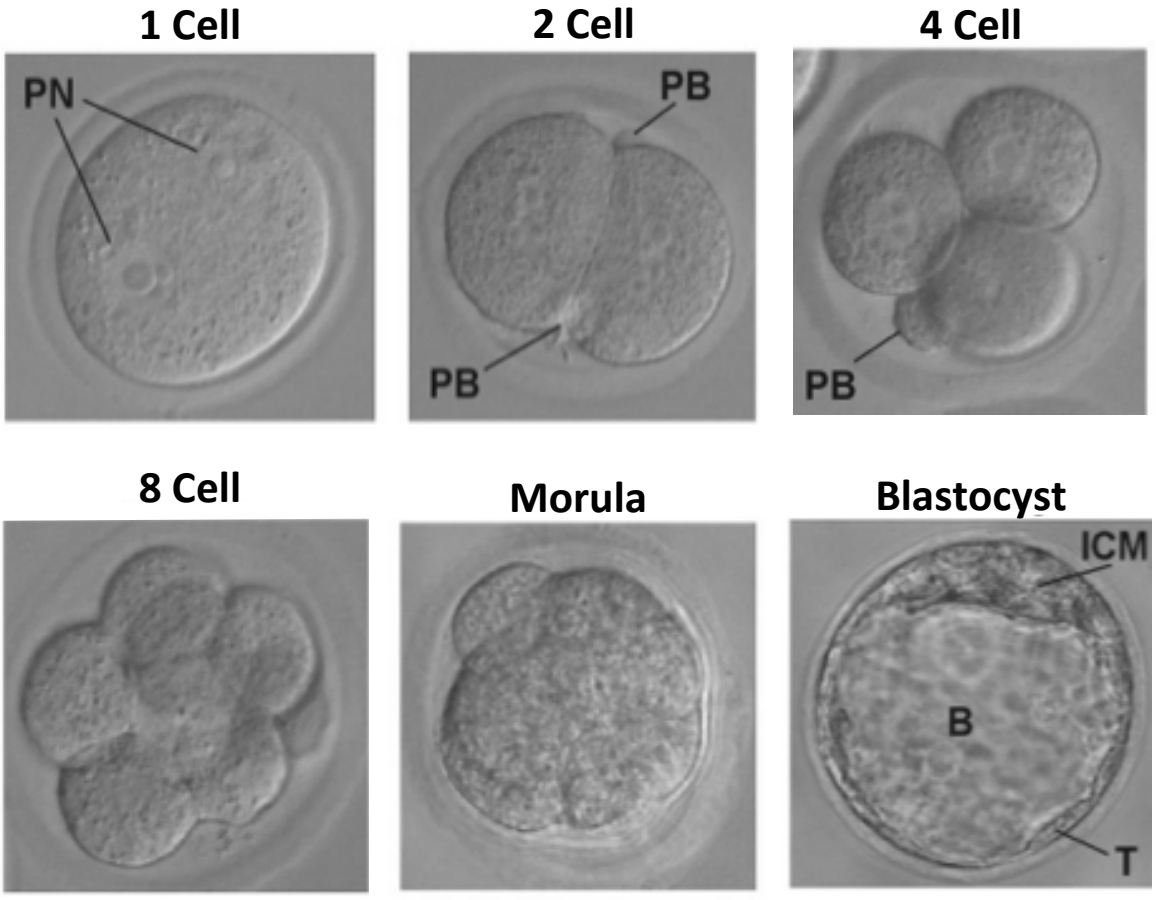

2. Oocyte Maturation

Oocyte maturation encompasses two stages: (1) nuclear and (2) cytoplasmic. Nuclear maturation includes the resumption and completion of the first meiotic division and re-arrest in metaphase II. Cytoplasmic maturation is a vital but incompletely characterized process that involves accumulation of mRNA, proteins, substrates, and nutrients required to complete nuclear maturation, fertilization and early embryo development (Eppig, 2004; Gandolfi and Gandolfi, 2001; Sirard et al., 2006).

2.1. Oocyte nuclear (meiotic) maturation

After oogenesis, oocytes are arrested in prophase I of meiosis and are distinguished by a prominent nucleus or *germinal vesicle* (GV) with a single nucleolus (Figure 2). Meiotic maturation is triggered *in vivo* by the ovulatory LH surge, which allows the transduction of the LH signal from the outer follicular layers to the oocyte (Eppig, 2004). Before ovulation is triggered, the oocyte is maintained in meiotic arrest by the follicular environment. This is confirmed by *in vitro* experiments that show spontaneous nuclear maturation of oocytes when removed from the follicle (Edwards, 1965; Eppig, 2004).

Prior to fertilization, the oocyte must undergo two consecutive rounds of meiosis, resulting in a reduction to a haploid number of chromosomes (Eppig, 2004). Before birth, the oocyte arrests in the diplotene stage of prophase I stage (McLaren and Southee, 1997), and arrest is maintained during oocyte growth identified as GV stage. After stimulation of ovulation, the oocyte resumes meiosis I (MI), the nuclear envelope is dissolved and the germinal vesicle is broken down (GVBD), which is followed by chromosome condensation and assembly of the metaphase I spindle. Upon completion of first meiotic cell division, the

oocyte undergoes an asymmetric cell division resulting in extrusion of half the chromosomes into a small polar body. The oocyte enters into meiosis II following cytokinesis, without an additional step of DNA synthesis, and re-arrests in metaphase II (MII) with chromosomes realigned on the spindle. Meiosis II completes upon fertilization with the extrusion of the second polar body (Eppig and O'Brien, 1996).

Meiotic competence is achieved during antrum formation (Erickson and Sorensen, 1974; Mehlmann, 2005) when the oocyte achieves a threshold level of maturation promoting (or M-phase) promoting factor (MPF), a complex that consists of CDK1 (cyclin-dependent kinase) catalytic subunit and Cyclin B (CyB) regulatory subunit (Figure 5A) (Tunquist and Maller, 2003). At the beginning of meiotic maturation, a decrease in cAMP leads to deactivation of protein kinase A (PKA), which activates phosphatase CDC25. Inhibitory phosphorylation of the CDK1/CyB complex is removed by CDC25 after its activation by the LH-surge, which leads to nuclear envelope breakdown and the resumption of meiosis I (Mehlmann, 2005). Entry into metaphase is mainly influenced by Cyclin B synthesis, while entry into anaphase is driven by a multi-subunit E3 ubiquitin ligase called anaphase-promoting complex/cyclosome (APC/C) and CyB degradation (Mehlmann, 2005; Peters, 2005). MPF inactivation (due mainly to cyclin B proteolysis) is prevented by the cytostatic factor (CSF) (Masui and Markert, 1971). CSF is a signaling complex of protein kinases including MOS, an oocyte - specific activator of MEK, which targets MAPK. MAPK is activated during the progression through MI, remaining high through MII metaphase arrest. Although some of the MAPK targets have been identified, the exact mechanism by which CSF maintains the metaphase II arrest has yet to be elucidated (Fan and Sun, 2004; Nishiyama et al., 2007).

The fertilizing sperm introduces phospholipase C zeta (PLCζ) into the egg which induces a series of transient calcium fluctuations in oocytes that cause oocyte activation (Swann and Lai, 2013). Ca^{2+}- dependent activation of anaphase-promoting complex leads to MPF inactivation, and to the completion of meiosis II and extrusion of the second polar body (Eppig, 2004).

2.2. Cytoplasmic maturation

Cytoplasmic maturation entails a myriad of changes to the cytoplasmic constitution that are vital for future egg activation, fertilization and preimplantation development. Cytoplasmic maturation usually occurs in parallel with nuclear maturation, however many key steps of cytoplasmic maturation occur during oocyte growth, well before the resumption of meiosis. Cytoplasmic maturation is vital for proper egg activation, embryo development and for the oocyte's ability to produce normal Ca^{2+} oscillations following fertilization. It also enables completion of meiosis I, oocyte cortical granules exocytosis, pronuclear formation, initiation of mitotic cell cycle and recruitment of maternal mRNA during embryonic genome activation (Ducibella et al., 2006; Eppig, 2004; Watson, 2007).

Proper cytoplasmic maturation is crucial for the initiation of Ca^{2+} oscillations, which is necessary for egg activation, triggers the resumption and completion of meiosis, blocks polyspermy (by releasing cortical granules) and mediates the recruitment of maternal mRNA required for the activation of the embryonic genome (Ducibella et al., 2002). Recent studies have demonstrated that while a low number of calcium transients are associated with impaired embryo development (Toth et al., 2006), an excessive amount of Ca^{2+} oscillations also interferes with embryo post-implantation development (Ozil et al., 2006), and thus the number of Ca^{2+} oscillations must be tightly regulated. The ability to produce Ca^{2+}

oscillations develops during meiotic maturation and requires several cytoplasmic changes: 1) reorganization of the endoplasmic reticulum (ER), the main stockpile of Ca^{2+} in oocytes, 2) increase in number and biochemical change of ER IP_3-receptors, 3) an increase in calcium stores in ER and 4) redistribution of ER calcium-binding proteins (Ajduk et al., 2008; Mehlmann et al., 1996).

During cytoplasmic maturation maternal mRNA is transcribed and stored until GVBD (during resumption of meiosis). Maternal RNA synthesized during oocyte growth is stockpiled in a dormant form and selectively translated at appropriate times after undergoing polyadenylation in the cytoplasm (Bachvarova, 1985; Eppig, 2004).

Accumulation of various oocyte cytoplasmic factors/proteins generated and/or accumulated during cytoplasmic maturation is key for ensuring the incorporation of sperm and its transformation into oocyte structures after fertilization. For example, it was shown that immature GV oocytes that do not have high enough stockpiles of the antioxidant compound glutathione are impaired in the formation of male pronuclei and thus embryo formation (Eppig et al., 1996; Yoshida et al., 1993). This factor is accumulated during cytoplasmic maturation and is involved in protamine dissociation on sperm chromatin during 1-cell embryo pronuclei formation, rendering the paternal DNA into an accessible template for transcription (Cooper, 1999). Although many facets of cytoplasmic maturation have been determined in the past decades, many components are yet to be defined.

Figure 5: Key molecules controlling the meiotic arrest or the progression through meiotic maturation.

(A) *Events of female meiosis:* In the fully grown (prophase I arrested) GV oocyte, both MPF and CSF are inactive. Following the stimulatory ovulatory LH surge, the intracellular cAMP decrease results in MPF activation. The oocyte undergoes germinal vesicle breakdown (GVBD) and enters metaphase I, becoming a MI oocyte. A transient decrease in MPF takes place at the end of meiosis I, coincident with emission of first polar body (PB). MPF is reactivated during meiosis II and the oocyte is rearrested in metaphase II, becoming a matured MII oocyte. MAPK, part of CSF, is activated slowly following GVBD, becoming fully activated in the MI oocyte. Its activity remains high throughout meiosis I and II**.** Upon fertilization the sperm induces a series of transient Ca^{2+} oscillations that cause egg activation. **(B)** *Schematics of events allowing maintenance of meiotic arrest.* A high steady-state level of cAMP within the GV oocyte activates PKA activity. Through steps unidentified to date, PKA activity mediates inactivation of CDC25 phosphatase, preventing dephosphorylation-dependent activation of CDK1, a component of MPF complex, resulting in maintenance of meiotic arrest. **(C)** *Schematics of major steps allowing oocyte release from meiotic arrest.* At the beginning of meiotic maturation, the decrease in oocyte intracellular cAMP level is followed by PKA inactivation. CDC25 phosphatase activity results in CDK1 dephosphorylation and ultimately activation of CDK1, allowing progression to metaphase I.

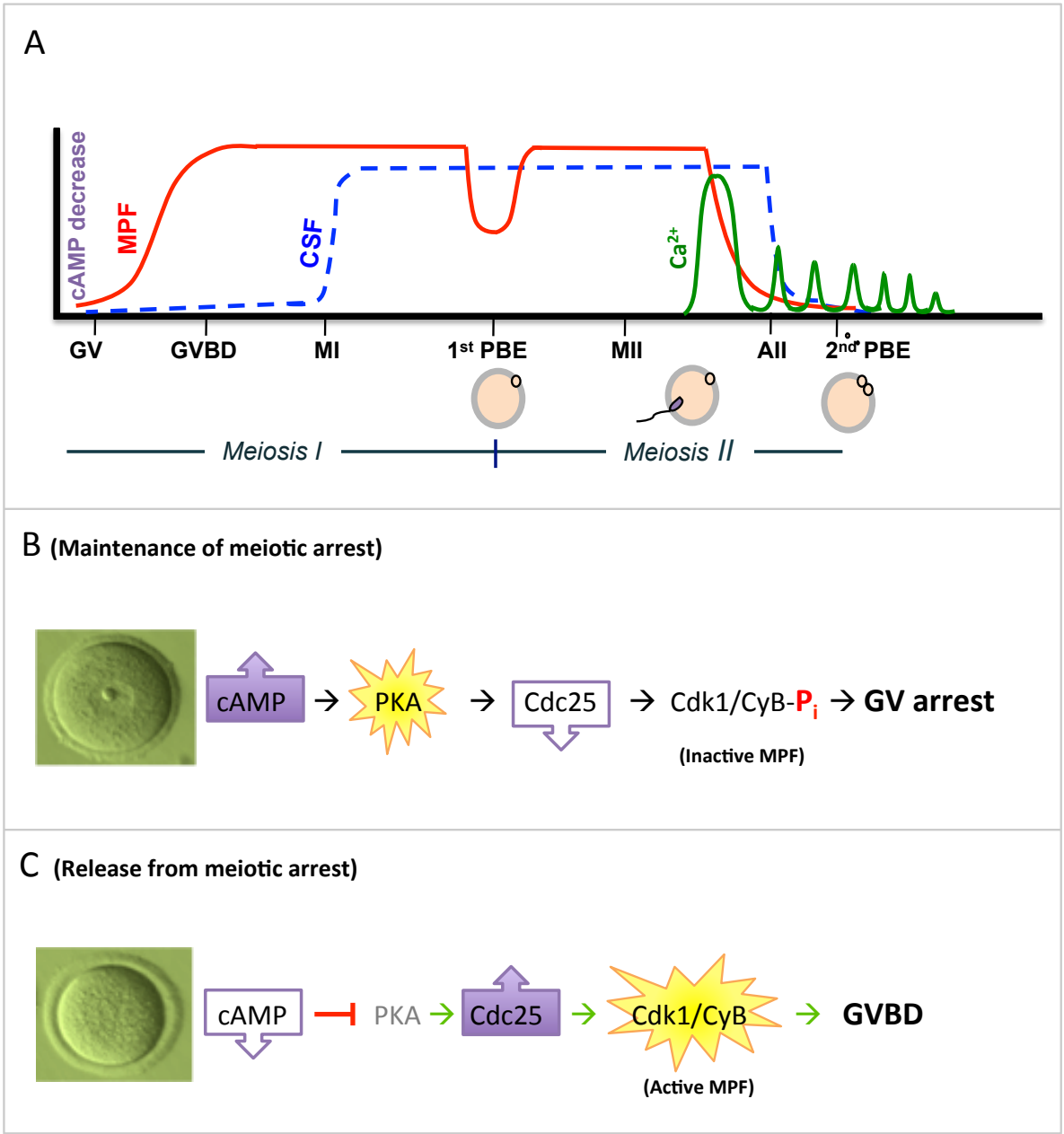
A
cAMP decrease
MPF
CSF
Ca2+
GV
GVBD
MI
1st PBE
MII
AII
2nd PBE
Meiosis I
Meiosis II
B (Maintenance of meiotic arrest)
cAMP
PKA
Cdc25
Cdk1/CyB-Pi
GV arrest
(Inactive MPF)
C (Release from meiotic arrest)
cAMP
PKA
Cdc25
Cdk1/CyB
GVBD
(Active MPF)

Figure 5

2.3. Ovulation

Ovulation is an intricate biological event occurring every reproductive cycle. Several hours after the stimulatory LH surge the antral follicle in the ovary ruptures into the perivitelline space and is propelled into the oviduct a mucified cumulus mass containing one or several matured oocytes, depending on the species (Bjersing and Cajander, 1975). Following stimulation of ovulation, the follicle undergoes several changes. The oocyte, previously arrested in prophase I, resumes first meiosis and is re-arrested in the second meiotic metaphase stage, and becomes a mature MII egg (Eppig, 2004; Eppig et al., 1996; Wassarman et al., 1979) by a process called meiotic maturation (Section 2.1). At the cumulus granulosa cell level, the LH surge triggers a cascade of events that lead to hyaluronic acid secretion and hydration, a process known as cumulus expansion or mucification (Eppig, 2001).

2.4. Fertilization

Sperm integration during fertilization is followed by a series of reactions that transform certain oocyte and sperm structures. First, the sperm undergoes the acrosome reaction, which initiates the release of hydrolytic enzymes to aid in the dissolution of the zona pellucida (ZP) to enable its penetration through the zona (Yanagimachi and Bhattacharyya, 1988). In mice, sperm-egg binding is facilitated by three zona glycoproteins, conveniently named ZP1, ZP2 and ZP3. Where ZP1 represents a key structural component of the zona pellucida, ZP3 is the primary sperm receptor (binding sperm prior to acrosomal reaction) and ZP2 is a secondary sperm receptor (Hogan, 1994; Yanagimachi and Bhattacharyya, 1988). After fertilization ZP2 and ZP3 are modified so that ZP3f can no longer bind or induce acrosome reaction in sperm and ZP2f can no longer interact with

acrosome-reacted sperm. These alterations to the ZP glycoproteins establish the ZP block to polyspermy and signify the early event of egg activation (Xu et al., 1994).

Fertilization is also accompanied by a large, transient increase in intracellular calcium ions in the egg. Sperm induced Ca^{2+} oscillations are stimulated through the activation of the oocyte-activating factor phospholipase C zeta (PLCζ), which cleaves phosphatidylinositol 4,5-biphosphate (PIP_2) to inositol triphosphate (IP_3) and diacylglycerol (Saunders et al., 2002). IP_3 binds to receptors on ER, initiating the opening of calcium channels and release of Ca^{2+} ions from the ER lumen to the cytoplasm (Mehlmann et al., 1996; Mehlmann et al., 1995). The increase in intracellular calcium stimulates cortical granule exocytosis, which are small, spherical, membrane-bound organelles containing hydrolytic enzymes. Their release after insemination leads to both chemical and physical changes of the ZP, making it refractory to any further sperm interaction (i.e. zona block to polyspermy) (Yanagimachi and Bhattacharyya, 1988).

The increase in intracellular Ca^{2+} also activates the ubiquitination pathway, whereby cyclin B is destroyed leading to inactivation of MPF and resumption of meiosis II (Figure 5A). The resumption of the cell cycle and progression into interphase by the destruction of MPF is a process known as *egg activation*. CSF activity is vital for metaphase II arrest in mice, and loss of its activity does not occur until several hours following the loss of MPF activity in interphase at the time of pronuclear formation. Once activated, the egg undergoes a second asymmetrical cell division, and a second polar body is extruded about 1-3 hours post insemination. Following cytokinesis, the egg is haploid and the remaining chromosomes form the female pronucleus (Howlett and Bolton, 1985).

3. Preimplantation Embryo Development

3.1. First cell cycle

Development of the early stage embryo is primarily controlled by the maternal genome, whose components were synthesized and stored during the oocyte maturation and are the activated and utilized in a controlled and sequential manner. In mice, this period of maternal control extends from ovulation to the early 2-cell stage ~18 - 22 hr post-fertilization (Bolton et al., 1984). Following formation of pronuclei, the embryo enters S-phase and begins DNA replication, ~10 - 12 hr post-insemination, with both pronuclei entering the S-phase at the same time (Howlett and Bolton, 1985).

3.2. Zygotic gene activation (ZGA)

The maternal mRNA and proteins support the progression of meiotic maturation, ovulation, fertilization and formation of pronuclei in the egg. Mouse maternal genes and proteins are also necessary to direct the first cell cycle (Bolton et al., 1984), since the newly fertilized egg is transcriptionally inactive with no new mRNA synthesized to complete fertilization (with only a few exceptions). Zygotic genome activation (ZGA) is an essential process for embryo development, whereby the embryo's reliance on maternally-derived factors is transitioned to the embryonic genome (Bellier et al., 1997). In mammals, most oocyte-derived mRNAs are degraded shortly after fertilization and cannot direct more than the first few cell divisions, thus ZGA is highly important for proper embryo development (Minami et al., 2007; Thompson et al., 1998).

The transition from maternal to embryonic control was found to occur during the 2-cell stage in the mouse. This process was shown to be independent of cytokinesis or DNA synthesis and involves a two-step process. The initial or minor ZGA phase begins in the middle of the 1-cell stage with very weak transcriptional activity and no translation of new transcripts, and the second or major ZGA phase occurs during the 2-cell stage with increased transcription and translation of embryonic genes (Bellier et al., 1997; Bolton et al., 1984).

In mouse embryos, the observed 2-cell block that occurs when embryos are stressed *in vitro* was related to the delay in zygotic genome activation rather than the inability to initiate ZGA (Qiu et al., 2003). It was demonstrated with α-amanitin, an RNA synthesis inhibitor, that there are serious effects on embryonic development when transcription was inhibited during the 1-cell to 2-cell transition. Zygotes progress to the 2-cell stage but fail to go to the 4-cell stage when α-amanitin is present, showing the requirement for transcription for development beyond the 2-cell stage (Golbus et al., 1973; Howlett and Bolton, 1985; Latham et al., 1991; Warner and Versteegh, 1974).

3.3. Cleavage and compaction

Following fertilization and formation of pronuclei, the embryo undergoes a series of successive cell divisions, producing increasing number of cells, called blastomeres, without increasing the overall size of the embryo. In the mouse at the 8- to 16-cell stage, blastomeres begin to compact. This period is associated with the formation of adherens and later tight junctions between cells. E-cadherin mediates adhesion between the cells, transforming the loose collection of blastomeres into a packed cluster of cells called the morula. E-cadherin is equally distributed within the early cleavage stages, with concentrations increasing around

the 4-cell stage (Vestweber et al., 1987). The E-cadherin binding partners α- and β-catenin, link E-cadherin to the actin cytoskeleton thus promoting cell adhesion and forming the morula (Pauken and Capco, 1999). The mechanisms of compaction are not clearly understood, but it was shown that PKC might play a regulatory role in cell to cell adhesion by directing both E-cadherin and β-catenin (Pauken and Capco, 1999) and its disruption leads to premature compaction of 2 and 4-cell embryos (Winkel et al., 1990).

As blastomeres adhere to one another, they rapidly polarize along the axis perpendicular to cell contact such that outward facing or apical regions becomes very different from the basolateral (or inward facing) region (Cockburn and Rossant, 2010). The cell surface also changes, with microvilli accumulating mainly on the apical surface, leaving no microvilli on the basolateral pole (Johnson and Maro, 1984; Maro et al., 1985). In the course of polarization the cytoplasm reorganizes and many organelles become unequally distributed throughout the cell: nuclei move basolaterally (Reeve and Kelly, 1983), actin and endosomes move to the apical domain (Ducibella et al., 1977; Houliston and Maro, 1989; Houliston et al., 1987), with mitochondria segregated to the blastomere cortex (Batten et al., 1987; Ducibella et al., 1977). The polarization results in two distinct populations of cells; large polar outside cells and small apolar inside cells (Ohsugi et al., 1993). Each cell type is destined for distinct developmental fates: the outer cells of the embryo are destined to become the trophectoderm cells, while the inside cells become the inner cell mass – see below.

3.4. Blastocyst formation

Blastocyst formation follows compaction. Blastocysts consist of a fluid-filled cavity, known as the blastocoel, the ICM, and an outer epithelial layer (or TE), which surrounds the

ICM and blastocoel. As stated above, the TE cells arise from the blastomeres on the outside of the compacted morula and are responsible for uterine contact and implantation of the embryo (Hogan, 1994). The trophectoderm goes on to form extra-embryonic membranes including the fetal contribution to the placenta (Cockburn and Rossant, 2010). The inner cell mass consists of pluripotent cells, that further divide into epiblasts (EPI) which develop into the fetus and the primitive endoderm (PE) that contribute to the yolk sac formation (Cockburn and Rossant, 2010; Gardner, 1982).

During blastocoel formation fluid enters the embryo via an osmotic gradient, mediated by the transportation of Na^+ out of the basolateral side of the TE into the blastocoel, by Na^+/K^+ ATPase located in the trophectoderm layer (Kidder and Watson, 2005; Van Winkle and Campione, 1991). In mice, apical Na^+ entry is regulated by Na^+/H^+ exchanger activity and possibly an amiloride-sensitive Na^+ channel (Manejwala et al., 1989). Cl^- transport into the blastocoel is apically mediated by chloride channels, with efflux mediated by HCO_3^-/Cl^- exchanger (Zhao et al., 1997). Water movement is facilitated by aquaporins, which are present within the blastocyst TE and functional by the compaction stage (Barcroft et al., 2003). Water leakage from the blastocoel is prevented by a seal that is produced by the expression of tight junctions in the apical surface of the TE cells, which form during the compaction period (Ducibella et al., 1977).

4. pH_i Regulation

Many cellular processes are highly dependent on intracellular pH (pH_i), including ion conductance, gap junctions, membrane transport and intracellular communication. Perturbations in pH_i may compromise cell function and viability, thus pH has to be regulated within a narrow range. Most vertebrate cells maintain a pH_i of about 7.2, which is regulated by several transmembrane transporters (Figure 6). Many mammalian cells regulate their internal pH by use of secondary active transport mechanisms. In addition to pH regulation, these transporters often function in the maintenance of ionic gradients, electrolyte balance and cell volume (Fliegel and Frohlich, 1993). The most common of these is Na^+/H^+ exchange by members of the NHE gene family (classified as Solute Carrier 9 or *Slc9* family), which appears to be nearly ubiquitous among mammalian cells. These transporters extrude H^+ in exchange for extracellular Na^+, to reduce intracellular acid loads (Figure 6). The other major group is a family of transporters related to the Band III anion exchanger of red blood cells (Grinstein, 1988). These include the HCO_3^-/Cl^- exchangers in the AE gene family (*Slc4* family), which regulate against intracellular alkalosis, by extruding bicarbonate out of the cell in exchange for external Cl^-, to reduce internal pH. The third exchanger, Na^+-HCO_3^-/Cl^- co-transporter (NDBCE, encoded by *Slc4a8*) which mediates cellular alkalization in response to an acid load, requires the presence of extracellular sodium in order to transport bicarbonate into an acidified cell in exchange for internal chloride, thus restoring the pH_i of the cell (Orlowski and Grinstein, 2004). The main foci of my study were the NHE exchangers, thus the following sections will focus on this family of transporters and their role in pH regulation.

Figure 6: **pH_i regulation.**

(A) *Major pH_i regulatory transporters. Acidosis:* Na^+-dependent HCO_3^-/Cl^- exchanger, Na^+/H^+ antiporter and Na^+-HCO_3^- co-transporter. *Alkalosis:* HCO_3^-/Cl^- exchanger and Na^+-HCO_3^- co-transporter. **(B)** *Dependence on pH_i for activities of three pHi regulatory transporters* (Na^+/H^+ exchanger, Na^+, HCO_3^-/Cl^- exchanger and HCO_3^-/Cl^- exchanger). Na^+/H^+ antiporter has high activity at low pH_i and functions to regulate intracellular acidosis. HCO_3^-/Cl^- exchanger has high activity at high pH_i and functions to mediate alkalosis. Na^+, HCO_3^-/Cl^- exchanger regulates intracellular acidosis but is active primarily at resting pH_i.

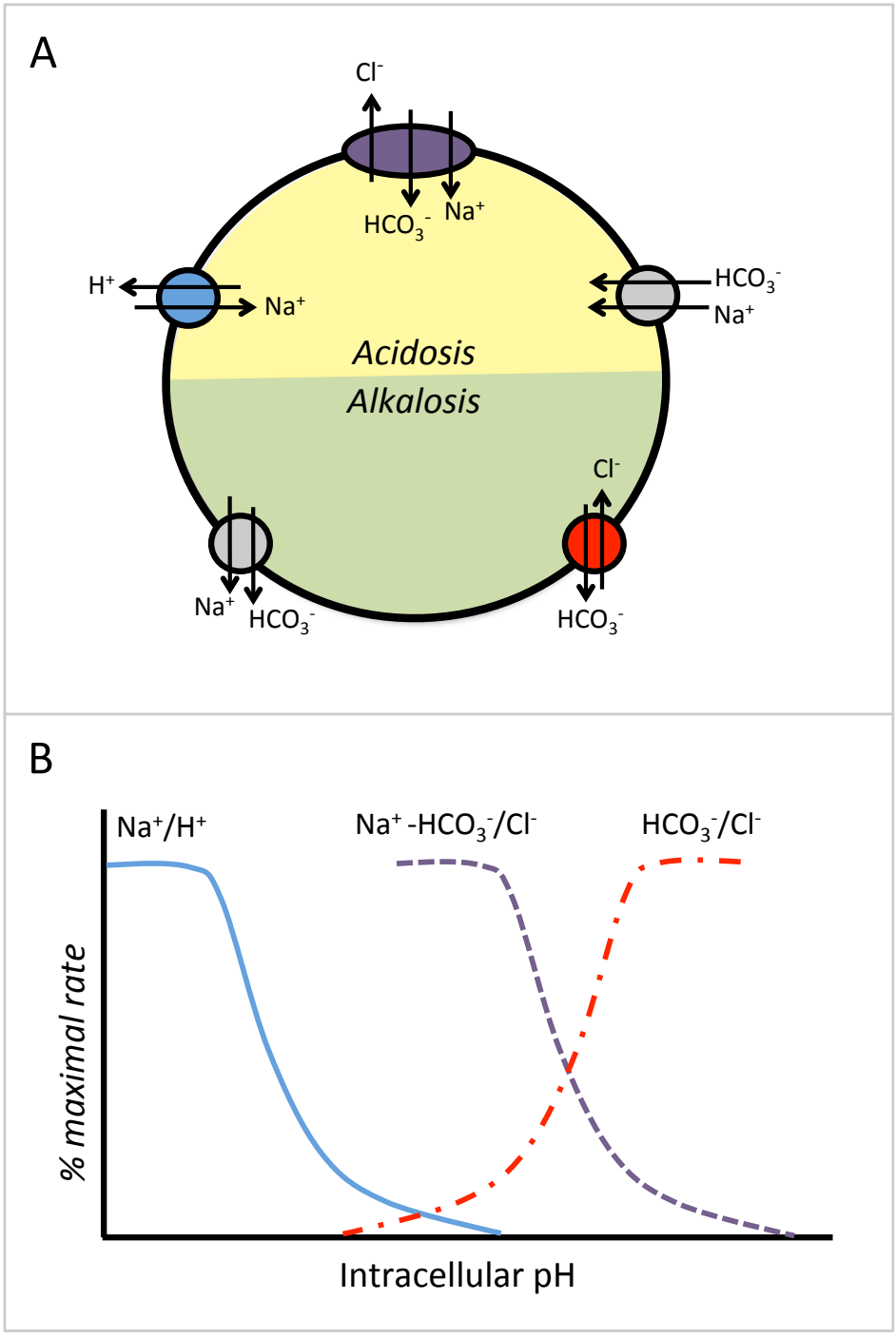
A
Cl-
HCO3-
Na+
H+
Na+
HCO3-
Na+
Acidosis
Alkalosis
Cl-
Na+
HCO3-
HCO3-
B
Na+/H+
Na+ -HCO3-/Cl-
HCO3-/Cl-
% maximal rate
Intracellular pH

Figure 6

5. Na^+/H^+ antiporters

NHE transporters are responsible for numerous physiological processes, ranging from pH homeostasis and epithelial salt transport, to systemic and cellular volume regulation (Orlowski and Grinstein, 2011; Puceat, 1999). The Na^+/H^+ exchanger mediates the electroneutral exchange of extracellular Na^+ for intracellular H^+ to increase pH_i. The SLC9 family of mammalian NHEs includes 10 isoforms designated SLC9A1-10 (Hoffmann et al., 2009).

Of these ten isoforms, NHE1-5 are of particular interest in this study, because they are localized to the plasma membranes of many cell types (Orlowski and Grinstein, 2004). In contrast, the NHE6-9 isoforms are mostly present within cellular organelles, i.e. Golgi, secretory vesicles, endosomes and lysosomes. SLC9A1/NHE1 is a ubiquitously expressed isoform, in epithelial cells localized to the basolateral domain (Coupaye-Gerard et al., 1996). SLC9A2/NHE2 and SLC9A3/NHE3 are found in many tissues, including the intestine (Bookstein et al., 1997; Dudeja et al., 1996), kidney (Soleimani et al., 1994; Sun et al., 1997) and apical membrane of epithelial cells (Counillon and Pouyssegur, 2000) (Hoogerwerf et al., 1996; Noel et al., 1996). SLC9A4/NHE4 is found within the basolateral plasma membrane in the stomach, intestine, kidney and hippocampus (Bookstein et al., 1997; Orlowski and Grinstein, 2011). SLC9A5/NHE5 is predominantly found in the brain (neurons), as well as the testis, spleen and skeletal muscle (Klanke et al., 1995; Orlowski and Grinstein, 2011).

NHE1 null mice did not show any obvious defect in acid-base homeostatic balance or in their kidney or intestine function. However, they do display defects in brain function, with epileptic-like seizures, ataxic gait of the hind legs and premature death due to convulsive seizures (Bell et al., 1999; Cox et al., 1997). NHE1 null mice were detectably smaller than their normal littermates, and ~67% of pups died before weaning. NHE2 knockout mice exhibit no detectable changes in intestine function, however the stomach was shown to be deficient in acid secretions due to modified gastric mucosa (Gawenis et al., 2002). NHE3 null mice are mildly acidotic and exhibit decreased blood pressure. As NHE3 is the main sodium absorption mechanism in intestines and kidney, its knockdown results in mice with poor Na^+- absorption and NHE3 null mice suffer from chronic diarrhea (Counillon and Pouyssegur, 2000; Schultheis et al., 1998).

5.1. Na^+/H^+ exchanger general structure

NHE proteins are highly conserved within a given isoform among numerous species and even among diverse isoforms of the same species (Fliegel and Frohlich, 1993). The molecular structures of mammalian NHEs are yet to be determined at the atomic level, although evidence suggests that they exist as homodimers (Figure 8B) of the respective monomers (Fafournoux et al., 1994; Hisamitsu et al., 2006; Hisamitsu et al., 2004). The consensus is that the NHE exchanger contains 12 membrane-spanning (or transmembrane, TM) segments at the N-terminal end (spanning ~ 400 - 500 amino acids) involved in ion translocation and drug recognition (e.g., amiloride; see Figure 8A). TM helices TM4 and TM11 are localized closely and have an unwound region in the middle of their respective segments, generating a pathway for ion permeation (Orlowski and Grinstein, 2011). Mutations of these regions lead to altered affinity for Na^+ and H^+, respectively

(Wakabayashi et al., 2003a, b). Along with the above, of particular note is a large exofacial reentrant loop (R-loop) between TM9 and TM10 that resembles an ion channel pore and may represent an analogous structure in NHEs (Orlowski and Grinstein, 2004; Schneider and Scheiner-Bobis, 1997). The hydrophilic C-terminus that faces the cytoplasm (ranging in length from ~50 - 450 amino acids) contains the residues involved in exchanger regulation and interactions with binding partners (Orlowski and Grinstein, 2011). TM6 and TM7 domains are highly conserved with 95% similarity among NHE isoforms and were shown to be central to Na^+ and H^+ transport (Slepkov et al., 2007). The transmembrane domains exhibit between 45-65% amino acid sequence identity between isoforms with only 25-35% identity of the cytoplasmic domain (Counillon and Pouyssegur, 2000). The monomeric NHE1 protein has three glycosylation sites with a molecular mass of 110kDa, while NHE3 and NHE4 have 3 to 5 glycosylation sites, depending on the species (Fliegel and Frohlich, 1993; Sardet et al., 1991).

5.2. Inhibitors

A number of pharmacological inhibitors are currently used to inhibit NHEs (Figure 7). Initially, a K^+-sparing diuretic, amiloride, was utilized to inhibit NHE1 activity, however this inhibitor is not particularly discriminating against other Na^+ transporters. It inhibits both the epithelial Na^+ channel (ENaC) and sodium calcium exchanger (NCX). Details can be found in comprehensive reviews (Kleyman and Cragoe, 1988a, b; Masereel, 2003). At physiological pH_i (~7.2 -7.4), amiloride exists primarily as a protonated (95%) monovalent cation and acts as a competitive inhibitor of Na^+ transport by NHE1 (K_i 1-100μM; (Aronson et al., 1982; Benos, 1982)) and other NHEs. Inhibition of NHEs by amiloride is almost immediate and is quickly reversed upon removal of amiloride from media (Grinstein and

Foskett, 1990). High external Na^+ reduces the inhibitory ability of amiloride and its analogs, suggesting that these compounds bind near an external Na^+ transport site (as indicated in Figure 8). In order to produce NHE-selective inhibitors a number of substitutions on the amiloride molecule yielded compounds with improved selectivity profiles with 10- to 100-fold higher K_i values for NHEs while losing potency for ENaCs and NCXs, such as 5-N-ethyl isopropyl amiloride (EIPA). The NHE isoforms vary in their sensitivity to amiloride and its analogs, generally following the order NHE1 > NHE2 >> NHE3 > NHE5 > NHE4 (Counillon et al., 1993; Orlowski and Grinstein, 2004).

Further research yielded a new group of drugs, benzoylguanidine-based compounds (Figure 7B), which selectively inhibit the NHE1 isoform. These include HOE-694 (3-methylsulphonyl-4-piperidinobenzoyl-guanidine hydrochloride) and cariporide (HOE-642; 4-isopropyl-3-methylsulphonyl-guanidine methanesulphonate). These compounds display a 1000-fold higher potency towards NHE1 than NHE3 and NHE4 (as summarized in Table 1) (Chambrey et al., 2001; Scholz et al., 1995; Schwark et al., 1998). A methacryloylguanidine-based compound, termed S3226 (3-[2-(3-guanidino-2-methyl-3-oxo-propenyl)-5-methyl-phenyl]-N-isopropylidene-2-methyl-acrylamide dihydrochloride), was developed to selectively block NHE3, and was determined to be up to ~100 fold more effective at inhibiting NHE3 than NHE1 or NHE2 (Masereel, 2003; Schwark et al., 1998). The differential effectiveness of these inhibitors has recently been used to determine the role of individual exchangers in the tissues where numerous isoforms are co-expressed (Scholz et al., 1995; Schwark et al., 1998).

Figure 7: **Molecular structures of Na^+/H^+ exchanger inhibitors.**

(A) Pyrazine-based compounds – EIPA, Amiloride; **(B)** Benzoylguanidine-based compounds – Cariporide and HOE; **(C)** Methacryloylguanidine-based compound – S3226 (Orlowski and Grinstein, 2011).

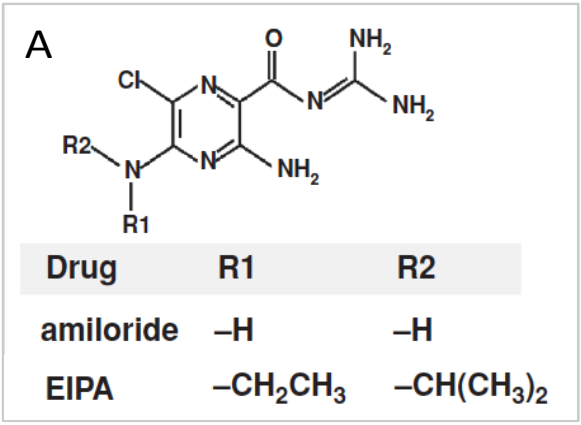

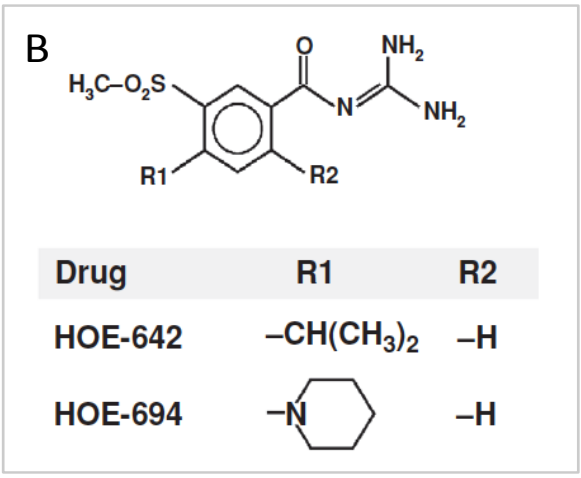

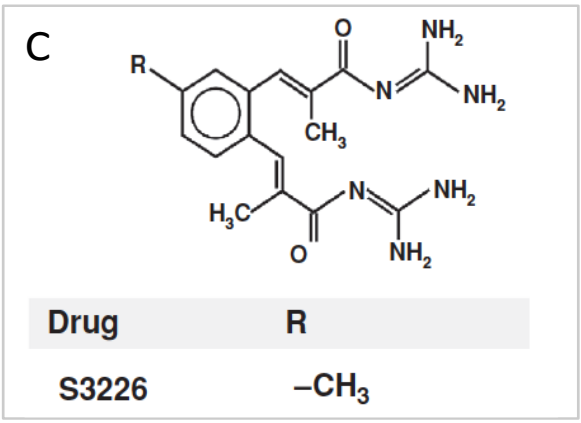

Table 1: Inhibitors of Na^+/H^+ Exchangers

Inhibitor	Isoform				
	NHE1	**NHE2**	**NHE3**	**NHE4**	**NHE5**
Amiloride	*3* [1] 1.6 [3] 5.3 [4] 10.7 [2]	*3* [1] 10.3 [2]	*100* [1,3] 283 [2] 438 [2]	813 [4]	21 [3]
HOE 694	*0.085 - 0.16* [2, 5]	*5* [1]	*640* [1,5]		*9.1* [5]
Cariporide	*0.05* [8] 0.08 [2] 0.05 - 3.4 [8, 5]	1.6 [2] 3.0 [6, 8] 4.3 – 62 [5]	900 – 1000 [2, 6, 8]	545 [7]	>30 [5]
S3226	3 – 3.6 [2, 5, 9]	80 [2]	0.023 [2]		

Values reported are IC_{50} or K_i in micromolar. Values are summarized from the following references: [1](Counillon et al., 1993); [2] (Schwark et al., 1998); [3] (Szabo et al., 2000); [4] (Chambrey et al., 1997b); [5](Masereel, 2003); [6](Scholz et al., 1995); [7](Chambrey et al., 2001); [8](Karmazyn et al., 2003); [9](Speake et al., 2005).

5.3. Transport Models

Currently, our knowledge of the transport mechanisms of NHE exchangers is incomplete. Most is known about NHE1 and NHE3, which have been generalized to describe the basic activity and transport model for all five trans-membrane isoforms. In their forward mode, the antiporter catalyzes an electroneutral exchange of extracellular Na^+ for cytosolic H^+, with a 1:1 stoichiometry. However, the transport can be operated in reverse depending on the combined gradients of Na^+ and H^+ (Grinstein et al., 1984; Semplicini et al., 1989). A more recent study has shown that the stoichiometry may in fact be $2Na^+$ for $2H^+$ (Fuster et al., 2008), however it can alternatively be explained by the coupling of two NHE monomers into one functional dimeric unit (as described above). NHE1-3, and 5 isoforms exhibit Michaelis-Menten kinetics, whereby the rate of Na^+/H^+ exchange exhibits a hyperbolic dependence on extracellular Na^+ concentration (Bookstein et al., 1994a). This suggests that Na^+ binds to a unique external binding site and is translocated into the cell. Unlike other isoforms that have been studied, NHE4 exhibits a sigmoidal dependence on external Na^+. However, the functional significance of this has not been elucidated, but could indicate regulation of its transport rate by a separate Na^+ binding site (Bookstein et al., 1996).

Under normal physiological conditions, Na^+ binding to the external binding site of any NHE antiporter occurs with a measured K_m about 3-fold below the physiological external Na^+ concentration. Thus, the antiporter operates close to saturation and any moderate changes in the external Na^+ have little effect on the transport rate of the exchanger (Counillon and Pouyssegur, 2000; Orlowski and Grinstein, 2011). The plasma membrane isoforms' external cation site, which normally binds Na^+, can also accommodate H^+ and Li^+ transport, while the endomembrane class (found within organelle membranes) also has the

ability to transport not only sodium but also K^+ and Rb^+ (Aronson et al., 1982; Orlowski and Grinstein, 2011; Paris and Pouyssegur, 1983).

5.4. Regulation of NHEs

NHE exchangers are secondary transporters whose activity is driven by the combined chemical gradients of Na^+ and H^+ and hence do not require direct ATP consumption. However, ATP was shown to be an integral part of optimal transporter activity. Acute cellular depletion of ATP reduces NHE1 and NHE2 activity and almost completely inhibits NHE3 and NHE5 activity, even with a high transmembrane H^+-gradient (Kapus et al., 1994; Wakabayashi et al., 1992). Reduction of intracellular ATP levels drastically decreases the activity of NHE1-3 by reducing the antiporter affinity for intracellular H^+ (Wakabayashi et al., 1997b). The pH setpoint of the antiporter (the threshold above which it is activated) can be shifted down by ATP-depletion, and are shifted up by growth or osmotic cell shrinkage (Grinstein and Foskett, 1990). ATP dependence is likely to be mediated by phosphoinositides (Figure 8). The inner portion of the plasma membrane is rich in phosphotidylinositol 4,5-bis phosphate (PIP_2), which at physiological pH has 3 to 4 negative charges. The high charge density attracts positively charged regions of the tail of the exchangers, which were shown to be essential for optimal NHE activity (see Figure 8). Two such motifs are discernible in the cytoplasmic domain of NHE1 (Aharonovitz et al., 2000; Sardet et al., 1989) and three in the case of NHE3 (Tse et al., 1992). ATP depletion also triggers dephosphorylation of NHE at critical sites, leading to conformational changes that reduce the affinity of the cytoplasmic domain H^+-modifier site (Wakabayashi et al., 1992).

Various stimuli have been identified that activate various protein kinases or G protein-coupled receptors, in turn activating signaling pathways which enhance or decrease activity of different NHE isoforms. NHE activation leads to intracellular alkalinization in the absence of activation of the NHE transporter by decreased pH_i, leading to a higher resting pH_i. Regulation of NHE transporters is mediated by a wide variety of mechanisms including receptor tyrosine kinases, the Ser/Thr kinases PKC and PKA, increases in $Ca^{2+}{}_i$, changes in cell volume (Fliegel and Frohlich, 1993) and p160ROCK, a RHO effector associated with the assembly of stress fibers and focal adhesions (Tominaga et al., 1998). Consensus sequences for PKA, PKC, CaMKII (Kemp and Pearson, 1990), and MAPK $p34^{cdc2}$ kinase are present in both the N-terminal and C-terminal regions of the Na^+/H^+ exchanger (Pelech and Sanghera, 1992).

It is thought that NHE1 antiporters are activated through the transduction of a common mitogen-activated protein kinase (MAPK) pathway involving mitogen-activated, extracellular signal-related kinase (MEK→ERK→$p90^{rsk}$). The $p90^{rsk}$ kinase phosphorylates Ser-703 of human NHE1 directly, enabling the binding of the multifunctional scaffolding protein 14-3-3 to that site (Lehoux et al., 2001). The bound 14-3-3 then serves as a focal point for the assembly of other signaling molecules (Fanger et al., 1998). NHE1 also acts as a substrate for NCK-interacting kinase (NIK), an adaptor protein, which transduces signals from a receptor tyrosine kinase (i.e. platelet-derived growth factor) diverging from the ERK-$p90^{rsk}$ pathway. NIK binds the middle portion of NHE1 C-terminus (Figure 8), while phosphorylating an unknown downstream site, yet to be elucidated. Also, NIK was found to act upstream of MEK kinase (i.e., it is a MEKK) to activate c-JUN N-terminal kinase JNK (mechanism activated during cell shrinkage) (Yan et al., 2001).

Although the mechanism by which protein phosphorylation enhances cation exchange by NHEs is yet to be determined, a study by Li et al. suggested that serum-induced phosphorylation of the distal C-terminus of NHE1 induces binding of carbonic anhydrase II (CAII), which catalyzes the hydration of CO_2 to form HCO_3^- and H^+ (Li et al., 2002). Co-expression of both proteins in a NHE-deficient CHO cell line increases NHE1 activity well above those that only express the antiporter; this activity is abolished by the presence of acetazolamide, a CAII antagonist. Thus, CAII binding to NHE1 stimulates transport activity and cellular alkalization rapidly by raising the local production of protons (which exit the cell) and elevate internal pH by increasing internal bicarbonate levels (Orlowski and Grinstein, 2004).

NHE activity can also be regulated by phosphorylation of secondary factors by protein kinases. Ca^{2+}/calmodulin binds to high affinity (CaM-A) or low affinity (CaM-B), positively charged clusters in the C-terminal regulatory domain of NHE1 (Wakabayashi et al., 1994). Ca^{2+}/calmodulin association with the CaM-A domain activates NHE1 by alleviating the autoinhibitory interaction, which increases the exchanger's affinity for internal protons, and is decreased by the presence of agonists that mobilize cytoplasmic calcium (Wakabayashi et al., 1997a).

Three other Ca^{2+}-binding phosphoproteins called calcineurin B homologous protein-1 and -2 (CHP1 and CHP2) and tescalcin (CHP3) associate with NHE residues in the juxtamembrane region of the C-terminus and are critical for binding and optimal basal transport activity (Pang et al., 2001). The outermost site can also be associated with the cytoskeletal-associated ERM proteins (Ezrin, Radixin and Meosin) (Denker et al., 2000). This C-terminal region is therefore of crucial importance in the regulation of NHE activity (Figure 8). Most of the foregoing has been elucidated only in NHE1, with regulation of the

other NHEs much less clear. Regulation of different NHE isoforms by two stimuli that are particularly relevant here - pH_i changes and cell volume decreases - is described in more detail below.

Figure 8: **Predicted molecular architecture of the mammalian Na^+/H^+ exchanger and binding partners.**

(A) Illustrates the proposed membrane topology of NHE1 and the approximate locations of direct interaction with identified binding partners (side view). See text for details. **(B)** Represents a higher-ordered dimeric structure of the mammalian Na^+/H^+ exchanger (top view). *Abbreviations:* CAII-carbonic anhydrase II; CaM- calmodulin; CHP-calcineurin homolog protein; ERM-ezrin/radixin/moesin; NIK- Nck-interacting kinase; PIP_2-phosphatidylinositol 4,5-bisphosphate (replicated from Hoffman et al. 2009 and Orlowski and Grinstein 2011).

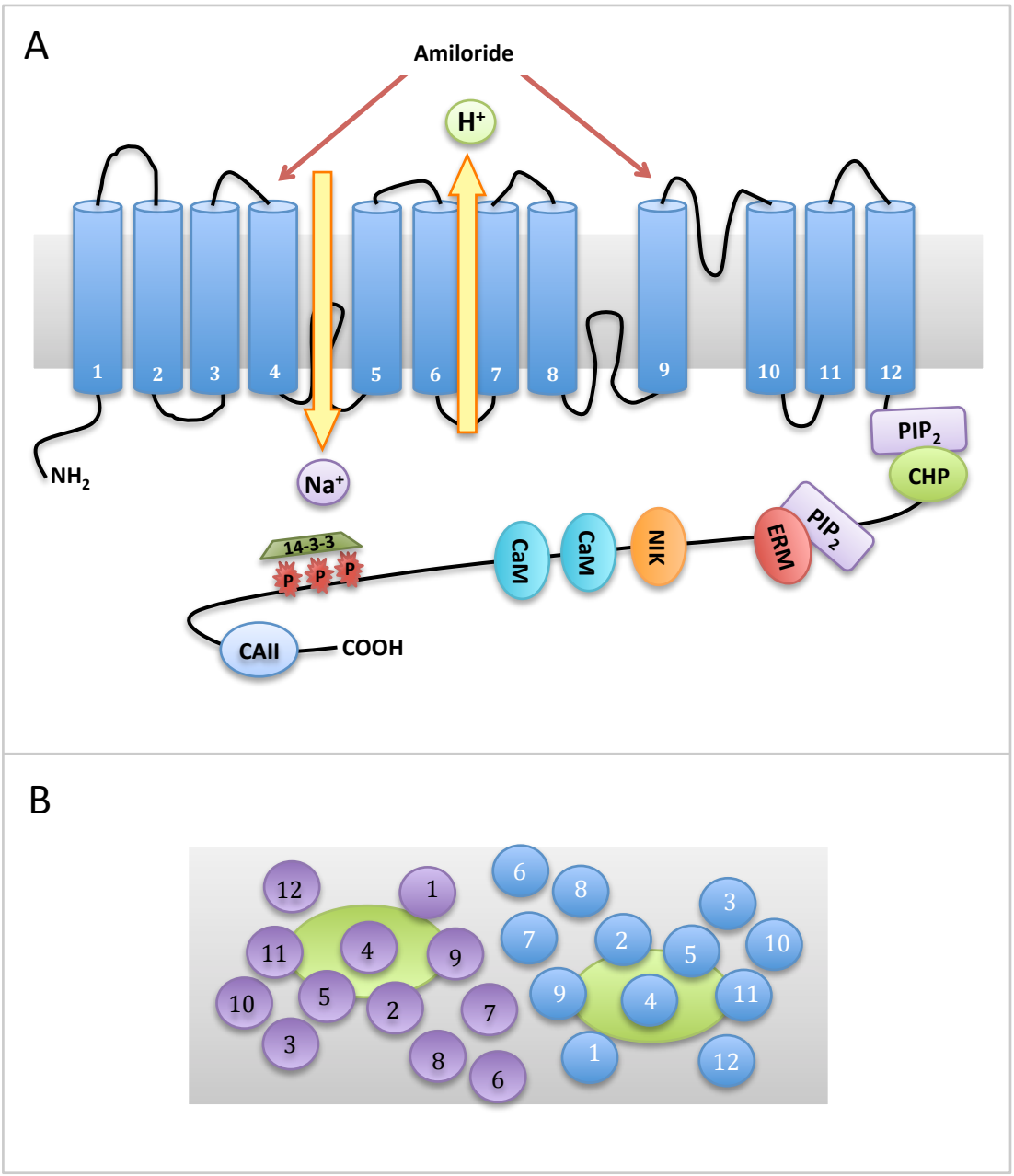
A
Amiloride
H+
1
2
3
4
5
6
7
8
9
10
11
12
NH2
Na+
PIP2
CHP
14-3-3
P
P
P
CaM
CaM
NIK
ERM
PIP2
CAII
COOH
B

Figure 8

5.5. Regulation by pH

A primary function of at least some NHE exchanger isoforms is to control intracellular pH. The activity of Na^+/H^+ exchange is controlled by the pH_i setpoint. A drop in the cytosolic pH below that setpoint activates the exchanger and enhances the rate of transport (Grinstein and Foskett, 1990). NHE1-3 isoforms are extremely sensitive to low intracellular pH. At normal physiological pH_i, NHE1 and NHE2 are practically dormant, and rapidly activated when pH decreases below the setpoint of that exchanger (Aronson et al., 1982; Paris and Pouyssegur, 1983), while NHE3 exhibits a lower affinity for intracellular H^+ and was shown to be active at resting pH_i (Wakabayashi et al., 1995).

As the cytosol is acidified due to a variety of normal intracellular metabolic activities (such as glycolysis and the Krebs cycle), the increased concentration of intracellular H^+ accelerates Na^+/H^+ exchange. The reported Hill coefficient (of more than 2) implied the existence of at least one H^+-binding sites in addition to the transport site (Aronson et al., 1982). The modifier site, which binds H^+ ions, exerts an allosteric effect on the exchanger during a pH drop below a threshold level, which leads to the rapid activation of the transporter (Kapus et al., 1994). Allosteric control of the rate of transport is required because of the large Na^+ gradient of >10 between the external and internal concentrations, to prevent intracellular pH rising above the physiological (setpoint) levels. As the cytosolic pH reaches neutrality, the decreased $[H^+_i]$ leads to decoupling of protons from the modifier site, which in turn deactivates the transporter (Orlowski and Grinstein, 2011).

Mutations of various domains on NHE1 and NHE3 isoforms have shown that complete deletion of the cytoplasmic domains leads to only 25% reduced activity (similar to that observed in cytosolic ATP depletion) suggesting that the N-terminal portion is sufficient for protein integration into the membrane and ion transport across the membrane (Aronson

et al., 1983). Deletion of the cytoplasmic domain has also shifted the sensitivity of NHE antiporter activity to the acidic range, rendering the modified exchanger inactive above pH_i 6.6. These results suggest that the proton modifier site is located on the N-terminal transmembrane domain, while the C-terminus regulates the setpoint value (Wakabayashi et al., 1992).

External pH (pH_o) may also affect the activity of NHE antiporter. In the range 6.0 - 8.5, external H^+ interacts with Na^+/H^+ at a single site with a reported pK_a of 7.3 - 7.5. This site is the external transport site that can also bind Na^+, H^+, Li^+, NH_4^+ and amiloride. The sequence of binding affinities for the external transport site of the renal Na^+/H^+ exchanger is $H^+ >>$ amiloride $>> Li^+ > NH_4^+ \geq Na^+ >> K^+$, Rb^+, Cs^+, choline (Aronson et al., 1983). Decrease in the external pH has been shown to inhibit Na^+ uptake and Na^+/Na^+ exchange, suggesting that external H^+ competes for the external sodium-binding site, consequently inhibiting exchanger activity (Aronson et al., 1983).

5.6. Volume regulation

To avoid excessive alterations of internal cell volume, cells have developed mechanisms to counteract these perturbations in volume both in the cell and the organism, thus regulating cellular as well as intravascular volume within a normal physiological range. The mechanisms employed in cells exposed to hypotonic extracellular fluid have been collectively termed regulatory volume decrease (RVD). Exposure to a hypertonic extracellular environment results in cell shrinkage, and is restored through a regulatory mechanism generally called regulatory volume increase (RVI). Ions are the main contributors of the intracellular (mainly K^+) and extracellular (by NaCl) osmolarity. Ions contribute up to 67% to cell volume regulation after an acute perturbation in the

extracellular osmolarity (Fisher and Spring, 1984; Lang et al., 1998; Verbalis and Gullans, 1991). Therefore, ion transport across the cell membrane is extremely imperative for the regulation of cell volume, largely because volume restoration through RVD and RVI are accomplished within minutes after exposure to anisotonic environments.

Mammalian cells regulate against unwanted cell volume increases through ubiquitous "volume-regulated anion channels" or VRACs (also known as "volume-sensitive organic osmolyte and anion channels," VSOAC) that are also permeable to a number of organic osmolytes (Okada, 1997; Strange et al., 1996). The mechanism by which cell volume leads to channel openings remains as elusive as their molecular identity and yet to be ascertained (for review refer to (Hoffmann et al., 2009). VRACs operate by releasing intracellular Cl^- and also a range of other organic osmolytes (Baltz and Zhou, 2012). During recovery from acute cell volume increases, any extruded Cl^- ions require the coupled efflux of cations (i.e. K^+) to maintain intracellular electroneutrality. K^+ efflux is carried out by K^+ channels, which are functionally coupled to VRACs (Hoffmann et al., 2009). Cell swelling recovery, therefore, is mediated by KCl efflux via coupled channels and by uncharged organic osmolyte extrusion through VRACs (Figure 9D).

During RVI, sodium is frequently driven intracellularly through an exchange of protons, a process regulated by the sodium/hydrogen exchanger (NHE). This was first demonstrated by Cala et al. while studying the volume regulation of red blood cells from *Amphiuma tridactylum* (giant salamander) (Cala, 1980). In red blood cells RVI is mediated by a NHE exchanger operating in parallel with AE, resulting in a net uptake of NaCl and water up the gradient (Figure 9A) (Cala, 1980). Shortly after, Sardet cloned the giant salamander NHE and showed a high similarity to the human NHE1 isoform (Sardet et al., 1989). Subsequently, NHE1 was found to be the isoform mediating RVI in a wide variety

of cell types (Alexander and Grinstein, 2006). Mutant cells lacking NHE1 were shown to be unable to regain volume after an imposed acute cell shrinkage (Grinstein et al., 1994; Kapus et al., 1994). In brief, during exposure to hypertonicity NHE1 is activated and internal protons are exchanged for external sodium ions, as protons leave the cell, the internal pH rises, and the internal bicarbonate concentration increases. The elevated pH_i in turn activates the bicarbonate/chloride exchanger (AE) to extrude the excess bicarbonate for Cl^-. This results in a net gain of sodium and chloride and expulsion of protons and bicarbonate. Increase in internal NaCl leads to increased osmolarity, which is remedied by influx of water into the cell and the restoration of cell volume (Humphreys et al., 1995; Jiang et al., 1997).

NHE1, being a ubiquitously distributed isoform thus is the most important mechanism of NHE-mediated RVI in most cells. This is not to say that the other isoforms have no role in RVI in cell types that express them. For example, NHE2 and NHE4 may also contribute to the RVI response in the stomach and gastrointestinal epithelia (Hoffmann et al., 2009). NHE4 is stimulated by cell shrinkage due to changes to actin cytoskeleton and was suggested to play a vital role in RVI in tissues exposed to very high osmolarities, such as in the kidney (Bookstein et al., 1996; Bookstein et al., 1994b). Unlike, NHE1, 2 and 4, NHE3 has been shown to be inhibited by cell shrinkage and activated by cell swelling in a variety of cell types. Also NHE3 sensitivity to volume changes plays a major role in control of systemic volume and hence blood pressure. Mutant mice lacking the NHE3 exchanger have shown a significantly decreased blood pressure compared with the wild-type littermates indicating a perturbation of fluid volume homeostasis (Hoffmann et al., 2009; Ledoussal et al., 2001; Schultheis et al., 1998).

Figure 9: Model of mammalian cell volume regulation.

When a cell decreases in volume (**A**), a common mechanism for acute recovery is the activation of NHE1 exchanger coupled with AE exchanger. This initiates the import of Na^+ and Cl^- into the cell, elevating the intracellular osmolarity and restoring the cell to normal size (**B**). As the resulting increased ionic strength in the cytoplasm would be detrimental, cells replace these ions with organic osmolytes with the aid of specific transporters, while still maintaining intracellular osmolarity (**C**). When a cell increases in volume, the volume-regulated anion channels (VRACs) are activated mediate the export of inorganic anions (accompanied by cation efflux via potassium channels) and organic osmolytes (**D**). These mechanisms (RVI vs. RVD) are vital for cell volume maintenance within a narrow, healthy range.

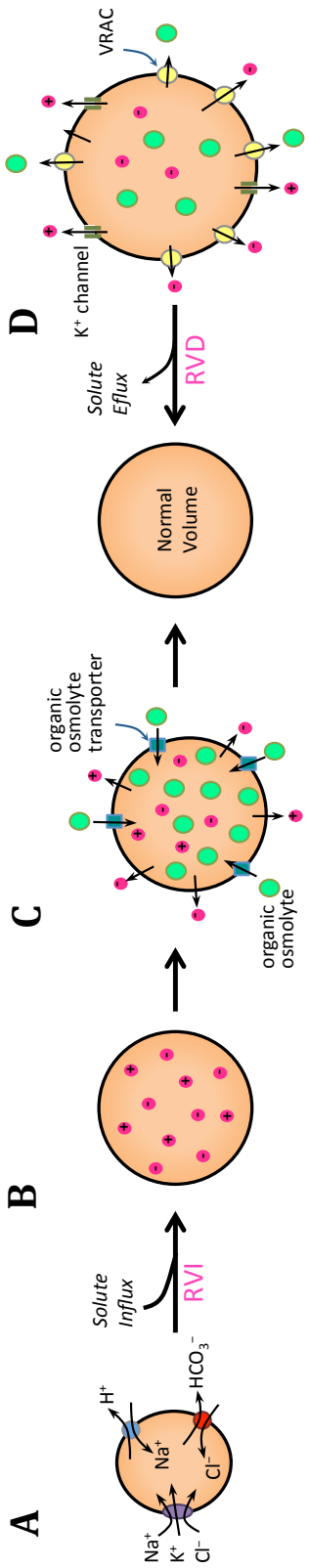
A
B
C
D
Na+
K+
Cl−
H+
Na+
Cl−
HCO3−
Solute Influx
RVI
organic osmolyte transporter
organic osmolyte
Normal Volume
K+ channel
VRAC
Solute Efflux
RVD

Figure 9

6. pH_i Regulation in Preimplantation Embryos

6.1. Na^+/H^+ exchanger

Sodium hydrogen exchangers became of particular interest in the study of fertilization upon Johnson and Epel's discovery of the considerable pH increase in eggs of sea urchins that immediately follows fertilization (Johnson and Epel, 1976). This rapid increase in pH was attributed to the activation of the Na^+/H^+ antiporter, which imported sodium ions into the cell in exchange for hydrogen ions. In mammals, no such rapid increase in pH after fertilization has been observed (Ben-Yosef et al., 1996; Phillips and Baltz, 1996); but the antiporter has been implicated in internal pH regulation of pre-implantation embryos (Steeves et al., 2001). Hamster and bovine 1-cell, 2-cell and 8-cell embryos are able to successfully develop to the blastocyst stage when cultured in acidic media, but blastocyst development is significantly decreased in the presence of the general NHE inhibitor EIPA (Lane et al., 1998; Lane and Bavister, 1999). Human GV, MII and PI stage embryos did not maintain baseline pH_i after being placed in moderately low pH medium before the blastocyst stage, the first stage that was able to maintain pH_i in the face of external acidosis (Dale et al., 1998). However, another study of cleavage-stage embryos demonstrated that these embryos can regulate pH_i against more profound acidosis, using Na^+/H^+ exchange with a setpoint of about 6.9 (Phillips et al., 2000). This implied that at least some mammalian embryos possess transporters capable of relieving intracellular acidosis.

Initial studies into the pH_i regulation of mouse 2-cell embryos from CF1 and BDF strains did not detect a sodium-dependent recovery component in response to induced acidosis (Baltz et al., 1990). Similar studies did not find bicarbonate-dependent recovery

from acidosis (Baltz et al., 1991b). However, later, a contradicting result was obtained in the Quackenbush Swiss (QS) strain of mice, where a robust recovery from acidosis was observed in 2-cell stage zygotes. This recovery was attributed to two components, the first was H^+-monocarboxylate transport, and the other was Na^+/H^+ exchange (Gibb et al., 1997). These contradictory results prompted the reevaluation of the earlier finding in 2-cell stage mouse embryos. Further investigation in several mouse strains demonstrated very different rates of recovery from acidosis via Na^+/H^+ exchange between each strain, with embryos from the Balb/C strain female mice having much higher Na^+/H^+ exchanger activity than either BDF or CF1 strains (Steeves et al., 2001). While the QS mice used in Gibb et al.'s (1997) study were not available to Steeves et al., they apparently have an even higher rate of Na^+/H^+ exchanger activity, judging by the reported rates of recovery.

NHE1 and NHE3 mRNA are expressed in mouse oocytes and unfertilized eggs. NHE1 mRNA was also detected in all preimplantation stages examined (Barr et al., 1998). The NHE1 protein was shown to be localized to the basolateral surface of the trophectoderm and the inner cell mass of the mouse blastocyst. Although no NHE3 mRNA transcripts were detected past the egg stage, the protein was present at the blastocyst stage and confined to the apical surface of the trophectoderm. Studies of growing and fully-grown oocytes in our lab yielded similar results, where mRNA expression for isoforms NHE1, 3 and 4 were observed in fully-grown oocytes (FitzHarris et al., 2007).

It is unclear which of these NHE isoforms is responsible for the Na^+/H^+ exchanger activity that mediates pH_i regulation in PI embryos. Most studies have used amiloride or its derivatives, which are general inhibitors of NHE isoform activity (Chambrey et al., 1997b; Counillon et al., 1993; Schwark et al., 1998; Szabo et al., 2000). Then, more selective NHE inhibitors than the amiloride derivatives have been developed, including cariporide

(HOE642) and related compounds that are highly selective for NHE1 (Counillon et al., 1993; Masereel, 2003; Schwark et al., 1998; Szabo et al., 2000), and S3226, which preferentially inhibits NHE3 (Schwark et al., 1998). We are aware of one attempt to elucidate the separate contributions of NHE isoforms to the regulation of pH_i in mammalian embryos. Harding et al. used the dose-response profile of HOE694, a compound related to cariporide that is selective for NHE1 (Counillon et al., 1993) in 2-cell stage mouse embryos and several concentrations of methylisopropylamiloride (MIA) at the MII egg, 1-cell and 2-cell stage and in the inner cell mass of blastocysts (Harding et al., 2002). According to Harding et al., a HOE694 concentration-response curve yielded a biphasic curve to a plot of the percent rate of recovery from acidosis versus inhibitor concentration ranging from 10^{-5} μM to 50 μM. This was interpreted as indicating two NHE isoforms of different affinities, one whose inhibition reached a plateau on the concentration-response curve that begins at ~10^{-3} μM HOE694 (attributed to NHE1), and the other represented by the final plateau that apparently was reached above 1 μM (NHE2 and/or NHE3). Since higher concentrations than 50 μM led to cell lysis, they opted to use an amiloride derivative MIA to elucidate which isoforms play a role in a myriad of PI stages. According to the dose-response curves obtained with MIA they reached the same conclusions obtained with HOE694, for at 1 μM (should only inhibit NHE1) at least 50% of the recovery was inhibited within all embryo stages tested, and at higher concentration almost complete inhibition was obtained at all stages except the blastocyst ICM cells, suggesting yet again a presence of NHE2 or NHE3 isoform activity. A small MIA-insensitive component was observed within the blastocyst ICM cell, which was attributed to NHE4 activity, due to its known insensitivity to amiloride and its analogs. However, the putative NHE2 and/or NHE3 activity was not confirmed by other means such as selective inhibitors (Harding et al., 2002).

Culturing of mouse embryos in various concentrations of the NHE1 inhibitor cariporide had no effect on development from the 2-cell stage to the morula stage. S3226 had no effect on embryo maturation up to 1μM from the 2-cell or morula stages, however development at 5 μM decreased dramatically and completely stopped at 10μM (Kawagishi et al., 2004). The concentration of S3226 that showed an effect, however, is high enough to completely inhibit NHE1 as well as NHE3, and the apparent IC_{50} near 5 μM for the effect on development is more consistent with NHE1 (Masereel, 2003; Schwark et al., 1998). The S3226 effect may instead have been due to a toxic effect.

6.2. HCO_3^-/Cl^- exchanger

Preimplantation embryo regulation against alkalosis has been well documented in the mouse (Baltz et al., 1991a; Zhao and Baltz, 1996; Zhao et al., 1995; Zhao et al., 1997) and hamster (Lane et al., 1999) from the 1-cell through blastocyst stage. First described in mouse 2-cell embryos, recovery from alkalosis was shown to be mediated by HCO_3^-/Cl^- exchanger activity. Recovery was shown to be HCO_3^- and Cl^--dependent and was inhibited by DIDS (Baltz et al., 1991a). Anion exchanger activity was highest at the zygote and 2-cell stages and decreases by the morula and blastocyst stages as the embryo entered the uterine horn (Zhao and Baltz, 1996). HCO_3^-/Cl^- exchanger activity was necessary for maintenance of normal physiological pH_i and recovery from intracellular alkalosis in PI embryos. Proper embryo development was hindered in the absence of functional exchangers (through inhibition with DIDS) when external pH was alkaline (near oviductal fluid pH) (Zhao et al., 1995).

Resting pH_i of 2-cell mouse embryos cultured under alkaline conditions (0.8% CO_2 ~ pH7.8) was 7.24, while in the presence of DIDS the internal pH rose to 7.57 (Zhao et al.,

1995). Under normal conditions (5% CO_2 ~ pH7.35) a similar effect was observed in the resting 2-cell embryo pH_i, with pH_i of 7.29 observed in embryos cultured with DIDS as compared to cultures in the absence of DIDS with pH_i of 7.10 (Zhao et al., 1995).

mRNA transcripts for AE1 were not detected in any PI stages, while AE2 mRNA was expressed throughout embryo development, with greatest amounts observed in the 1-cell and blastocyst stages. AE3 was present from the 2-cell stage through to blastocyst stage, with very weak expression in the 1-cell stage. Thus, AE2 is both maternally and embryonically derived, while AE3 is a product of the embryonic genome, since it only appears after ZGA at the 2-cell stage (Zhao et al., 1995). Since at the blastocyst stage there is little exchanger activity detectable in the apical trophectoderm, the basally located AE2 is believed to function in Cl^- and fluid transport to the blastocoel cavity (Zhao et al., 1997).

HCO_3^-/Cl^- exchanger is active in first meiotic prophase (GV) oocyte but inactivated during meiotic metaphase before the MI to MII transition. These exchangers are quiescent in the unfertilized eggs and become highly active in regulating pH in early embryo development (Erdogan et al., 2005). Since mammalian fertilization and early embryo development occur in the alkaline environment of the oviduct, expression and function of HCO_3^-/Cl^- exchangers is fundamental for PI embryo development.

6.3. Na^+-HCO_3^-/Cl^- exchanger

A third pH regulatory mechanism that may alleviate internal acidosis is Na^+ dependent HCO_3^-/Cl^- exchanger. Its activity was observed in human (Phillips et al., 2000) and mouse (Erdogan et al., 2011) GV, MII and 1-cell embryos. In mice, the presence of bicarbonate/CO_2 media doubled the rate of pH_i recovery from acidosis in zygotes. In bicarbonate-free medium, EIPA and cariporide inhibited recovery to the level seen in Na^+-

free medium (Erdogan et al., 2011). In bicarbonate/CO_2 containing medium, EIPA or DIDS each inhibited recovery to about 50%. Quantitative PCR analysis of 1-cell zygotes showed the presence of NHE1 (SLC9A1) and NDBCE (SLC48A) transcripts (Erdogan et al., 2011). Studies with other mammalian species, hamster (Lane et al., 1998) and bovine (Lane and Bavister, 1999) have failed to show presence of this antiporter.

7. Cell Volume Regulation in Oocytes and PI Embryos

The ability of the preimplantation embryo to maintain its internal environment is crucial for its survival and successful implantation. The earliest stages of PI embryos are extremely susceptible to increased osmolarity, even within the normal physiological range. This sensitivity contributes to the developmental block that occurred in traditional culture media (Biggers, 1998; Goddard and Pratt, 1983), a phenomenon called the "2-cell block" in mice and rats (Kishi et al., 1991). Similar developmental blocks were also observed in other mammalian species including the hamster in the 2- to 4-stage embryos (Schini and Bavister, 1988), 8-cell in bovine (Camous et al., 1984) and 4- to 8-cell in human embryos (Bolton et al., 1984). Such blocks to development were attributed to high osmolarity of the media, although the culture media used mimicked the *in vivo* oviductal fluid osmolarity of 300 - 310 mOsM range (measured in mice) (Collins and Baltz, 1999; Fiorenza et al., 2004). Similarly measurements of osmolarities of oviductal fluid in other species have also shown them to be essentially isosmotic to blood in the same species and thus not hypotonic (Knudsen et al., 1979; Waymouth, 1970; Williams et al., 1972). It was found that the developmental arrest could be overcome by either lowering the culture media osmolarity (to ~250 mOsM in mice) or by adding any of several amino acids or amino acid derivatives to the higher osmolarity culture media. Addition of glutamine, betaine, proline, glycine or β-alanine each enabled development of mouse embryos past the 2-cell stage at higher osmolarities (Biggers et al., 1993; Dawson and Baltz, 1997; Van Winkle et al., 1990). This suggested that organic osmolytes are required for embryo volume regulation and successful embryo development. Organic osmolytes are small, neutral organic compounds accumulated by different cells to provide intracellular osmotic support (Garcia-Perez and Burg, 1991;

Yancey et al., 1982). Accumulated organic osmolytes are required to substitute for a portion of the inorganic osmolytes (i.e. Na^+, Cl^-, K^+) accumulated in the embryo during recovery from acute volume decreases. If the inorganic osmolytes remain in the cell at too high a level for prolonged periods, they have a deleterious effect on embryos due to high intracellular ionic strength.

Studies in our lab have found that, as in somatic cells, acute cell volume decreases in preimplantation embryos are regulated by the RVI system, as described above. Early preimplantation mouse embryos respond to cell volume decreases by activating NHE1 in concert with AE exchangers. The role of Na^+/H^+ exchangers in volume regulation was confirmed by exposing embryos to hypertonic solutions (of 310 to 500 mOsM), which led to an instant volume decrease and subsequent pH_i increase due to NHE activation. NHE1 was clearly implicated as the isoform regulating cell volume since pH_i increase and recovery from cell volume decrease was blocked by removal of Na^+, or the addition of 1 mM amiloride or 1 μM cariporide into the culture media (Zhou and Baltz, 2012). Those experiments were done in the absence HCO_3^- and in atmospheric CO_2, to block HCO_3^-/Cl^- exchanger activity that would counter alkalosis, and thus reveal the NHE-mediated pH_i increase. In the presence of HCO_3^- and CO_2, HCO_3^-/Cl^- exchange is activated secondary to NHE1 activation (by the increased pH_i) during volume decrease (Humphreys et al., 1995; Jiang et al., 1997; Zhou and Baltz, 2012), resulting in very small net shift in pH_i. Addition of a broad spectrum AE inhibitor DIDS to HCO_3^- containing media led to a robust pH_i increase, confirming the activity of the HCO_3^-/Cl^- exchanger. Thus it was concluded that mouse preimplantation embryos do possess a functional RVI volume regulatory mechanism, in which NHE1 is stimulated by acute volume decrease, increasing internal pH_i, that in turn

stimulates the secondary activation of HCO_3^-/Cl^- exchanger to ensure the influx of NaCl and water into the embryo to counteract the decrease in cell volume (Zhou and Baltz, 2012).

The mechanism for NHE1 activation by cell volume decrease is largely unknown, however some portions of the pathway have been identified. While NHE1 is not directly phosphorylated upon a cell volume decrease, several tyrosine kinases are activated and phosphorylated during cell volume decrease (Hoffmann et al., 2009; Zhou and Baltz, 2012). In preimplantation mouse embryos, Janus kinase 2 (JAK2 tyrosine kinase) is activated by cell volume decrease (Zhou and Baltz, 2012). Increased JAK2 phosphorylation is required for the proper activation of NHE1 by decrease cell volume, where JAK2 activates NHE1 through phosphorylating and activating Calmodulin (CaM), which then binds to and stimulates NHE1 activation, while expression of a dominant negative JAK2 or use of pharmacological JAK2 or CaM inhibitors block NHE1 activation (Zhou and Baltz, 2012).This suggests that perhaps the role of NHE1 in PI embryos is to regulate its volume prior to implantation into the uterus.

Objective and Specific Aims

Intracellular pH affects many cellular mechanisms including gene expression, cellular metabolism, calcium homeostasis, cell volume regulation, cell proliferation and cell death. Two general pH_i - regulatory mechanisms used by most cells are the bicarbonate-chloride exchangers of the AE gene family that regulate against intracellular alkalosis (Alper et al., 2002), and the sodium-hydrogen antiporters of the NHE family that regulate against acidosis (Orlowski and Grinstein, 2004). Sodium hydrogen exchangers became of interest to experts in the study of fertilization upon Johnson et al.'s discovery of the considerable intracellular pH increase in eggs of sea urchins immediately following fertilization (Johnson and Epel, 1976). This rapid increase in pH was attributed to the activation of the sodium hydrogen-exchanger, which imported sodium ions into the cell in exchange for hydrogen ions.

In mammals, no such rapid increase in intracellular pH after fertilization has been observed, but the antiporter has been implicated in internal pH regulation of pre-implantation embryos (Steeves et al., 2001). A study of the HCO_3^-/Cl^- antiporter determined that it is present in all preimplantation stage embryos and is required for proper embryo development. Determining which of the five NHE plasma membrane isoforms are present in preimplantation embryos and what role if any each isoform plays in pH regulation and embryo development will increase our basic understanding of embryo physiology and developmental potential.

Objective: The overall objective of this study is to improve our understanding of preimplantation embryo physiology by focusing on five known plasma membrane Na^+/H^+ exchangers and their role in pH_i regulation and embryo development.

Specific Aim #1: *To determine which of the NHE isoforms regulates pH_i at each stage of preimplantation embryo development.*

Multiple NHE isoforms were shown to be expressed in mammalian oocytes including NHE1, NHE3 and NHE4 (FitzHarris et al., 2007). Studies of various mouse strains have shown that NHE1 was expressed at all preimplantation stages, while another isoform NHE3 and/or NHE4 was also proposed to be active based on the characteristics of recovery from acidosis (Barr et al., 1998; Harding, 2002), however no conclusive quantitative expression or activity profiles have been compiled. According to a study by Barr et al., although no NHE3 mRNA transcripts were observed past the early PI stage, the protein was present within the blastocyst and found in the basal part of polarized TE cells. In contrast, NHE1 protein was reportedly localized to the apical surface of the TE cells in the blastocyst (Barr et al., 1998). To elucidate which NHE isoforms contributed to the regulation of pH_i in QS mouse embryos, Harding et al. (Harding et al., 2002) used the NHE1-selective inhibitor HOE-694. They interpreted their results to indicate that there were several NHE isoforms (proposed as NHE1 and NHE3) operating in the 2-cell embryo. However, their results were not consistent with the known effective concentration range for HOE-694 inhibition of NHE1 and NHE3. Their results could also be interpreted as suggesting that only one NHE isoform was actually present. Thus we aimed to systematically determine which isoforms were expressed and active in preimplantation mouse embryos through the morula stage, hypothesizing that at least one of the three

expressed NHE isoforms will be responsible for regulating the recovery from acute induced acidosis in preimplantation embryos.

Specific Aim #2: *Determine which of the isoforms aids in embryo development during prolonged exposure to an acidic environment*

Zhao et al. had shown in their study of the bicarbonate/chloride exchangers that inhibition of these isoforms at elevated external pH lead to alkalization of the internal pH of the blastomeres and ultimately the death of embryos (Zhao et al., 1997). Thus we hypothesized that the decrease of external pH will lead to a similar effect, whereby inhibition of the active NHE isoform will inhibit embryo development at lower external pH, due to the acidification of its internal environment.

Materials and Methods

1. Chemicals and Solutions

Embryo culture media components were obtained from Sigma (St. Louis, MO, USA) and are listed in Table 2. Media components were embryo grade or cell culture grade. Other chemicals and reagents used and their sources are listed in Table 3.

1.1. Oocyte and embryo culture and handling media

Culture media were based on KSOM (K^+ supplemented Simplex Optimized Medium) developed by Lawitts and Biggers (Lawitts and Biggers, 1993). To obtain and manipulate gametes and embryos, Hepes-buffered KSOM (H-KSOM) media was used, wherein 21 mM (of 25 mM) $NaHCO_3$ in KSOM was replaced by equimolar Hepes (and pH adjusted with NaOH to 7.4). Refer to Table 4 for more details.

1.2. Media for pH_i measurements

Bicarbonate-CO_2 buffered media used for pH_i measurements were based on KSOM, with lactate concentration reduced to 1.0 mM (from the original 10 mM) and replaced with equimolar amounts of NaCl (total 104 mM), equilibrated with CO_2/air mixtures as specified and with BSA omitted to ensure embryo adhesion to the microscope chamber cover slip (Steeves et al., 2001). This medium was designated p-KSOM. In experiments where intracellular acidosis was induced, a medium containing 25 mM NH_4Cl was employed (replacing 25 mM NaCl for a final concentration of 79 mM), this medium was designated NH_4-KSOM. For sodium-free p-KSOM (labeled $0Na^+$-KSOM), NaCl was replaced with 104

mM choline chloride, and Na^+ pyruvate, Na^+ lactate and $NaHCO_3$ were replaced by K^+ pyruvate, lactic acid and choline HCO_3^-, respectively (for more details refer to Table 4).

For bicarbonate-free media used for most experiments to determine the role of Na^+/H^+ exchanger in recovery from induced acute acidosis, a modified form of H-KSOM was used in which lactate was reduced to 1.0 mM and all $NaHCO_3$ replaced with equimolar of NaCl (for total of 108 mM). Intracellular acidosis was achieved using a medium containing 25 mM NH_4Cl (replacing 25 mM NaCl). This medium was labeled NH_4-H-KSOM (Table 4). The sodium-free version of this medium was prepared by replacing NaCl with equimolar choline chloride, sodium pyruvate with potassium pyruvate and sodium lactate with lactic acid, with final concentration of ~0.04 mM Na^+, with BSA excluded from all media, and designated $0Na^+$-H-KSOM (FitzHarris et al., 2007). The pH of all Hepes-buffered media was adjusted to 7.4 using NaOH, while in Na^+-free media KOH was employed.

Calibration solutions used in pH_i measurements contained 100 mM KCl, 25 mM NaCl, 21 mM Hepes, 75 mM sucrose, 10 μg/mL nigericin and 5 μg/mL valinomycin. Solutions were adjusted to approximately pH 6.7, 7.0, 7.4, and 7.8 with NaOH or KOH before the addition of nigericin or valinomycin, which were added immediately before calibration (Thomas et al., 1979).

Table 2: List of media components and their source.

Name of chemical or compound	Source
4-(2-hydroxyethyl)-1-piperazineethane-sulfonic acid (HEPES)	Sigma
Ammonium chloride (NH4Cl)	Sigma
Bovine serum albumin (BSA)	Sigma
$CaCl_2 \cdot 2H_2O$	Sigma
Choline Cl	Sigma
EDTA (tetra Na)	Sigma
Glucose	Sigma
L-Glutamine	Sigma
K penicillin G	Sigma
KCl	Sigma
K pyruvate	Sigma
$KH_2PO_4 \cdot 7H_2O$	Sigma
DL-Lactic acid	Sigma
$MgSO_4$	Sigma
Na lactate	Sigma
Na pyruvate	Sigma
NaCl	Sigma
$NaHCO_3$	Sigma
Potassium hydroxide (KOH)	Sigma
Sodium Hydroxide (NaOH)	Sigma
Streptomycin SO_4	Sigma
Sucrose	Sigma

Table 3: List of chemicals

Chemical Name	Description/ Uses	Supplier
DIDS (4,4'-diisothiocyanatostilbene-2,2'-disulfonic acid, disodium salt)	AE and NDBC inhibitor	Invitrogen
H_2DIDS (4, 4'-diisothiocyanatodihydrostilbene-2,2'-disulfonic acid, disodium salt)	AE and NDBC inhibitor Not fluorescent under UV illumination	Invitrogen
SNARF-1-AM (5-(and-6)- carboxyseminaphthorhodafluor-1-acetoxymethyl ester)	pH-sensitive fluorophore	Molecular Probes
5-(N-ethyl-N-isopropyl) amiloride, hydrochloride (EIPA)	Na^+/H^+ antiporter inhibitor	Sigma
5-5-dimethyl-2-4-oxazolidinedione (DMO)	Non-metabolizable weak acid Used to decrease pH_i	Sigma
Amiloride, hydrochloride hydrate	Na^+/H^+ antiporter inhibitor	Sigma
Cariporide (4-isopropyl-3-methylsulphonylbenzoyl-quanidine methanesulphonate, HOE642)	NHE1 specific inhibitor	Aventis Pharma
Chorionic gonadotropin (hCG)	Used to trigger ovulation in mice	Intervet Canada
Dimethyl sulfoxide (DMSO)	Used to dissolve chemicals for stock solutions	Sigma
Ethyl Alcohol, 95%	Used to dissolve chemicals for stock solutions	Commercial Alcohols
Pregnant Mare Serum Gonadotropin (PMSG)	Used to stimulate follicle development	Intervet Canada
Hyaluronidase	Enzyme used to disperse cumulus cells	Sigma
Nigericin, sodium salt	H^+/K^+ exchanger Used for pH_i calibration	Sigma
S3226 (3-[2-(3-Guanidino-2-methyl-3-oxo-propenyl)-5-methyl-phenyl]-N-isopropylidene-2-methyl-acrylamide dihydrochloride)	NHE3 and NHE1 inhibitor	Aventis Pharma
Valinomycin	K^+ ionophore Used for pH_i calibration	Sigma

Table 4: Media for pH_i measurements and pH experiments (concentrations stated in mM).

Component	H-KSOM	pH-KSOM	$0Na^+$-H-KSOM	NH_4-H-KSOM	KSOM	p-KSOM	$0Na^+$-KSOM	NH_4-KSOM
NaCl	95	108	--	83	95	104	--	79
KCl	2.5	2.5	2.5	2.5	2.5	2.5	2.5	2.5
KH_2PO_4	0.35	0.35	0.35	0.35	0.35	0.35	0.35	0.35
$MgSO_4$	0.2	0.2	0.2	0.2	0.2	0.2	0.2	0.2
Na lactate	10	1	--	1	10	1	--	1
Glucose	0.2	0.2	0.2	0.2	0.2	0.2	0.2	0.2
Na pyruvate	0.2	0.2	--	0.2	0.2	0.2	--	0.2
$NaHCO_3$	--	--	--	--	25	25	25	25
Hepes	21	21	21	21	--	--	--	--
$CaCl_2$	1.7	1.7	1.7	1.7	1.7	1.7	1.7	1.7
Glutamine	1	1	1	1	1	1	1	1
EDTA (tetra Na)	0.01	0.01	0.01	0.01	0.01	0.01	0.01	0.01
K penicillin G	0.16	0.16	0.16	0.16	0.16	0.16	0.16	0.16
Streptomycin SO_4	0.03	0.03	0.03	0.03	0.03	0.03	0.03	0.03
NH_4Cl			--	25			--	25
Choline Cl			108				104	
Lactic acid			1				1	
K pyruvate			0.2				0.2	
Choline HCO_3							25	

2. Animals, gamete and embryo manipulation

2.1. Animals and super-ovulation

The Animal Care Committee of the Ottawa Hospital approved all experimental protocols involving animals. Female mice of the CF1 strain (acquired from Charles River, St-Constant, PQ, Canada) were used to obtain oocytes, eggs, and preimplantation embryos. This strain was selected because it was successfully used in previous studies of pH regulation in oocytes and PI stage embryos (FitzHarris et al., 2007; Steeves et al., 2001; Zhao and Baltz, 1996). Female mice were super-ovulated using equine chorionic gonadotropin (eCG, or pregnant mare's serum gonadotropin – PMSG, which is the designation used here), to mimic follicle-stimulating hormone (FSH) for the production of a maximal number of antral follicles. To circumvent the release of endogenous luteinizing hormone (LH) in response to PMSG, which is estimated to occur 50 – 55 hr post PMSG injection, and ensure a synchronized oocyte population and maximal numbers at ovulation, human chorionic gonadotropin (hCG) was used 47 hr post PMSG injection to induce oocyte maturation and ovulation, as would LH *in vivo* (Hogan, 1994). Animals were maintained on a 12 hr light (7am to 7pm) and 12 hr dark cycle (7pm to 7am). At 4:00 pm, 5 IU PMSG was administered via an intraperitoneal (IP) injection, and 47 hr later the mice were IP injected with 5 IU hCG and mated overnight with BDF1 males (Charles River; 8 – 30 weeks old). To collect zygotes and gametes, animals were sacrificed by cervical dislocation at appropriate times (Hogan, 1994), this method is favored over the (CO_2)-induced asphyxia for it avoids the lowering of the animals normal internal pH.

2.2. Oocyte collection

Female mice were primed with PMSG 45 – 47 hr prior to gathering GV oocytes. The ovaries were removed and mechanically homogenized using a razor blade. The minced tissue was then transferred to H-KSOM media containing 300 μM dbcAMP to prevent release from meiotic arrest and germinal vesicle break down (Cho et al., 1974; Phillips et al., 2002). Cumulus oocyte complexes (COC) were then collected and transferred to wash drops, where the cumulus cells were removed from the GV oocytes via a narrow-bore pipette. GV oocytes were kept in media containing dbcAMP prior to use to prevent spontaneous GVBD, unless otherwise stated.

2.3. Egg and embryo collection

In vivo matured MII oocytes (unfertilized eggs) were collected 15 hr post hCG injection. To obtain embryos, female mice were mated with BDF1 males, immediately following hCG administration and embryos were collected at ~22, 43, 56, 67, 76 and 91 hr post hCG corresponding to 1-, 2-, 4-, 8-cell, morula and blastocyst stages, respectively. Excised oviducts were flushed with H-KSOM and adherent cumulus (in MII and 1-cell embryos) removed by brief exposure with 300 μg/ml hyaluronidase (Hogan, 1994). To obtain later stage embryos, the oviduct together with the uterine horns were excised from the mouse, flushed with H-KSOM and embryos collected. Freshly collected embryos were used immediately for pH experiments, culture or flash frozen with liquid nitrogen to be used later for RNA extractions.

2.4. Blastocyst diameter

Two-cell embryos were collected and cultured for 72 hr until they reached the blastocyst stage. Measurements of the blastocoel diameters were made using a stereomicroscope Nikon Coolpix 4500 digital camera on a Zeiss IM35 microscope fitted with Hoffman optics. The focal plane was placed at the center of the embryo, to encompass the largest diameter. For calculation of the mean diameter, blastocysts were assumed to be perfect spheres, even though they were frequently somewhat ellipsoidal. In aspherical specimens, the diameters were estimated as averages between the shortest and longest measurements.

3. Molecular Biology Techniques

3.1. Nomenclature

pH_i-regulatory mechanisms are commonly designated by nomenclature based on their functional characteristics, many of which were defined before the discovery of the underlying proteins. Thus, the Na^+/H^+ exchanger activities designated NHE1 through NHE5 have been established to correspond to the proteins SLC9A1 through SLC9A5 (*Slc9a1-a5* genes). Similarly, sodium-dependent bicarbonate/chloride exchanger activity NDBCE corresponds to SLC4A8 (*Slc4a8*). Throughout, mRNA and proteins are indicated by their official SLC nomenclature, while functional activities are given their conventional designations.

3.2. Determination of NHE exchanger mRNA in embryos via RT-PCR

RNA extraction was performed using an RNAeasy Micro kit (Qiagen), and reverse transcription performed using a Retroscript kit (Ambion), according to manufacturers' instructions. RNA extraction and reverse transcription were performed upon groups of no fewer than 30 oocytes, eggs or embryos at a time. PCR (35 cycles at appropriate annealing temperatures listed in Table 5) was performed using HotStarTaq PCR kit (Qiagen) on an appropriate amount of cDNA template corresponding to 1.5 oocytes, eggs, or embryos. Kidney (*Slc9a*1, 2 and 4), liver (*Slc9a*3) and brain (*Slc9a*5) cDNA were used as positive controls. The amount of positive control tissue cDNA used was chosen to approximate that of 1.5 oocytes based upon measurement of total RNA content of control tissue RNA preparations, and the known total RNA content of one oocyte (~0.6 ng) based upon

spectrophotometric measurement (Ultraspec 2000, Pharmacia Biotech, Cambridge, England) (Sternlicht and Schultz, 1981).

Samples of the final drops of medium in which oocytes were washed were subjected to the same reverse transcription protocol and used as negative controls. Amplicons were visualized on a 1.7% agarose gel containing 0.13ng/ml ethidium bromide. Primer pairs were designed (OligoPerfect, Invitrogen, Carlsbad, CA, USA) using mouse mRNA reference sequences spanning exon-intron borders (Table 5). All products were of the predicted size according to their position on the gel, and the identities of products from all five primer pairs were confirmed by direct sequencing. PCR with primers for H2A histone family member Z (*H2afz*), a basic nuclear protein that is involved in determining the nucleosome structure of the chromosomal fiber and that has been shown to be very stably expressed in a well-established pattern during early developmental stages (from oocyte to blastocyst) (Mamo et al., 2007), was utilized to confirm correct RNA extraction, reverse transcription, PCR and loading. PCR was repeated on a minimum of three different sample preparations.

Quantitative RT-PCR was carried out using the LightCycler 480 SYBR Green I Master Mix (Roche Applied Science). A negative control (H_2O replacing cDNA template) and a positive control (liver, kidney or brain cDNA) were included in each run. As in RT-PCR we used a cDNA equivalent of 1.5 oocyte or embryo, and run for a minimum of 45 cycles at optimum annealing temperatures (as listed in Table 5). A range of 6 different temperatures was used to empirically determine the annealing temperature (i.e. T_m, T_m-1, T_m-3, T_m-5, T_m-6, T_m-7), where T_m is the lowest melting temperature of the primer set. T_a of the amplicons that produced a single clear band at the expected size (and confirmed by sequencing) was selected as the optimum annealing temperature for the selected primer set.

At the end of the run, melting-curve analysis was performed to confirm the PCR

product. Each sample was run in duplicates that were simultaneously amplified and the results averaged to constitute one independent repeat.

A standard curve was created using serial 10-fold dilutions of a known concentration of template from positive control organ tissue cDNA. The number of mRNA copies per embryo was determined using the absolute quantification method according to the manufacturer's instructions.

Table 5: Primers used for isoform-specific detection of NHE mRNA by RT-PCR

Primer	Sequence (5'-3')	T_a (°C)	Amplicon size (bp)	Accession number
Slc9a1	F: CACCAGTGGAACTGGACCTT R: AAGGTGGTCCAGGAACTGTG	55	372	NM_016981.1
Slc9a2	F: ATCACGGCTGCTATTGTCGTT R: GTGACCCCAGTGTCCACACACA	60	189	NM_001033289
Slc9a3	F: TATCTTCGCCTTCCTGCTGT R: GCTCTGAGATGTTGGCCTTC	60	191	NM_001081060.1
Slc9a4	F: TGTGTGTGGGCAGTGGAGTCAC R: GACTGATAGGGTGTGGGAGAAGCCA	60	204	NM_177084.3
Slc9a5	F: CCTCCCTGTTTGTGGTCAGT R: TATGGGAGATGTTGGCTTCC	55	235	NM_138858
H2afz	F: ACAGCGCAGCCATCCTGGAGTA R: TTCCCGATCAGCGATTTGTGGA	60	202	NM_138858

T_a - annealing temperature; F – forward; R- Reverse

4. Immunocytochemistry

4.1. Embryo fixation and whole-mount indirect immunofluorescence

Blastocysts and cumulus oocyte complexes (COC) were collected and washed with phosphate buffered saline (PBS) for 5 min at room temperature. The cells were then fixed in 2% paraformaldehyde in PBS for 20 min at room temperature, followed by two 5 min washes in PBS at room temperature. Cells were then blocked with 0.01% Triton X-100 and 5% normal donkey serum (NDS) in PBS for 1 hr at room temperature followed by incubation with primary antibodies in antibody dilution buffer overnight at 4°C (1^{o} antibody diluted 1:100; ADB = 0.005% Triton X-100 + 1% NDS in PBS). After overnight incubation, the cells were washed four times for 15 min in ADB at 37°C. They were then incubated with fluorescently labeled secondary antibodies [diluted to 1:200; Alexa 594 goat α-mouse (Invitrogen, cat. A11032) or Alexa 594 goat α-rabbit (Invitrogen, cat. A11072)] in ADB, overnight at 4°C. To label cells for F-actin, embryos and COCs were incubated for 30 min at 37°C with Phalloidin-488 (1:40, Invitrogen Cat. No. A12382) in ADB, followed by three final 15 min washes in ADB at 37°C. Embryos were mounted in 5 μL Fluoro-Guard Antifade Mounting Reagent (Bio-Rad, Mississauga, Ontario, Canada) on glass slides. Fluorescence patterns were examined using confocal microscopy (Nikon Diaphot 200 with MRC-1024 Laser Sharp, BioRad, Life Science Group, Mississauga, ON, Canada).

Primary antibodies for NHE1 were rabbit polyclonal (H-160, Santa Cruz Biotech., Cat. No. SC28758), against epitope corresponding to AA656 – 815 in C-terminal of human cytoplasmic domain and rabbit polyclonal antibody (Abcam, Cat. No. AB67314), 17AA synthetic peptide from the center of human NHE1. NHE3 (H-170) rabbit polyclonal

antibody (Santa Cruz Biotech., Cat. No. SC28757) was used, against an epitope corresponding to amino AA665-834 mapping within a C-terminal cytoplasmic domain of NHE-3 of human origin. In addition, NHE3 mouse monoclonal antibody, clone 4F5 (Millipore, Cat. No. MAB3136), generated against fusion protein containing C-terminal 131AA of rabbit NHE3, was used.

4.2. Blastocyst differential staining

In order to distinguish between the inner cell mass (ICM) and the trophectoderm (TE) cells, we utilized a simplified method of differential blastocyst staining (Thouas et al., 2001). In brief, cultured blastocysts were first incubated in 500 µL of H-KSOM containing 1% Triton X-100 and 100 µg/mL propidium iodide for 5-10 seconds, until it was observed under the dissection microscope that the trophectoderm discernibly changed colour to red and slightly contracted. Immediately after, the embryos were transferred into a fixative solution of 100% ethanol with 25 µg/mL bisbenzimide (Hoechst 33258). The embryos were left in this solution overnight at 4^{o}C. The embryos were then mounted onto a microscope slide in a drop of SlowFade Antifade solution (Invitrogen, Carlsbad, CA, USA). The embryos were gently flattened using a glass cover slip and visualized under a standard fluorescent microscope for cell counting. Cell counting was performed on digital images obtained on a Zeiss fluorescence microscope fitted with an ultraviolet lamp and excitation filters (560 nm for red and 360 nm for blue), using Image J software with the cell-count plug-in (NIH, Bethesda, MD, USA).

5. Measurement of Intracellular pH

5.1. Intracellular pH measurements

Intracellular pH of embryos was measured using a quantitative imaging fluorescence video-microscopy system, as previously described in detail (Baltz et al., 1990; Phillips et al., 2000; Phillips et al., 1998; Steeves et al., 2001; Zhao and Baltz, 1996; Zhao et al., 1995). The pH-sensitive fluorophore carboxyseminaphthorhodafluor-1 (SNARF-1) was loaded into embryos by incubation with 5 μM SNARF-1-acetoxymethyl ester (SNARF-1-AM; Molecular Probes, Eugene, OR, USA) at 37^{o}C for 30 min in pH-KSOM (Figure 10). After SNARF-1 loading, the embryos were washed several times with pH-KSOM and placed into a temperature-controlled chamber with a glass coverslip bottom that holds up to 2.5 mL of liquid (model PDMI-2 with TC202A controller, Harvard Apparatus, South Natick, MA, USA). The controller was set to maintain embryos at 37^{o}C (±0.5^{o}C). The chamber was outfitted with inlet and outlet tubes to allow for gas-phase control (when using bicarbonate/CO_2-buffered media). Tubes were also provided for solution changes (Baltz and Phillips, 1999). Solutions were changed with the aid of an automated syringe pump driving inflow (Sage model 362, ATI Orion, Thermo Fisher Scientific, Waltham, MA, USA) and vacuum aspiration for outflow (Thermo Scientific Air Cadet Vacuum Pump, Fisher Scientific, Pittsburg, PA, USA). Inflow and outflow was turned off except during solution changes, which took ~1 min.

Concurrent pH_i measurements were made on groups of embryos with data collected for each embryo individually. The fluorescence images were obtained using a Zeiss Axiovert 135 inverted epifluorescence microscope (Zeiss Canada, Toronto, ON) outfitted with a Photometrics CoolSnap ES camera (Photometrics/Roper Scientific, Tucson, AZ). Output

was to an image storage and quantification system running RatioTool software (Isee Imaging Systems, Raleigh, NC) on a Dell 380 computer with a Redhat Linux operating system (supplied custom-configured by Isee Imaging Systems). Excitation illumination was provided by a type 75XE 75 watt Xenon arc lamp using a LPS220 power supply (Photon Technologies International, Birmingham, NJ) with a monochometer (model 5010, Photon Technologies International) and an Optikon shutter (model VS35S27MO, Vincent Associates, Rochester, NY) connected to the microscope by a fiber optic cable. Emission wavelengths were selected through bandpass filters in a LEP filter wheel (model EM DC FW) with MAC5000 controller (Ludl Electronics, Hawthorne NY).

SNARF-1 is a ratiometric, pH-sensitive fluorophore, (with an excitation wavelength of 535 nm), whose emission intensity increases with increasing pH at the emission peak near 640 nm but does not change at its isosbestic point (a specific wavelength at which the total absorbance of a sample does not change during a chemical reaction or a physical change of the sample; in this case, it is the wavelength at which SNARF-1 fluorescence is independent of pH) that is near 600 nm (Figure 10B). Measurements were obtained at two emission wavelengths, 640 nm (pH sensitive) and 600 nm (pH insensitive), with the excitation set at 535 nm (Figure 10C). Ratiometric images were obtained using RatioTool by dividing each image at 640 by the paired image at 600, pixel by pixel, after subtracting the background for each to produce images whose values at each point in the oocyte or embryo depended essentially only on their internal pH. The timing of image acquisition during an experiment and the emission and camera settings were pre-programmed and controlled using RatioTool. The emission ratio for each oocyte or embryo was calculated by placing a region of interest over each and obtaining the average value for the ratio for each oocyte or embryo.

Emission ratios were calibrated to pH_i using calibration curves obtained by exposing the oocytes or embryos to calibration solutions containing 10 μg/mL nigericin and 5 μg/mL valinomycin with 100 mM K^+. Nigericin a K^+/H^+ exchanger, leads to equilibration of both K^+ and H^+ across the cell membrane. Valinomycin (K^+-selective ionophore) was included to ensure the complete K^+ gradient collapse. Thus, when the external and internal K^+ concentrations are equilibrated, pH_i will have the same value as that of the external calibration solution. Using four different calibration solutions of known pH, a calibration curve was obtained for embryos at the end of an experiment, at least weekly. The emission ratio was essentially linearly related to pH in the selected pH range (pH 6.6-8.1) as shown in an example calibration curve (Figure 10D).

In brief, calibration experiments were carried out as following: a solution with the highest pH (30 mL out of 40 mL total solution, with 10 mL reserved) was introduced into the chamber and the oocytes or embryos exposed to it for 7 min to let the pH equilibrate. Following this equilibration period, five consecutive readings at 7 sec intervals were obtained. The solution was then changed to the next lower pH calibration solution in the sequence and the procedure was repeated three more times. Using the reserved 10 mL of each solution (heated to 37^{o}C to be the same temperature as the media in the chamber) the pH of each solution was measured using a standard pH meter and used for constructing the calibration curve.

Figure 10: SNARF-1 fluorescence.

(A) *AM loading.* SNARF-1 is available as an acetocymethyl (AM) ester derivative. In the AM form, this fluorophore is membrane permeable and the dye is not fluorescent. Once the fluorophore enters the cell, the AM group is cleaved by intracellular esterases, making the dye fluorescent and membrane impermeable [adapted from (Han and Burgess, 2010)]. **(B)** *Fluorescent emission spectrum for SNARF-1, at excitation wavelength of 535nm.* Fluorescence emission is maximal at 640nm and increases with increasing pH. The isosbestic point (pH independent wavelength) is observed at 600 nm and used for ratiometric imaging (Haugland et al., 1996). **(C)** *Schematic diagram of SNARF-1, a pH_i sensitive fluorophore that is used for measuring embryo pH_i.* SNARF-1 is excited at 535 nm and emission is detected at two wavelengths - 640 nm (pH sensitive) and 600 nm (pH insensitive). Ratiometric analysis is calibrated to pH_i, by dividing the intensities of the images at the two wavelengths 640 nm/600 nm. **(D)** *A sample of SNARF-1 calibration curve* (for 2-cell stage embryos in pH-KSOM media).

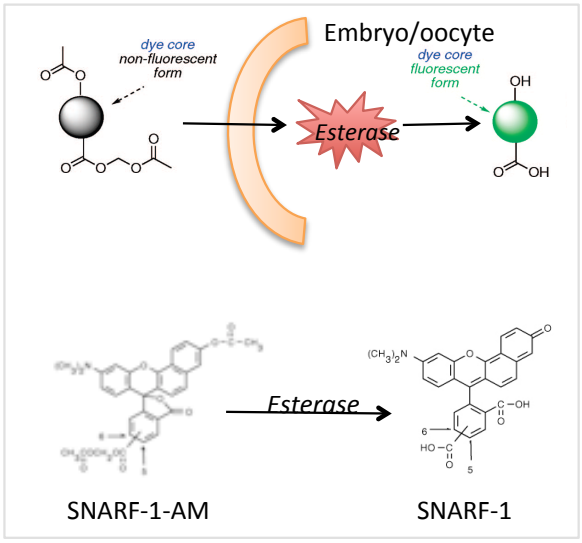
dye core
non-fluorescent
form
Embryo/oocyte
dye core
fluorescent
form
Esterase
OH
OH
Esterase
SNARF-1-AM
SNARF-1

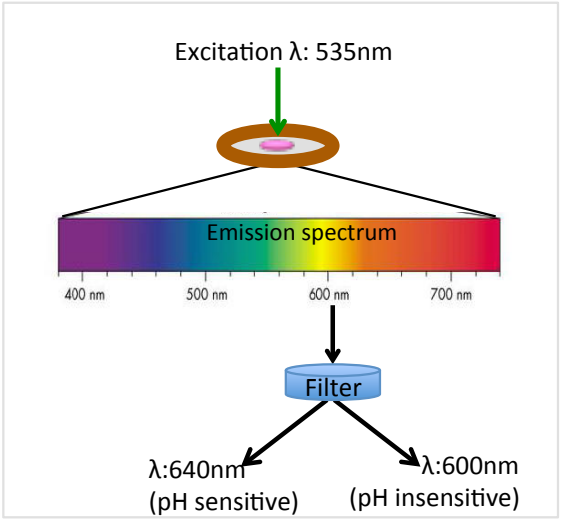
Excitation λ: 535nm
Emission spectrum
400 nm
500 nm
600 nm
700 nm
Filter
λ:640nm
(pH sensitive)
λ:600nm
(pH insensitive)

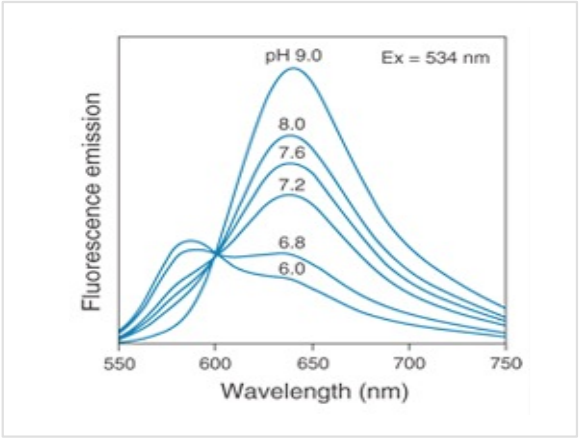
pH 9.0
Ex = 534 nm
8.0
7.6
7.2
6.8
6.0
Fluorescence emission
550
600
650
700
750
Wavelength (nm)

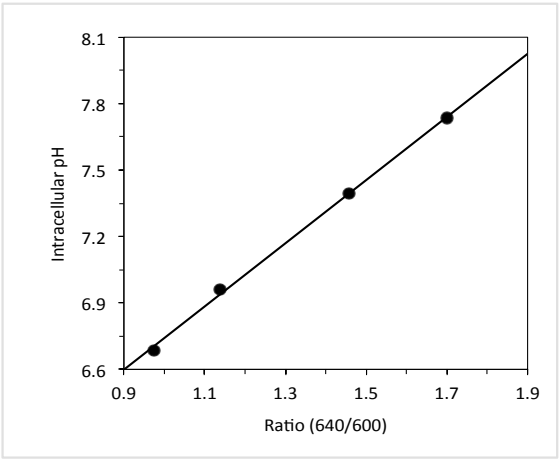
8.1
7.8
7.5
7.2
6.9
6.6
Intracellular pH
0.9
1.1
1.3
1.5
1.7
1.9
Ratio (640/600)

Figure 10

5.2. Probing Na^+/H^+ exchanger activity in PI embryos

To detect the presence of functional sodium hydrogen exchangers, an ammonium pulse assay (Boron and De Weer, 1976; Roos and Boron, 1981) was used for all stages of PI embryos. Normal medium was first present for 10 min, while images were obtained every 60 sec, to establish the baseline pH_i. Acidosis was then induced by a 10 min exposure to ammonium chloride (25 mM) in the chamber containing the embryos, with images obtained every 30 sec (Figure 11). This causes an immediate substantial increase in internal pH due to rapid influx of cell-permeant NH_3 molecules into the cell raising the internal pH of the embryo as the NH_3 equilibrates with intracellular H^+ to form NH_4^+. During the period in which NH_4Cl is present, external NH_4^+ slowly enters the cell, where it dissociates to NH_3 and H^+, thus causing a slow decrease in pH_i. Removal of NH_4Cl from the chamber results in the swift decrease in pH_i, resulting in net acidosis. This occurs due to the rapid efflux of NH_3 molecules out of the cell, including those that entered as NH_4^+, which leave their H^+ behind in the cell. Thus, the pulse of NH_4Cl results in a net acidification of the cell (Figure 11).

The medium introduced upon NH_4Cl washout was Na^+-free, to prevent any immediate Na^+-dependent recovery (e.g., by Na^+/H^+ exchange) and reveal the extent of net acidosis and any non-NHE-dependent recovery. After a 10 minute Na^+-free period, pH-KSOM or p-KSOM media (containing sodium) was reintroduced into the chamber to allow recovery by Na^+-dependent mechanisms such as Na^+/H^+ exchange, and the embryo response observed for 20 minutes with measurements at 30 sec intervals (Figure 11).

The rates at which embryos recovered from induced acidosis were compared by determining the recovery rates immediately following the Na^+-free period, by calculating the linear regression during the linear portion of the recovery within approximately the initial 5 min after pH-KSOM or p-KSOM addition (indicated by the red line in Figure 11). The first

one or two points following the solution change were not included in the regression in order to avoid the effects on apparent pH from perturbations during the solution change.

5.3. Inhibition of Na^+/H^+ exchangers with pharmacological agents

In order to inhibit recovery from acidosis due to NHE activity, we utilized several inhibitors: amiloride, cariporide and S3226. The inhibitors were added to the $0Na^+$ media, to ensure that the drug had the time to fully inhibit the transporter. Stock solutions were prepared by dissolving the drugs in DMSO, to obtain 1M amiloride, 10 mM cariporide and 10mM S3226. To inhibit the activity of NDBCE transporter, DIDS was used from a stock solution of 0.1M in DMSO. Control experiments contained 0.1% DMSO, to account for the DMSO used to dissolve the inhibitors. Stock solutions were kept in a dark and cool place. Immediately prior to use the inhibitor was diluted to a desired final concentration in 30 mL of pre-equilibrated, heated solution and introduced to the chamber with the aid of an automated syringe pump and vacuum pump aspiration as described above.

Cariporide (HOE 642), which is selective for NHE1 over both NHE3 and NHE4 by more than 1000-fold (Chambrey et al., 2001; Scholz et al., 1995; Schwark et al., 1998), was utilized to determine whether NHE1 activity played a role (Refer to Introduction section 4.1.2. Inhibitors, Table 1). Complete inhibition of NHE3 and NHE4 activities by cariporide occurs only in the 1000 μM range (Chambrey et al., 2001; Scholz et al., 1995; Schwark et al., 1998). Thus, cariporide was employed at each PI embryo stage to determine the dose-response of recovery over the range of 0-10 μM. The extent of maximal inhibition by cariporide was compared with that of amiloride, a general Na^+/H^+ exchanger inhibitor that should completely block activity of all plasma membrane NHE isoforms at the concentration

used (1mM) except NHE4, which could be only partly blocked at this concentration (Refer to Table 1).

The NHE3-selective inhibitor S3226 blocks rodent NHE3 activity with an IC_{50} on the order of 0.1 μM while blocking NHE1 activity at somewhat higher concentrations with an IC_{50} of about 3 μM (Schwark et al., 1998; Speake et al., 2005). To block recovery from acidosis in 2-cell embryos 0.1 μM S3226 was utilized to block only NHE3, 1.0 and 10 μM to block both NHE1 and NHE3 (Table 1). To determine whether any significant portion of the recovery from acidosis could be attributable to NHE3, we used cariporide and S3226 in concert and compared the rate of recovery to those obtained when each drug was used individually. Our rationale was that if NHE3 contributes to embryo recovery from acidosis, complete inhibition of NHE1 only with 10 μM cariporide would result in a higher recovery rate than that obtained with either 10 μM S3226 (a level that completely inhibits both NHE1 and NHE3) or in the presence of both cariporide and S3226 (at 10 μM each). To inhibit NHE4 activity, 5 mM amiloride was used with 2-cell and 8-cell stage embryos, for amiloride has a very high IC_{50} ~800 μM for NHE4 (Chambrey et al., 1997b; Chambrey et al., 2001).

5.4. Effect of changes in external pH

To determine the effect of a chronically acidic external environment on the internal pH of embryos, 2-cell embryos were loaded with SNARF-1-AM for 30 minutes and placed into pre-equilibrated media containing either 0.1% DMSO (vehicle control), 3 or 10 μM cariporide, 100 μM DIDS or 10 μM cariporide plus 100 μM DIDS together. These embryos were cultured for 3-5 h in an incubator at 37^0C, 100% humidity with 5, 10, 15, 20 or 25% CO_2 or with 10, 20, or 30 mM of the permeant weak acid 5-5-dimethyl-2-4-oxazolidinedione (DMO) at 5% CO_2. After the incubation period, embryos were transferred onto the heated

microscope stage and tubing was attached to the cover-lid and the dish perfused with appropriate CO_2% so as to maintain appropriate medium pH. The dish was equilibrated for 5 -10 minutes on the stage. After the background images were taken the embryos were brought into the field of view and 10 consecutive images at 30 sec intervals were taken (at 640 and 600 nm). The ratio was converted to pH values using the nigericin/high K^+ method, described above.

Figure 11: Assay for Na^+/H^+ exchanger (NHE) or Na^+-dependent HCO_3^-/Cl^- exchanger (NDBCE) activity (ammonium pulse assay).

The baseline pH_i was determined for 10 min, with images taken at 60 sec intervals. Intracellular acidosis was then achieved by a transient exposure (10 min) to NH_4Cl. Acidosis was maintained after NH_4Cl washout for 10 minutes with sodium free medium (0 Na^+), and then recovery from acidosis observed after introducing sodium-containing medium: pH-KSOM or p-KSOM buffered with 5% CO_2 (for 20 min). Introduction of NH_4Cl to the media, results in an instantaneous increase in internal pH due to the rapid influx of the weak base NH_3 into the embryos, followed by the slower entry of NH_4^+ (a weak base), which gradually decreases the pH_i. Upon the removal of NH_4Cl, NH_3 rapidly leaves the embryo, leaving behind the excess protons brought in by NH_4^+, resulting in rapid intracellular acidification. 0Na^+-media maintains acidosis due to lack of NHE (or NDBCE) activity. When NHE or NDBCE is active, the addition of Na^+ back to the medium results in a rapid increase in pH that is measured by extrapolating a linear regression line during the initial time of recovery from acidosis (indicated by a red line). The orange box indicates the image acquisition specifications, which represent #images/time interval (sec). When pharmacological agents (inhibitors) were utilized they were added to the sodium-free media at t=20 and maintained within the media until the conclusion of the experiment.

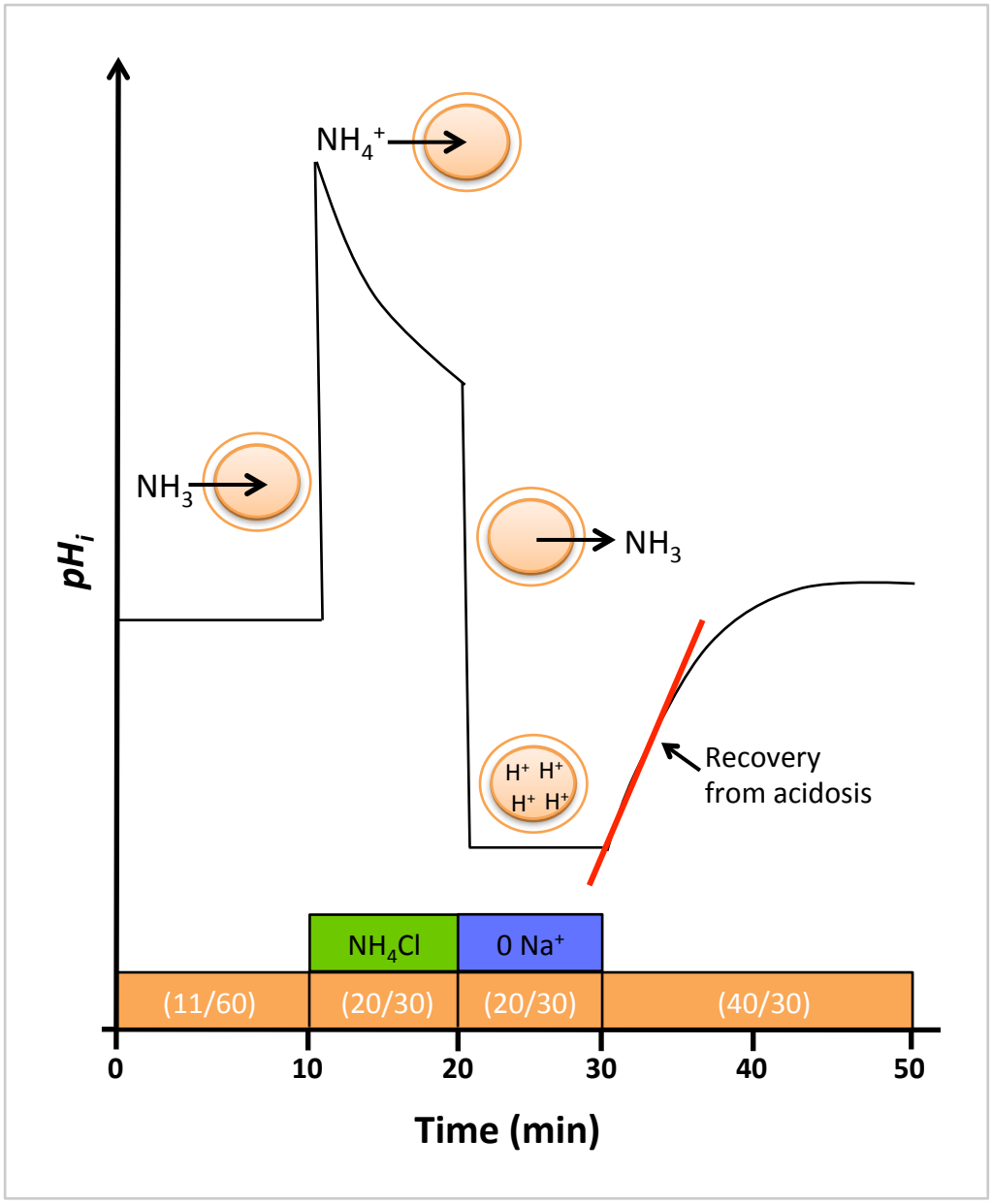
NH_4^+
NH_3
NH_3
H^+ H^+
H^+ H^+
Recovery
from acidosis
pH_i
NH_4Cl
0 Na^+
(11/60)
(20/30)
(20/30)
(40/30)
0
10
20
30
40
50
Time (min)

Figure 11

6. Embryo Cultures in Varying pH Conditions

6.1. Culture of embryos under varying CO_2 concentrations in the presence and absence of NHE1 inhibitor cariporide

To study the effect of chronic acidosis on embryo development, embryos were cultured *in vitro* in media of different pH from about 7.4 to 6.4. One- or 2-cell embryos were flushed from oviducts and placed into culture, and embryo development scored daily for a period of 3 days (2-cell embryos) or 4 days (1-cell embryos). For different CO_2 concentrations, modular chambers (Billups-Rothenburg, Inc., Del Mar, CA) were filled with the appropriate gas mixture before being sealed and placed in a 37°C incubator. Embryos were cultured in groups of 10 – 15 per 50 µL drop of KSOM under mineral oil (embryo-tested), which had been equilibrated in the incubator overnight (Hogan, 1994; Zhao et al., 1995) at 37^{o}C and 100% humidity. Chambers were replenished with the gas mixtures daily. CO_2 concentrations of 5, 10, 15, 20 or 25% CO_2 in pre-mixed gases (20% O_2, balance N_2) were used. To inhibit NHE1, 3 µM cariporide was added to the culture media. The control media contained 0.1% DMSO. Cultures were scored daily, and the number of embryos that reached the blastocyst stage (large cavity and visible inner cell mass) was recorded.

6.2. Embryo cultures with various DMO concentrations

A second method to decrease culture pH (and thus embryo pH_i) was performed by culturing 2-cell embryos in KSOM-media containing the weak acid DMO at 10, 20 or 30 mM DMO. DMO was added to KSOM culture medium in a conventional incubator (5% CO_2 in air, 37°C and 100% humidity). To inhibit NHE1, 3 µM cariporide was added to the

culture media; the control media contained 0.1% DMSO. The number of embryos that reached the blastocyst stage after 70-72 hr in culture was recorded.

6.3. Inhibiting NDBCE and NHE1 while culturing embryos with varying CO_2 concentrations

The media used for embryo cultures contained bicarbonate as a buffering agent, and thus the Na^+-dependent HCO_3^-/Cl^- exchanger could be active. NDBCE was inhibited with 100 mM DIDS (Molecular Probes, Eugene, OR, USA), alone or in concert with 10 μM cariporide to ensure complete inhibition of these exchangers. These cultures were carried out in organ dishes, with the center-well being filled with 500 μL pre-equilibrated KSOM and the outer-well with distilled-water to create a humid environment. To ensure full drug potency the media was changed daily and no mineral oil layer was present in these experiments. The embryos were cultured for ~72 hr at 37^{o}C and 100% humidity with 5, 10, 15 or 20% CO_2. The fully expanded blastocysts in each group were then collected and fixed for cell counts (refer to the above section *4.Blastocyst differential staining*). The non-fluorescent DIDS analog, H_2DIDS, was used for these experiments to avoid fluorescence interference of DIDS with cell counting that employed bisbenzimide.

7. Statistics

Plots were prepared using GraphPad Prism 5.00 (GraphPad Software, San Diego CA, USA). All data were expressed in mean±s.e.m. Statistical analysis of the data was performed by ANOVA followed by Tukey-Kramer multiple comparison test (when three or more were compared), or by Student's two-tailed t-test (to compare two groups), using Instat (GraphPad Software, San Diego CA, USA). N is used to indicate the number of independent repeats and n corresponds to the total number of embryos. In all cases, statistical tests were performed using the means of the N independent repeats, while n is provided for information only.

Results

1. Na^+/H^+ Exchanger Expression in Preimplantation Embryo

1.1. Slc9 transcript expression in preimplantation embryos

Ovarian oocytes (GV), ovulated eggs, and preimplantation embryos at the 1-, 2-, 4-, 8-cell, morula and blastocyst stages were examined by RT-PCR for the presence of mRNA coding for products of five known plasmalemmal Na^+/H^+ exchanger genes, *Slc9a1-a5* (corresponding to SLC9A1-5 proteins with NHE1-5 activities). Amplicons for *Slc9a1*, *Slc9a3* and *Slc9a4* were detected at the GV, egg and at several embryonic stages. However, no amplicons were detected for *Slc9a2* or *Slc9a5* at any stage. Figure 12A shows the results. *Slc9a1* transcripts appeared to be present in oocytes and throughout PI development, while *Slc9a3* amplicons were detectable in GV oocytes, eggs, and 1-cell embryos, and slightly at the 2-cell stage, while *Slc9a4* amplicons appeared to be present in GV oocytes, eggs, and 1-cell embryos.

Quantitative analysis of the mRNA expression patterns of *Slc9a1*, *Slc9a3* and *Slc9a4* by RT-Q-PCR revealed a similar pattern (Figure 12B), with transcripts of all three genes being relatively high in GV oocytes, eggs, and 1-cell embryos. Neither *Slc9a3* nor *Slc9a4* appeared to be present at appreciable levels from about the 4- to 8-cell stage onward. *Slc9a1*, however, may increase expression slightly in blastocysts. A ubiquitously expressed gene, *H2afz* (Histone H2A family member Z), whose stable expression pattern in PI embryos was previously validated (Jeong et al., 2005; Mamo et al., 2007) was used as a control (Figure 12C). However, since no transcript has yet been identified that remains constant throughout

PI development, *H2afz* was only used to confirm that the expected expression pattern was obtained, rather than for normalization.

1.2. Expression of NHE isoforms at a protein level

Based on the transcript presence, the candidates for NHE isoform activities mediating Na^+/H^+ exchange in PI embryos were NHE1, NHE3, and NHE4. It was suggested by previous studies with mouse blastocysts that NHE1 and NHE3 were found on the basolateral and apical surfaces of the TE cells, respectively (Barr et al., 1998; Kawagishi et al., 2004). In our pilot experiments with the western blot analysis, we were not able to detect any bands using protein extracted from 200 - 250 GV oocytes or 2-cell embryos with equivalent amounts of kidney protein used as a positive control (not shown). We then proceeded to detect protein localization within the blastocyst via immunofluorescence.

Several antibodies were tested for NHE1 and NHE3, which are currently available commercially (refer to Materials and Methods, *4.1 Embryo fixation and whole-mount Indirect Immunofluorescence*). Previous findings indicated that NHE1 and NHE3 were active in cumulus cells surrounding the GV oocyte (FitzHarris et al., 2007). We found here that antibodies to SLC9A1 (NHE1) and SLC9A3 (NHE3) localized to the cumulus cell membranes in cumulus-oocyte complexes (Figure 13A). However, clear membrane staining for SLC9A1, whose NHE1 activity is present in GV oocytes (FitzHarris et al., 2007), was not consistently detectable in the oocyte within the complex, nor was there any membrane staining in isolated GV oocytes (not shown). Previous attempts in our lab to stain for the protein within 1-cell and 2-cell embryos have also been unsuccessful (C. Zhou and J.M. Baltz, unpublished). In blastocysts, there was occasional staining with a subset of the antibodies tried, which appeared similar to staining obtained in previous reports, where

staining was observed in the membrane of some TE and ICM cells. However, no polarized, consistent staining was achieved by any antibodies utilized in this study. In contrast, we were able to detect other membrane proteins such as the Na^+/K^+ ATPase α subunit with the same protocol (not shown). Thus we concluded that perhaps PI embryos before the blastocyst stage have levels of NHE protein in their membrane that are below detectable levels.

Figure 12: Expression of *Slc9* NHE family Na^+/H^+ exchanger mRNA.

(A) *Conventional RT-PCR of Slc9a1-a5* (NHE1-5) *and a control gene H2afz*. The lane markings indicate positive control tissue (+), negative control (-), GV oocytes (GV), MII eggs (E), 1-cell to 8-cell embryos (1C-8C), morulae (M), and blastocysts (B). Lanes at far right and left are size markers. Amplicons were confirmed by direct sequencing. The results shown here for GV oocytes are consistent with those previously reported by FitzHarris et al. (FitzHarris et al., 2007). **(B)** *Quantitative RT-PCR of Slc9a1* (NHE1)*, Slc9a3* (NHE3) and *Slc9a4* (NHE4*), as indicated in panels, for in vivo-derived oocytes and PI embryos.* NHE1 exhibited an expression pattern typical for a constitutively expressed message in PI embryos, with a decrease at the 2- to 4-cell stage (during the maternal-to-zygotic transition) followed by apparently increased expression, although the increase at the blastocyst stage was small. NHE3 and NHE4 appeared to be exclusively of maternal origin, with essentially no mRNA detected by the blastocyst stage. Purified, sequenced amplicon was used to quantitate NHE1, NHE3 and NHE4 message and convert to number of transcripts. Each bar represents the results of triplicate independent mRNA isolations (mean ± SEM). Bars not sharing letters were significantly different ($P<0.01$ by ANOVA). **(C)** *Expression level of H2afz in same samples shown in (B) normalized relative to eggs (arbitrarily set to 1).* The expression pattern is essentially identical to that previously reported as the reference pattern (Mamo et al., 2007). Figure originally published in Siyanov and Baltz (2013).

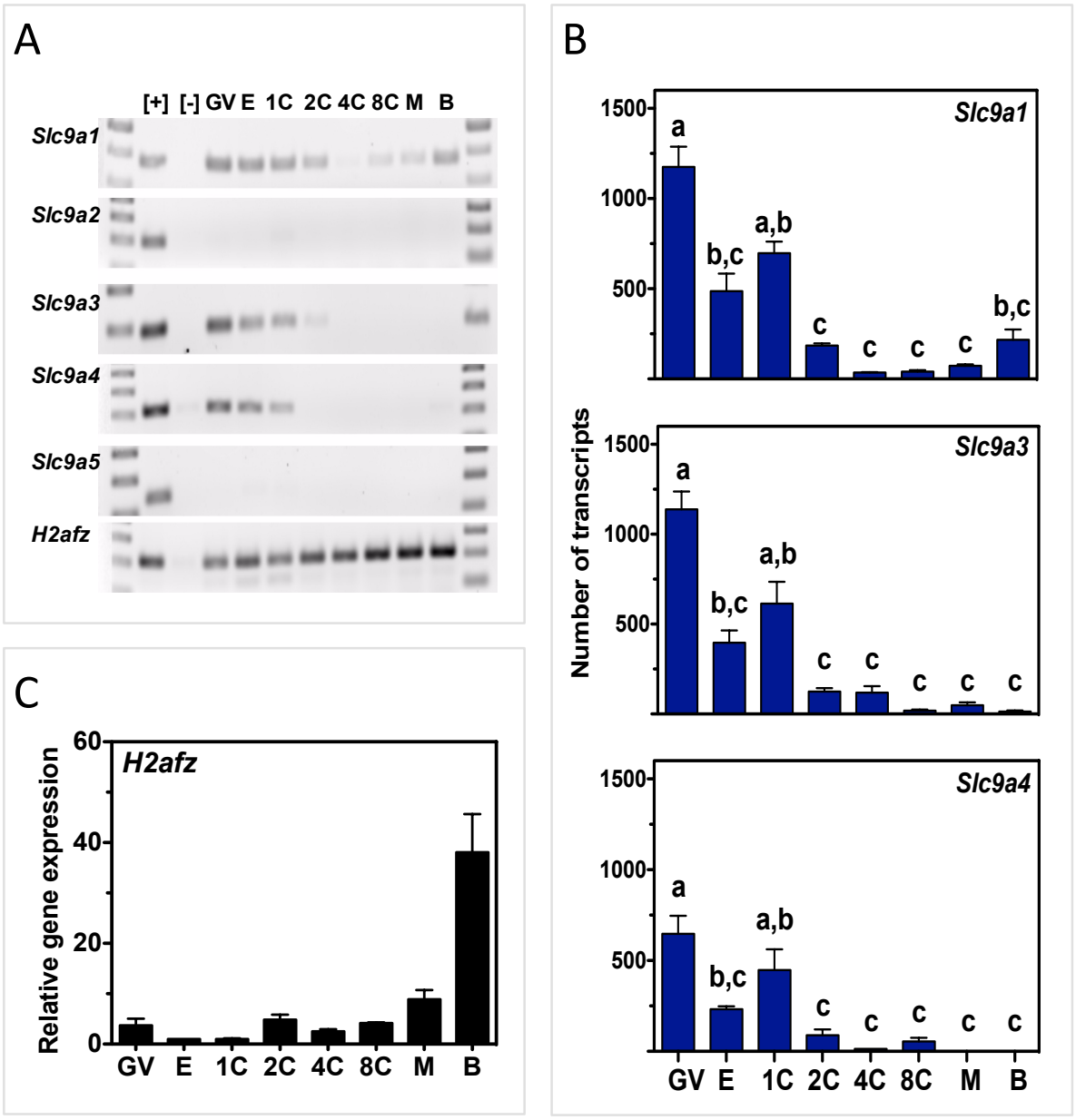
A
[+] [-] GV E 1C 2C 4C 8C M B
Slc9a1
Slc9a2
Slc9a3
Slc9a4
Slc9a5
H2afz
B
Slc9a1
Slc9a3
Slc9a4
Number of transcripts
1500
1000
500
a
b,c
a,b
c
b,c
GV E 1C 2C 4C 8C M B
C
H2afz
Relative gene expression
60
40
20
0
GV E 1C 2C 4C 8C M B

Figure 12

Figure 13: Localization of NHE1 and NHE3 (SLC9A1 and SLC9A3) proteins in freshly collected (A) mouse cumulus-oocyte complexes and (B) blastocyst stage embryos.

(A) Confocal microscopic imaging of mouse cumulus-oocyte complex was used after permeabilization and incubation with antibodies to NHE1 and NHE3. DNA was visualized with Hoechst 33258 (green). Both NHE1 and NHE3 showed a distinct localization to the cell membrane in granulosa cells. **(B)** Immunofluorescence imaging localization pattern of NHE1 and NHE3 in blastocysts. F-actin labeled with Alexa Fluor 488 Phalloidin (green) was used to visualize blastocyst embryo cell structures. Two different types of primary antibodies were used for each isoform, diluted 1:200 and obtained from (*a)* NHE1 rabbit IgG polyclonal antibody (SC28758) (*b)* NHE1 rabbit IgG polyclonal antibody (AB67314), *(c)* NHE3 (H-170) rabbit IgG polyclonal (SC28757) and *(d*) NHE3 mouse MBP monoclonal antibody, clone 4F5 (MAB3136). Scale bar, 50 μm.

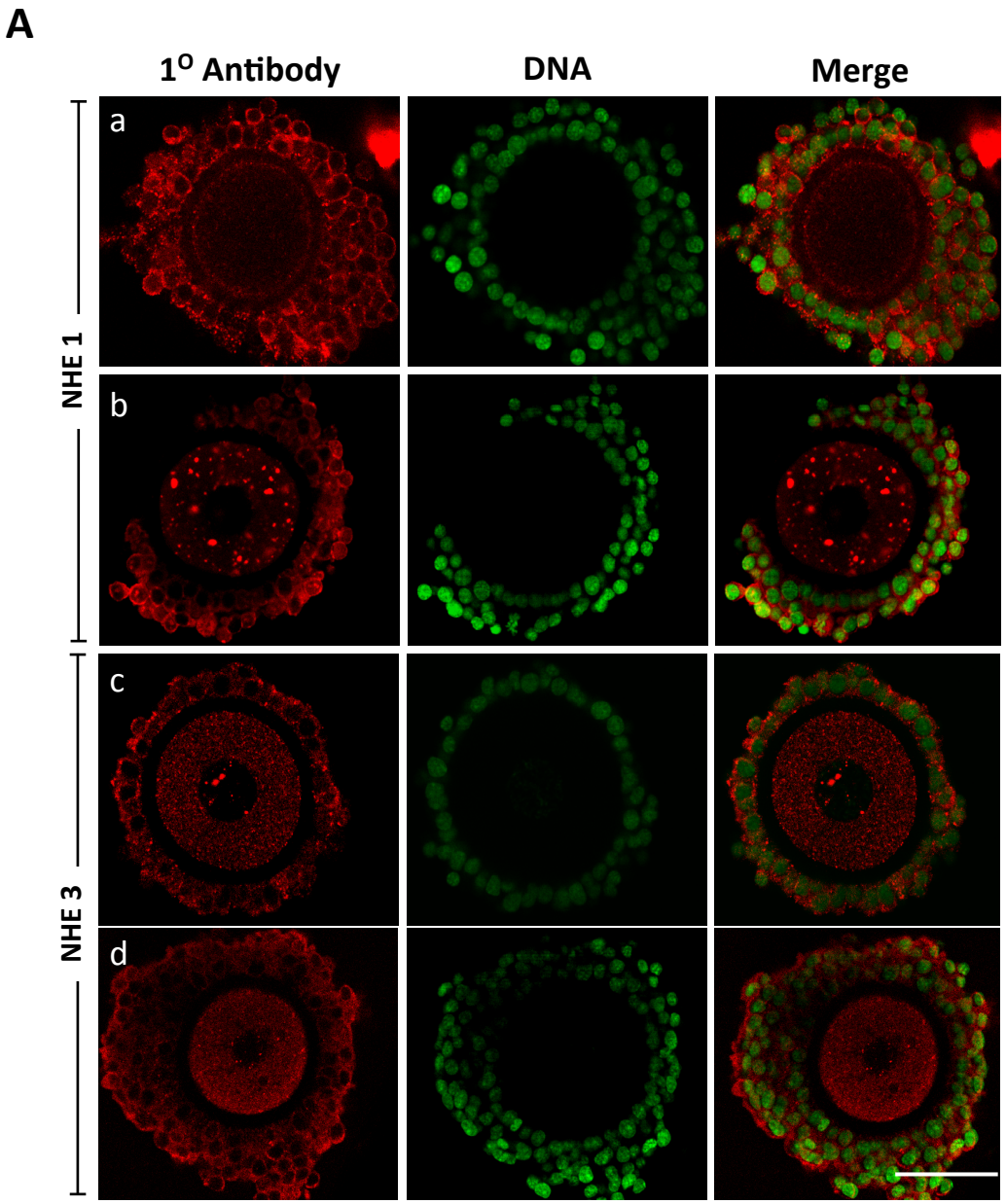

Figure 13A

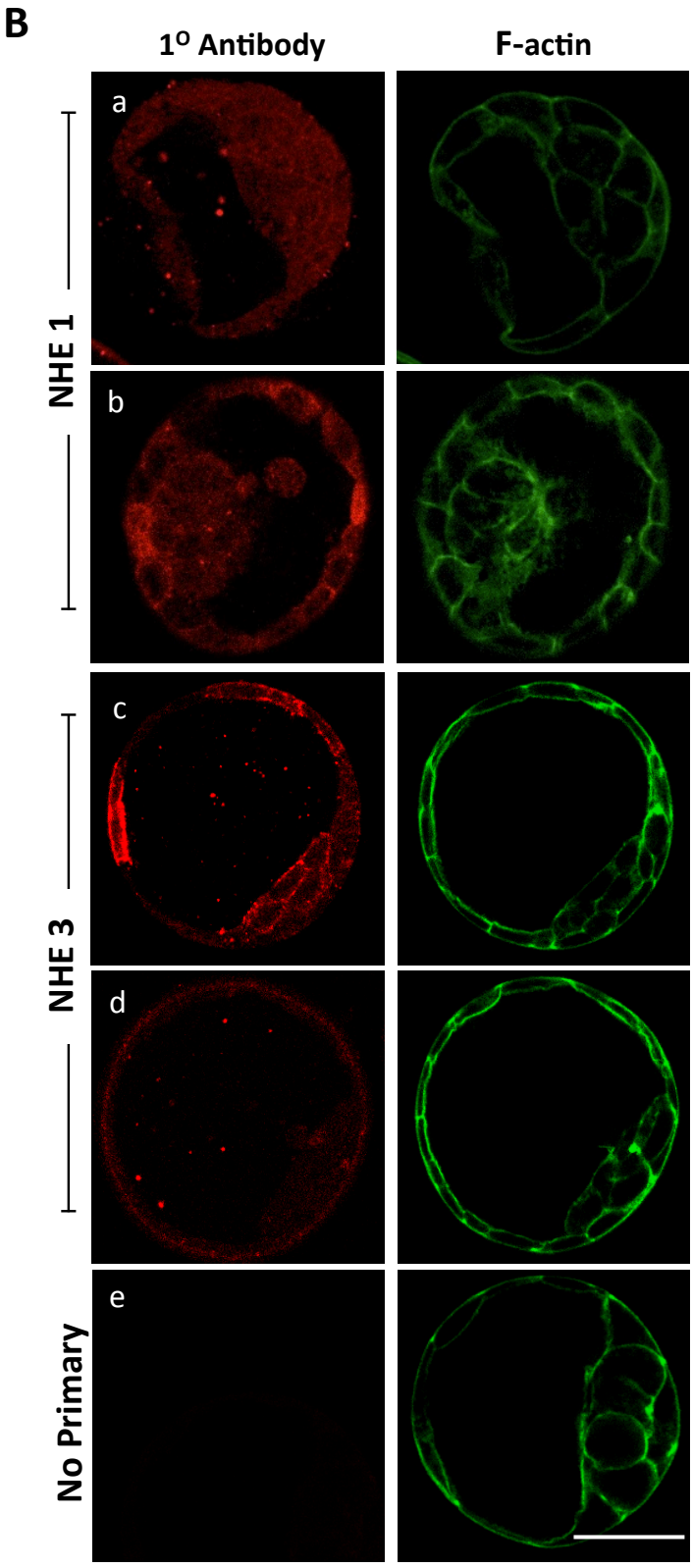

Figure 13B

2. Presence of Functional Na^+/H^+ Exchange During Embryo Development

To determine if the Na^+/H^+ exchanger is active within the PI embryo, we utilized the ammonium pulse assay and bicarbonate depleted media (refer to Materials and Methods, Figure 11). Briefly, net intracellular acidosis was induced by exposing 2-cell embryos to NH_4Cl (25 mM) for 10 min and then washing it out with Na^+-free medium (to confirm that subsequent recovery from acidosis was sodium dependent). Furthermore, to ensure that the observed recovery was solely due to NHE activity (rather than the Na^+ dependent HCO_3^-/Cl^- exchanger) all media were bicarbonate depleted. Relatively little recovery occurred in the Na^+-free medium (0.007 ± 0.001 pHU/min), but upon re-introduction of Na^+, a rapid increase in pH_i was observed (0.089 ± 0.015 pHU/min) that restored pH_i to approximately its baseline level (Figure 14A top panel).

To verify that the recovery was due to NHE activity, amiloride, a general Na^+/H^+ exchanger inhibitor, was employed. Amiloride at 1 mM concentration should completely block activity of all plasma membrane NHE isoforms except NHE4, which may be only partly blocked (refer to Table 1 in Introduction). In 2-cell embryos, amiloride decreased recovery from acidosis by approximately 4.7-fold when compared to the control (0.019 ± 0.001 vs. 0.089 ± 0.015 pHU/min; $P<0.001$; Figure 14B), consistent with suppression of NHE activity.

Figure 14: Recovery from induced acidosis in 2-cell mouse embryos by Na^+/H^+ exchangers.

(A) Representative traces of pH_i versus time during recovery from acidosis (left panel) and effect of the non-selective NHE inhibitor amiloride (right panel) on recovery. Each trace is a single experiment in which pH_i of a group of 2-cell embryos was assessed simultaneously by quantitative fluorescence imaging of SNARF1-loaded embryos. Symbols represent the mean pH_i of 5-10 embryos per experiment, red straight lines show initial recovery rate, and green dashed line indicates the recovery rate in sodium-free media. **(B)** Summary of mean rate of recovery (± SEM) from induced acidosis, in the absence of sodium (0 Na^+) and upon the reintroduction of sodium in bicarbonate free medium (Control and 1mM Amiloride). There was a significant difference between the control and amiloride treatment. The numbers above the bars: n (N) where n represents the total number of embryos and N represents the number of experiments (***$P<0.0001$ by ANOVA with N=3-5).

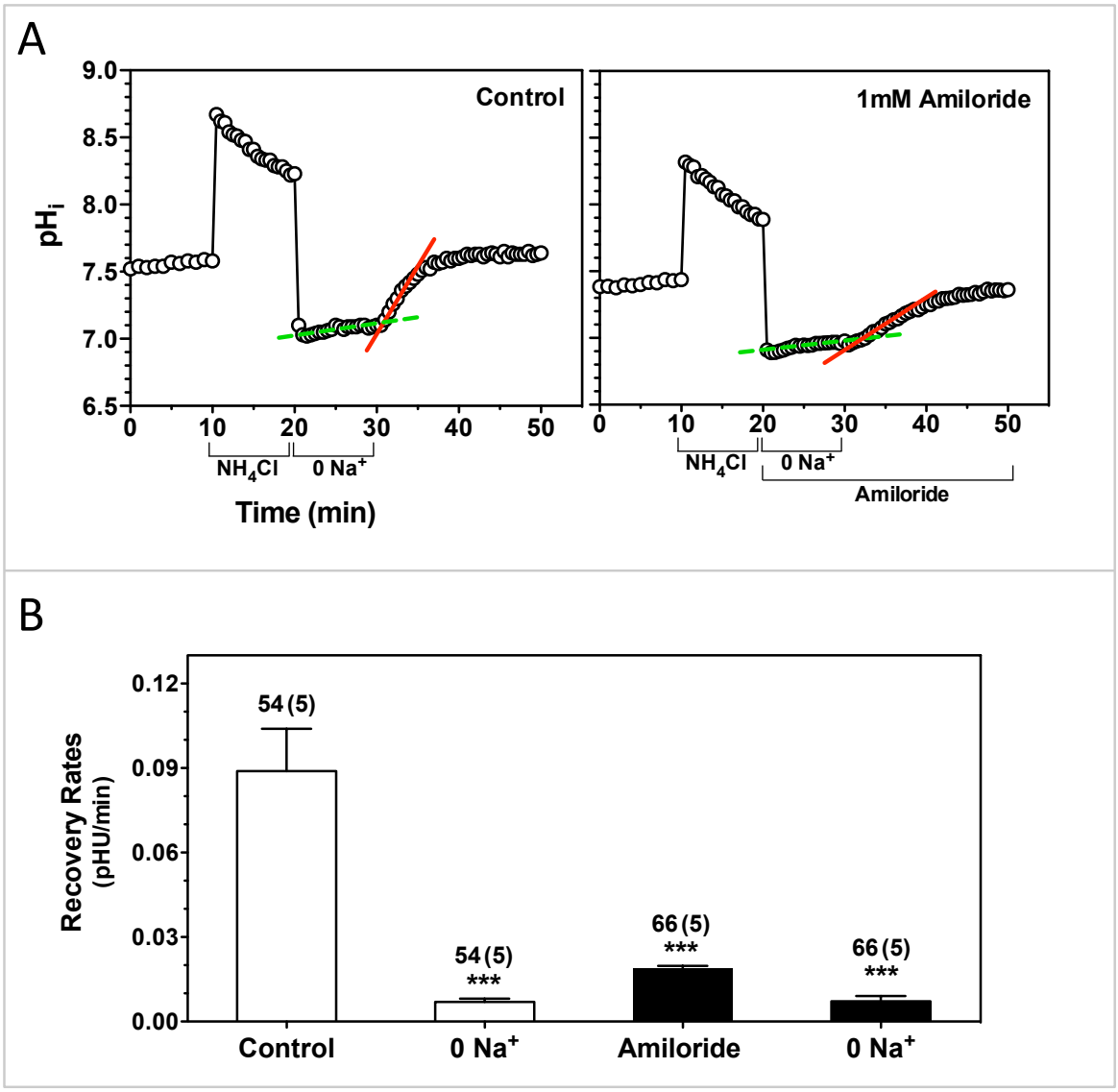
A
Control
1mM Amiloride
pH_i
9.0
8.5
8.0
7.5
7.0
6.5
0
10
20
30
40
50
NH4Cl
0 Na+
Amiloride
Time (min)
B
Recovery Rates
(pHU/min)
0.12
0.09
0.06
0.03
0.00
54 (5)
54 (5)
***
66 (5)
***
66 (5)
***
Control
0 Na+
Amiloride
0 Na+

Figure 14

2.1. Role of NHE1 in embryo recovery from acidosis

2.1.1. Effect of cariporide on 2-cell embryo recovery from acidosis

Based on the transcript presence, the candidates for NHE isoform activities mediating Na^+/H^+ exchange in PI embryos were NHE1, NHE3, and NHE4. We used cariporide (HOE 642), which is selective for NHE1 over both NHE3 and NHE4 by more than 1000-fold (Chambrey et al., 1997b; Counillon et al., 1993; Scholz et al., 1995), to determine whether NHE1 activity played a role. Two-cell stage embryos were used to establish a working concentration for cariporide, via a series of dose-response experiments. Cariporide data was fit (by nonlinear least squares) to: rate = $r_\infty + r_o*IC_{50}/(IC_{50} +$ [cariporide]), where r_∞ is the residual rate at infinite cariporide, r_o is the additional rate with no cariporide (i.e., the total rate is $r_\infty + r_o$ when [cariporide] = 0, or the residual rate), and IC_{50} is the concentration of cariporide that is half-maximally effective, each determined from the fit (Van Winkle, 1999). Refer to the Appendix for extended explanation of how we arrived at this equation.

Measurement of the concentration dependence of inhibition yielded an IC_{50} value of ~ 0.25 μM, r_∞ equals 0.021 pHU/min and r_o was calculated to be 0.049 pHU/min (Figure 15). When compared, the recovery rates for 2.5 μM cariporide were not significantly different from those obtained with 1 mM amiloride in 2-cell embryos, 0.21 ± 0.001 and 0.19 ± 0.001 pHU/min, respectively thus confirming NHE1 as an active participant in pH regulation at this stage of PI development (Figure 15).

2.1.2. NHE1 role in various PI embryo stages

After having defined the effective range for cariporide, a similar dose-response experiment was performed with various PI stages to determine the role of NHE1 in 1-cell, 2-cell, 8-cell and morula embryos using 0, 0.1, 1, 3 and 10 µM cariporide. As with the initial study of the effect of cariporide on 2-cell embryos, maximal inhibition was achieved by 1 - 3 µM at each stage (Figure 16). The extent of maximal inhibition by cariporide (1, 3 and 10 µM) was not significantly different from the residual recovery in the presence of amiloride within each embryo stage (Figure 16).

Since complete inhibition of NHE3 and NHE4 by cariporide occurs only in the 1000 µM range (Chambrey et al., 2001; Scholz et al., 1995; Schwark et al., 1998), these results are consistent with NHE1 mediating most or all recovery from acidosis in PI embryos at these stages.

Figure 15: Concentration-response curve for the effect of cariporide (NHE1 inhibitor) on the Na^+-dependent pH_i recovery at the 2-cell stage following an ammonium pulse.

Initial recovery rates were plotted at each concentration of cariporide (0-10 μM, circles) and amiloride (1mM, bar). Cariporide data were fit (by nonlinear least spares) to rate = r_∞ + r_o*IC_{50}/(IC_{50} + [cariporide]), where r_∞ is the residual rate at infinite cariporide, r_0 is the additional rate with no cariporide (i.e., total rate is r_∞+ r_0 when cariporide = 0), and IC_{50} is the concentration of cariporide that is half-maximally effective, each determined from the fit. IC_{50} from the fit was 0.25 μM. At the maximally effective level, cariporide inhibited to the same extent as amiloride. The residual rate may reflect non-specific permeability of H^+ equivalents driven by the membrane potential after Na^+ reintroduction, or alternatively NHE4 activity, which is relatively amiloride-resistant. Five independent repeats were done for each point and reported as means ± SEM, different letters indicate statistical significance (ANOVA; Tukey-Kramer post hoc), amiloride results have been added as a bar, N=5, and represents mean ± SEM.

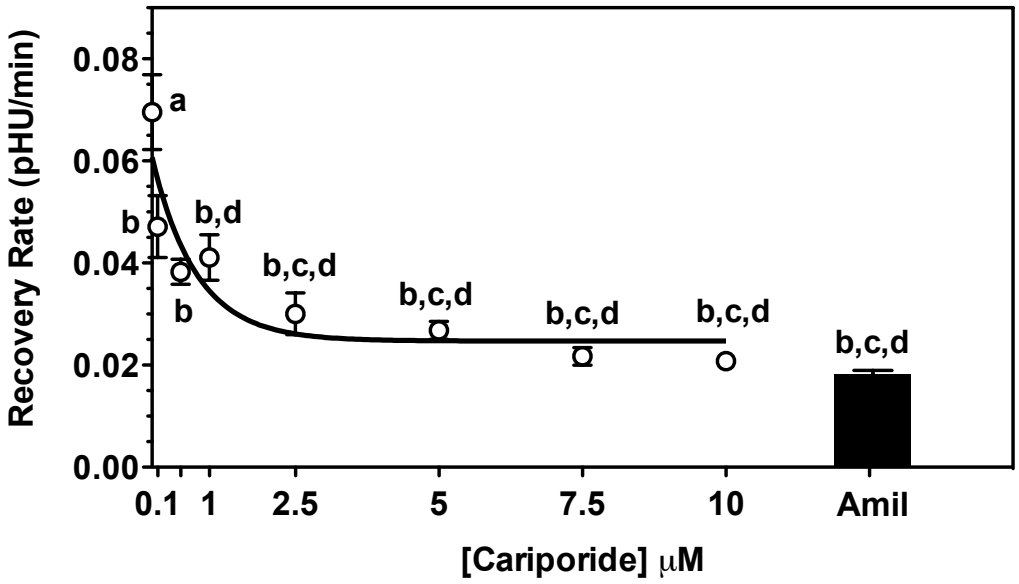
Recovery Rate (pHU/min)
0.08
0.06
0.04
0.02
0.00
a
b
b
b,d
b,c,d
b,c,d
b,c,d
b,c,d
0.1
1
2.5
5
7.5
10
Amil
[Cariporide] μM

Figure 15

Figure 16: Dose dependent inhibition of NHE1 in preimplantation mouse embryos.

Summary of all experiments performed in 1-cell to 8-cell and morula stages of development, with corresponding IC_{50} values for each stage listed in the upper right corner. 0.1% DMSO was used as a vehicle in all experiments (in control experiments it was demonstrated to have no effect on pH_i recovery). The results of amiloride have been added as a bar, N=4-5, reported as mean ± SEM. Different letters indicate statistical significance (ANOVA followed by Tukey-Kramer post hoc test). Parts of this figure were originally published in Siyanov and Baltz (2013).

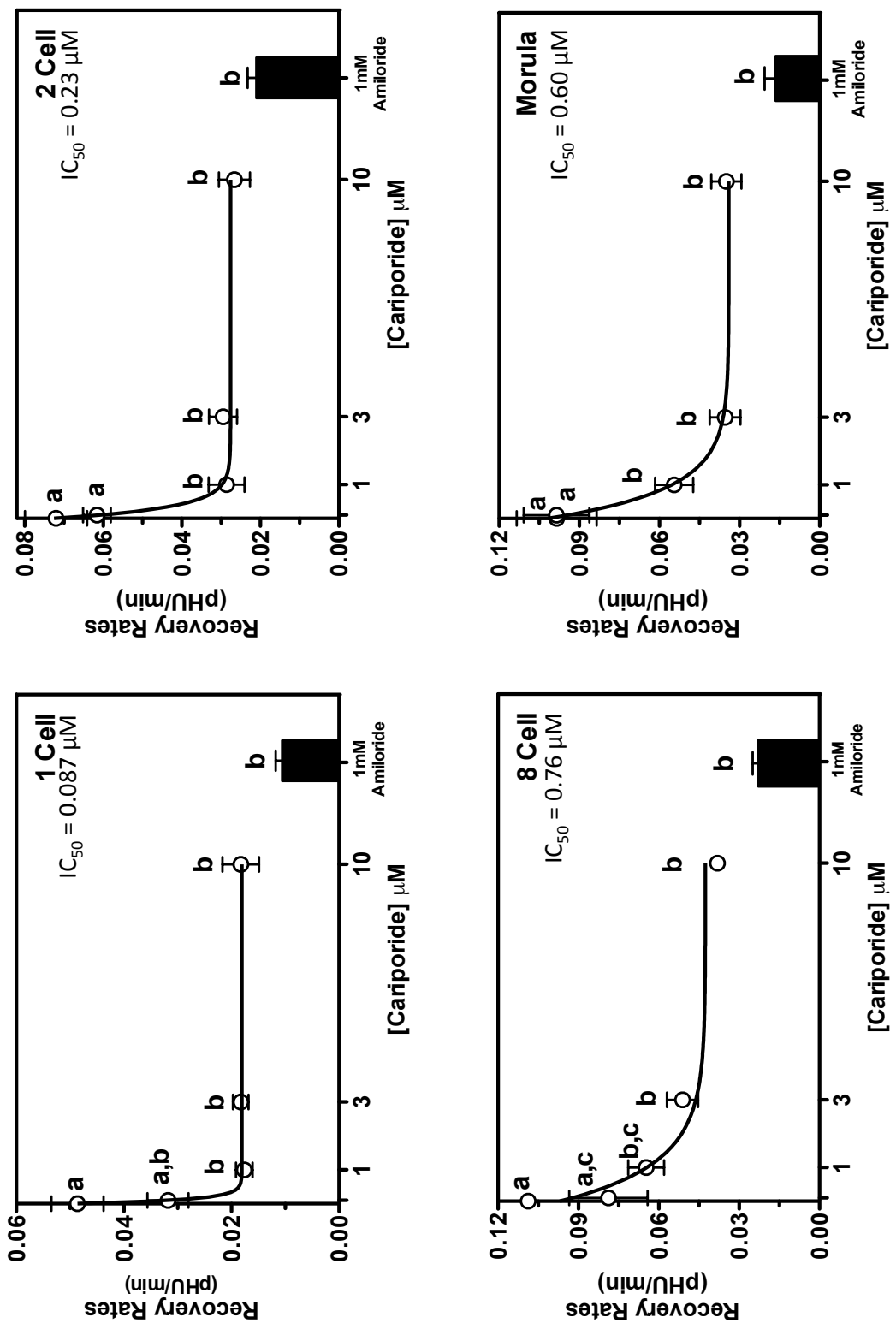
1 Cell
IC50 = 0.087 µM
2 Cell
IC50 = 0.23 µM
8 Cell
IC50 = 0.76 µM
Morula
IC50 = 0.60 µM
Recovery Rates (pHU/min)
[Cariporide] µM
1mM Amiloride
a
a,b
b
a,c
b,c

Figure 16

2.2. Role of NHE3 in PI embryo recovery from acidosis

The NHE3-selective inhibitor S3226 blocks rodent NHE3 activity in fibroblasts with an IC_{50} less than 0.1 μM while blocking NHE1 activity at about 10-fold higher concentrations (Schwark et al., 1998; Speake et al., 2005). The ability of 0.1, 1.0 and 10 μM S3226 to block recovery from acidosis was assessed in 2-cell embryos (Figure 17A). At 0.1 μM the recovery from acidosis was not significantly impeded when compared to the control (0.107 ± 0.026 vs. 0.124 ± 0.01 pHU/min). Essentially complete inhibition was achieved at 1 and 10 μM S3226, comparable to that achieved with 1 mM amiloride (1 μM – 0.047 ± 0.004; 10 μM – 0.027 ± 0.003 vs. amiloride at 0.0209 ± 0.001 pHU/min; N=4-9).

To determine whether any significant portion of acidosis recovery could be attributable to NHE3, 3 μM cariporide (should inhibit NHE1) and 0.1 μM S3226 (should inhibit NHE3, with known IC_{50} = 0.023 μM, (Schwark et al., 1998)) were used in concert and compared the rate of recovery to that obtained with 10 μM S3226 alone. There was, however, no statistically significant difference between levels of inhibition in the presence of S3226 alone, the two inhibitors in combination, or amiloride (1mM) as demonstrated by Figure 17A. This indicated that NHE3 was unlikely to contribute detectably to recovery from acidosis in PI mouse embryos at the stages examined. Furthermore, when compared to the cariporide dose response curve, S3226 was not more effective at inhibiting recovery in 2-cell embryos. This is consistent with a lack of a role for NHE3 as the major component of recovery from acidosis in 2-cell mouse embryos, since the cariporide curve would then have been shifted well to the right of the S3226 curve (Figure 17B).

To determine whether NHE3 plays any detectable role in pH_i regulation in PI embryos at a later stage cariporide and S3226 were used in concert to inhibit both isoforms and compared those values to those obtained when each drug was used individually, to reveal

whether there could be two components to recovery due to NHE1 and NHE3 acting in concert (Figure 18). For this study 2-cell and 8-cell embryos were assessed. Our rationale for this experiment was that if NHE3 contributes to embryo recovery from acidosis, inhibition with 10 μM cariporide (inhibits only NHE1) would have a higher recovery rate than that obtained with either 10 μM S3226 (a concentration that inhibits both NHE1 and NHE3) or the two-drug cocktail (inhibits NHE1 and NHE3). In 2-cell stage embryos there was a substantial decrease in the recovery rates in all inhibitor treatment groups when compared to control (Figure 18B). Similar results were obtained with 8-cell stage embryos (Figure 18B). There was no significant difference between the different drug treatment groups in both the 2-cell and 8-cell embryos, consistent with NHE1 being the primary pH_i regulator in PI mouse embryos in the acidic range, with no detectable component due to NHE3.

2.3. Effect of inhibition of NHE4 in 2-cell embryos

Even in the presence of maximally-inhibiting concentrations of cariporide or S3226, or in the presence of 1 mM amiloride, a small recovery often was observed after introduction of Na^+. This could be due to recovery not mediated by NHEs, or it could be due to an inhibitor - resistant NHE isoform. Since *Slc9a4* mRNA was present in very early PI embryos (Figure 12), and NHE4 activity is resistant to inhibition by amiloride with an IC_{50} near 1 mM (Chambrey et al., 1997b) and thus some NHE4 activity could persist with 1 mM amiloride. To test this theory the concentration of amiloride was increased to 5 mM. However, as Figure 19 shows, the recovery rates for 1 and 5 mM amiloride were essentially identical and were not significantly different from the recovery values obtained during the sodium-free period. Thus, the apparent amiloride-insensitive recovery is not likely due to

NHE4 but more likely arises from passive processes such as diffusion of protons or the equivalent across the membrane, driven by the large induced pH gradient.

Figure 17: Concentration-response curve for the effect of S3226.

(A) *Initial rates of pH_i recovery following induced acidosis in 2-cell embryos in the presence of NHE3-selective inhibitor S3226* (IC_{50}= 0.23 μM; Table 1). At higher concentrations S3226 inhibits the NHE1 isoform (IC_{50}=3 - 3.6 μM; Table 1). The addition of both inhibitors to the media (0.1 μM S3226 and 3 μM Cariporide) did not have an additive effect at decreasing the rates of recovery from acidosis (grey bar) and not significantly different from the 1 mM amiloride recovery rates (black bar). These data show that the residual recovery during cariporide inhibition is not dependent on NHE3 activity. Each point represents 4 - 9 individual repeats, with 5-15 embryos per experiment (ANOVA; Tukey-Kramer post hoc test; $P<0.05$). **(B)** *Maximal recovery rates of 2-cell embryos in the presence of S3226 or cariporide.* The residual recovery rate in the presence of amiloride was subtracted from all values. Each point represents the mean ± SEM of N=4-9 repeats with 5-15 embryos per each experiment. Parts of this figure were originally published in Siyanov and Baltz (2013).

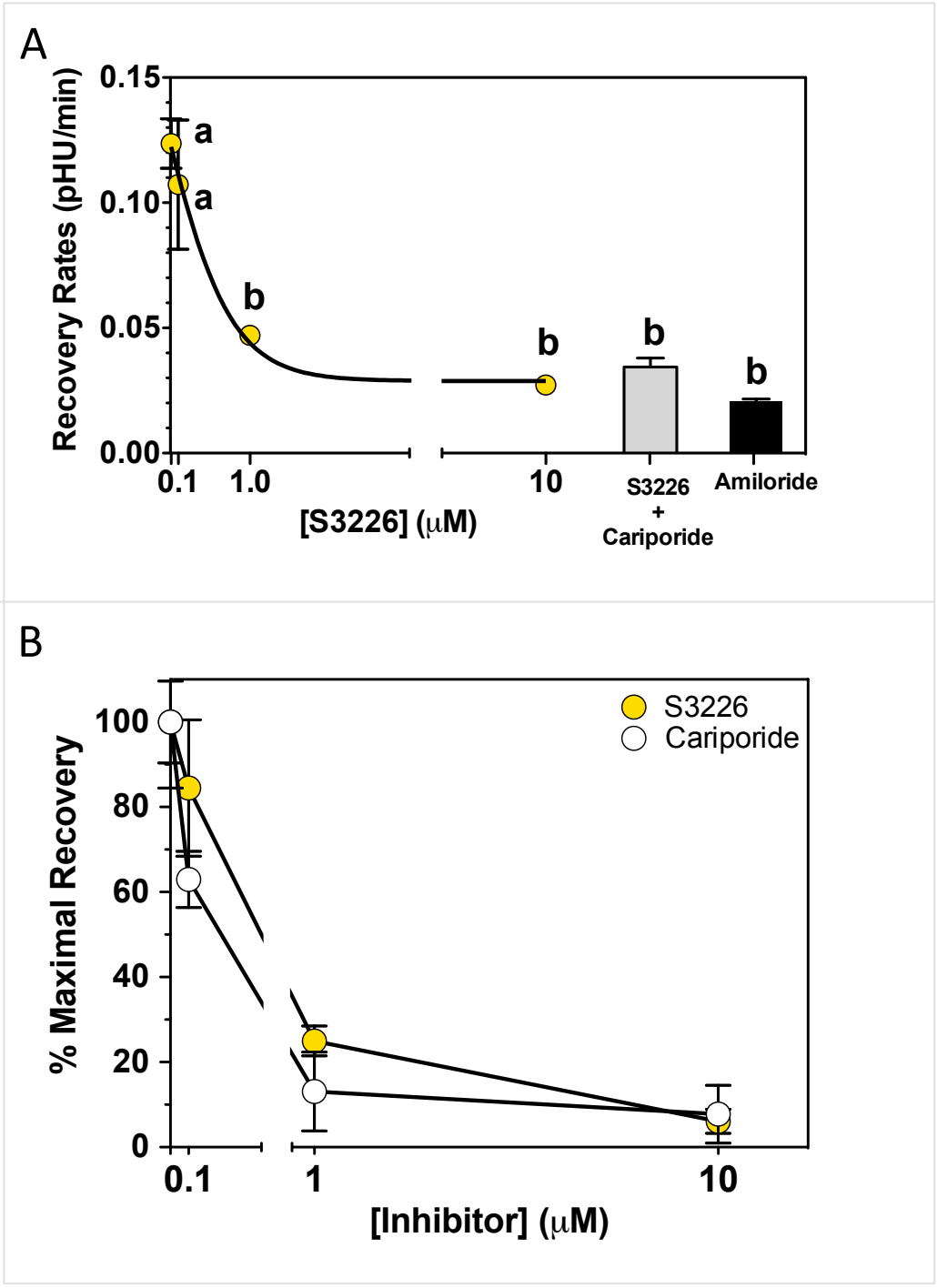
A
Recovery Rates (pHU/min)
0.15
0.10
0.05
0.00
a
a
b
b
b
b
0.1
1.0
10
S3226
+
Cariporide
Amiloride
[S3226] (μM)
B
% Maximal Recovery
100
80
60
40
20
0
S3226
Cariporide
0.1
1
10
[Inhibitor] (μM)

Figure 17

Figure 18: Identification of NHE isoforms that aid in the recovery from acidosis in preimplantation embryos.

(A) Representative examples of recovery from acidosis by 2-cell and 8-cell embryos (as indicated at right) in the presence of 0.1% DMSO (control), 10 μM cariporide, 10 μM S3226, both cariporide and S3226 (Carip+S3226) or 1 mM amiloride. **(B)** Summary data in 2-cell and 8-cell embryos indicates only NHE1 is actively regulating the embryos recovery from induced acidosis. The addition of 10 μM cariporide + 10 μM S3226 (pink bar) does not show additional inhibition of recovery rates in either the early and late stage PI embryos. Each bar represents a mean ± SEM of Na^+-dependent recoveries of pH_i with N=5-6, with 5-12 embryos per replicate. Different letters above bars indicate statistical difference (ANOVA with Tukey-Kramer test, $P<0.001$). This figure was modified from Siyanov and Baltz (2013).

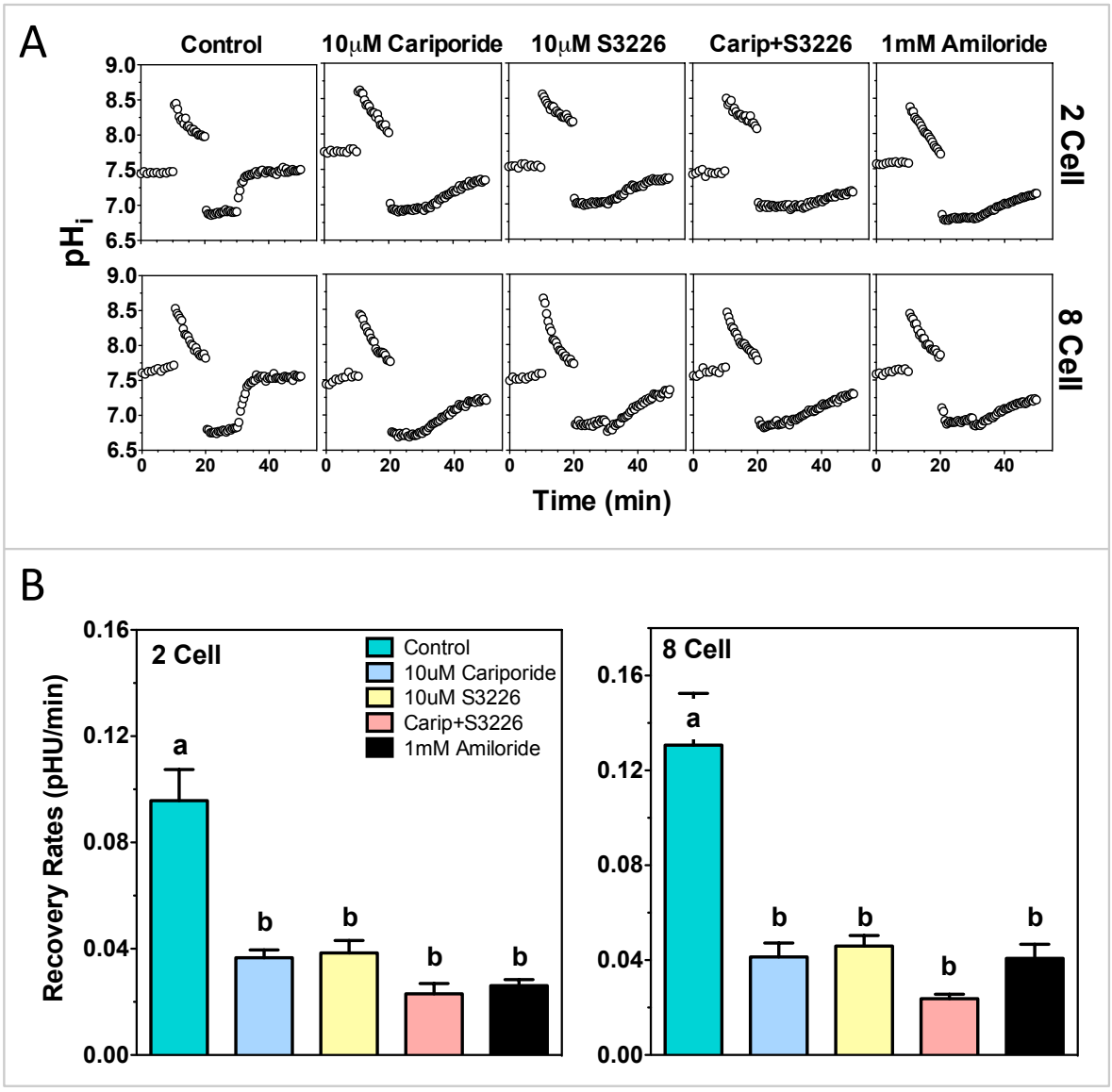
A
Control
10μM Cariporide
10μM S3226
Carip+S3226
1mM Amiloride
2 Cell
8 Cell
pH_i
Time (min)
B
2 Cell
8 Cell
Control
10uM Cariporide
10uM S3226
Carip+S3226
1mM Amiloride
Recovery Rates (pHU/min)
a
b

Figure 18

Figure 19: Effect of increased amiloride on recovery from acidosis in 2-cell embryos.

The mean rate of recovery from acidosis in 2-cell embryos was determined in the presence of 0 (Control), 1 or 5 mM amiloride in experiments similar to those shown in Figure 14. Recoveries were measured in pH-KSOM. The second bar of each pair represents the mean recovery in the absence of sodium ($0Na^+$; $0Na^+$-H-KSOM medium). Each bar represents a mean ± SEM with the numbers above the bars: n (N) where n corresponds to the total number of embryos and N represents the number of experiments (a vs. b: $P<0.001$ by ANOVA). Figure was originally published in Siyanov and Baltz (2013).

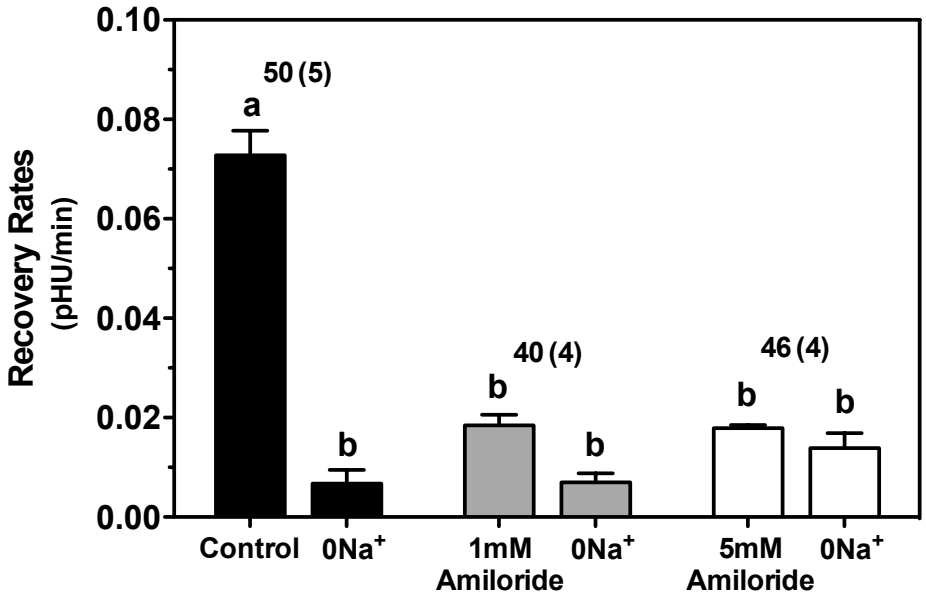
0.10
0.08
0.06
0.04
0.02
0.00
Recovery Rates
(pHU/min)
50 (5)
a
b
40 (4)
b
b
46 (4)
b
b
Control
0Na+
1mM
Amiloride
0Na+
5mM
Amiloride
0Na+

Figure 19

3. Effect of Chronic Acidosis and NHE Inhibitors on PI Embryos in Culture

3.1. Embryo development in the presence of cariporide at various CO_2 concentrations

Our pilot culture experiments with the general NHE inhibitor amiloride and the amiloride derivative EIPA (ethylisopropylamiloride) revealed these drugs to be toxic to embryo development even under control conditions (in KSOM at 5% CO_2, 37^{o}C). Since amiloride has effects on cellular processes other than Na^+/H^+ exchange, such as DNA synthesis and other modes of Na^+ transport, the culture with amiloride or its derivatives was not further pursued. Given that cariporide inhibited essentially all NHE-specific, Na^+-dependent recovery from acidosis in PI mouse embryos (above), the effect of cariporide on PI embryo development was assessed at different levels of chronic acidosis by increasing CO_2 levels in the incubation chamber. The measured pH of KSOM media at 5%, 10%, 15%, 20% and 25% CO_2 was 7.3, 7.0, 6.9, 6.7 and 6.6, respectively (Figure 20A – top axis).

One-cell embryos were used since this stage is most sensitive to stress during development. The percentage of 1-cell embryos that reached the expanded blastocyst stage by 96 hours in culture decreased sharply with increasing CO_2 and decreasing medium pH (Figure 20A). These embryos arrested at the 2-cell stage and many failed to develop to the blastocyst stage even at pH 7 at 10% CO_2 (40.4 ± 12.5 vs. control 74.1 ± 4.8% blastocysts).

Next, 2-cell embryos were used to culture for 70 - 72 hours, until they reached the expanded blastocyst stage. Decreasing pH_i reduced embryo development only slightly until CO_2 was increased to 25%, when the majority of the 2-cell embryos failed to develop to the blastocyst stage (41.6±14.3% when compared to 5% CO_2 control 89.8±2.9%).

To block NHE1 activity at each CO_2 concentration, 3 μM cariporide was added to the culture medium. The addition of cariporide did not by itself detectably perturb

development to the blastocyst stage for either 1-cell or 2-cell embryos, since there was no effect of cariporide at the normal 5% CO_2 concentration (pH 7.3). Indeed, cariporide unexpectedly had no effect on development to the blastocyst stage at any CO_2 level when culturing 2-cell embryos (Figure 20A, B).

3.2. Internal pH of 2-cell embryos in various acidic environments

Next we sought to do determine if decreasing media pH by increasing external [CO_2] in combination with 3 μM cariporide had perturbed the internal pH of 2-cell embryos, even though we had not detected an effect on development. Increasing [CO_2] both in the control and cariporide treated embryos had only a small effect on pHi after 3 - 5hr in culture (Figure 20C). Decreasing pH_o below 6.9 (CO_2 15%) lead to a significant decrease in pH_i in both control and inhibitor treated groups (Figure 20C). However, analysis of the data showed no significant difference in pH_i values between the control and cariporide treated embryos at any CO_2 level. These results suggested that embryos either do not possess an active mechanism capable of regulating against prolonged acidosis, or the increasing CO_2 concentration itself is toxic to embryo development, or there is another mechanism that compensates for the inactivation of NHE1.

Figure 20: Effect of cariporide on PI embryo development and resting pH_i with chronic acidosis *in vitro*.

(A) *1-cell and* (**B)** *2-cell embryos* were cultured (for 72 hr or 96 hr, respectively) to the expanded blastocyst stage. Embryos were cultured in KSOM medium with the NHE1-selective inhibitor cariporide (3 μM) or without the inhibitor (control; 0.1% DMSO alone). The CO_2 concentration (lower axis) was increased to decrease pH of the medium (upper axis). No significant difference in development was detected between the control and cariporide-treated groups at any CO_2 level (ns; $P>0.05$ by ANOVA), but development at 5% CO_2 was significantly higher than other levels of CO_2 as indicated (*$P<0.05$ by ANOVA). Each point represents the pH_i (mean ± SEM) of N=4-14 independent repeats for 1-cell and N=5 for 2-cell. **(C)** *Steady-state pH_i of 2-cell embryos after 3 - 5hr at each CO_2 concentration.* There was no significant effect of cariporide on pH_i at any CO_2 level, but pH_i differed significantly from 5% CO_2 vs. 15% - 25% as indicated (*$P<0.05$ by ANOVA; N=3-4 independent repeats). This figure was modified from Siyanov and Baltz (2013).

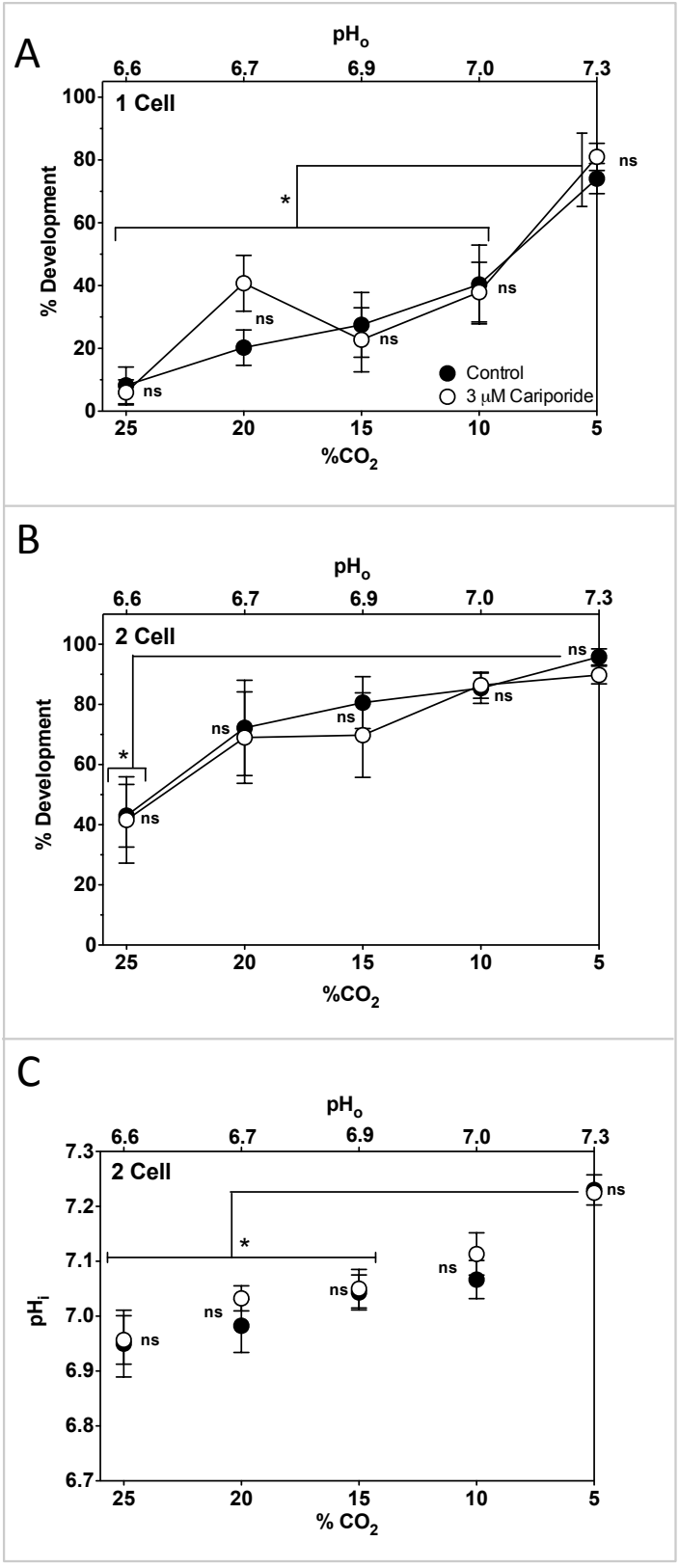
A
pH$_o$
6.6
6.7
6.9
7.0
7.3
1 Cell
% Development
100
80
60
40
20
0
*
ns
ns
ns
ns
ns
Control
3 μM Cariporide
25
20
15
10
5
%CO$_2$
B
pH$_o$
6.6
6.7
6.9
7.0
7.3
2 Cell
% Development
100
80
60
40
20
0
*
ns
ns
ns
ns
ns
25
20
15
10
5
%CO$_2$
C
pH$_o$
6.6
6.7
6.9
7.0
7.3
2 Cell
pH$_i$
7.3
7.2
7.1
7.0
6.9
6.8
6.7
*
ns
ns
ns
ns
ns
25
20
15
10
5
% CO$_2$

Figure 20

3.3. Embryo development in the presence of cariporide and various DMO concentrations

It was possible that increasing CO_2 is itself detrimental to embryo development independent of pH_i. To test this theory, a non-metabolizable weak acid DMO was used for embryo cultures, which has been previously shown to decrease medium pH and pH_i of embryos (Zander-Fox et al., 2010). The measured pH of KSOM media at 0, 10, 20 and 30 mM DMO was 7.4, 7.0, 6.6 and 6.3, respectively (Figure 21A).

The highest concentration of DMO (30 mM) completely prevented embryo development (Figure 21A). However, 2-cell embryos developed to blastocysts in up to 20 mM DMO. As with the CO_2 culture experiments, the addition of the NHE1 inhibitor cariporide did not have any significant effect on embryo development when compared to the paired controls.

As for CO_2 experiments, it was determined that the presence of DMO with or without cariporide in the medium perturbs steady-state pH_i after 3-5 hours in 2-cell embryos (Figure 21B). Increasing [DMO] both in the control and cariporide treated embryos had no effect on pH_i with mean values at 0, 10, and 20 mM DMO were 7.26 ± 0.04, 7.27 ± 0.04 and 7.26 ± 0.03 and respectively in the control group and 7.28 ± 0.03, 7.26 ± 0.02 and 7.30 ± 0.07 in the presence of cariporide, respectively. Analysis of the data showed no significant difference in pH_i values between the control and cariporide treated embryos. Two-cell embryos were able to maintain normal pH_i until exposed to 30 mM DMO where both the control and cariporide treated group pH was significantly lower than that in groups treated with 0-10 mM DMO.

Figure 21: Development of 2-cell embryos in the presence of the cell-permeant weak acid DMO.

(A) Increased DMO (lower axis) decreased pH of the KSOM medium (upper axis). There was no significant effect of cariporide (3 μM) on development within each DMO concentration (ns; $P>0.05$ by ANOVA). Development was significantly lower at 30mM DMO than at other DMO concentrations as indicated (*$P<0.05$ by ANOVA). Each point in the graph represents the mean ± SEM of N=4-5 independent repeats. **(B)** pH_i was not significantly different at any DMO concentration in the presence vs. absence of cariporide, but was significantly lower at 30mM DMO than at lower DMO concentrations as indicated (*$P<0.05$ by ANOVA). Each point represents the mean ± SEM of N=2-3 independent repeats. Modified from a figure originally published in Siyanov and Baltz (2013).

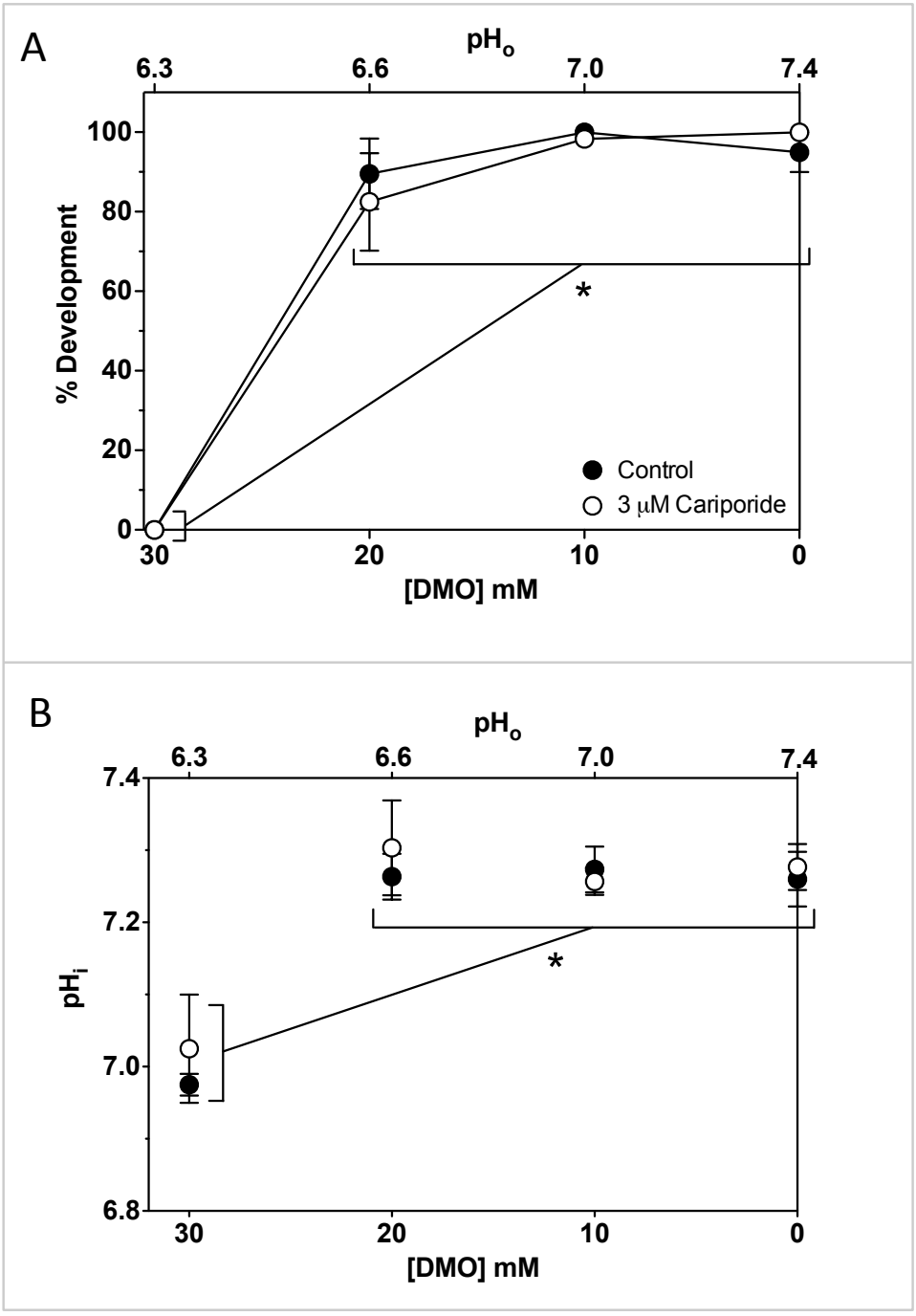
A
pH$_o$
6.3
6.6
7.0
7.4
100
80
60
40
20
0
% Development
*
Control
3 μM Cariporide
30
20
10
0
[DMO] mM
B
pH$_o$
6.3
6.6
7.0
7.4
7.4
7.2
7.0
6.8
pH$_i$
*
30
20
10
0
[DMO] mM

Figure 21

4. Role of NDBCE and NHE in Embryo Recovery from Acidosis

Previously, Erdogan et al. showed that Na^+ dependent HCO_3^+/Cl^- exchanger (NDBCE; SLC4A8 protein) activity was present in GV oocytes, mature MII eggs, and 1-cell embryos (Erdogan et al., 2011). Thus, in KSOM culture medium that is buffered by bicarbonate (25 mM) and CO_2, any NDBCE present could contribute to maintenance of baseline pH_i, recovery from acidosis, and the ability of embryos to develop under conditions of chronic acidosis.

4.1. Recovery from acidosis in media containing bicarbonate

First the observations of Erdogan et al. on NDBCE in oocytes and 1-cell embryos were extended to 2-cell embryos, while confirming their previous results in GV oocytes as a control. In bicarbonate-containing p-KSOM medium where any NDBCE would be active, the NDBCE inhibitor DIDS (100 μM) substantially inhibited recovery in GV oocytes (0.019 ± 0.002; n=52; N=4 vs. control 0.051 ± 0.005 pHU/min; Figure 22A), consistent with previous results (Erdogan et al., 2011), as did cariporide (0.016 ± 0.004 pHU/min; n=59, N=5). The combination of DIDS and cariporide did not further inhibit pH_i recovery significantly in GV oocytes (Figure 22A).

Under the same conditions in 2-cell embryos however, DIDS had only a small insignificant effect (0.09 ± 0.008 pHU/min) vs. control (0.11 ± 0.011 pHU/min), while 10 μM cariporide significantly inhibited recovery (0.057 ± 0.01; Figure 22A). The combination of DIDS and cariporide did not further inhibit recovery significantly in 2-cell embryos. Thus, while NDBCE appears to play a significant role in recovery from acidosis in GV

oocytes (Figure 22A) and 1-cell embryos (Erdogan et al., 2011), a substantial component of NDBCE activity does not appear to persist into the 2-cell stage.

4.2. Removal of bicarbonate from media prevents the activity of NDBCE

In bicarbonate-free medium (pH-KSOM) where NDBCE would be inactive, DIDS (100 μM) had no effect on recovery from induced acidosis in either GV oocytes (0.055 ± 0.005 vs. control 0.054 ± 0.001 pHU/min; Figure 22B) or 2-cell embryos (0.085±0.005 vs. control 0.093 ± 0.01 pHU/min), indicating that there was no NDBCE activity. Cariporide inhibited recovery as expected (GV 0.018 ± 0.004 and 2-cell 0.030 ± 0.002 pHU/min). The combination of cariporide and DIDS did not further inhibit recovery (GV 0.008±0.002 and 2-cell 0.027±0.002 pHU/min).

Figure 22: NDBCE activity in GV oocytes and 2-cell embryos.

Mean recovery rates from acidosis in GV oocytes and 2-cell embryos **(A)** in bicarbonate-containing CO_2-buffered p-KSOM medium, or **(B)** in bicarbonate-depleted pH-KSOM medium for control (0.1% DMSO vehicle only), 100 μM H_2DIDS, 10 μM cariporide or both inhibitors together (D+C). In (A) all experiments were carried out in p-KSOM and $0Na^+$-KSOM media, buffered with 5% CO_2 gas during pH_i measurements. Different letters above bars indicate significant difference $P<0.01$ (ANOVA). Each bar represents the mean ± SEM with the numbers above the bars showing N(n), where n corresponds to the total number of embryos and N represents the number of independent experiments. Modified from a figure originally published in Siyanov and Baltz (2013).

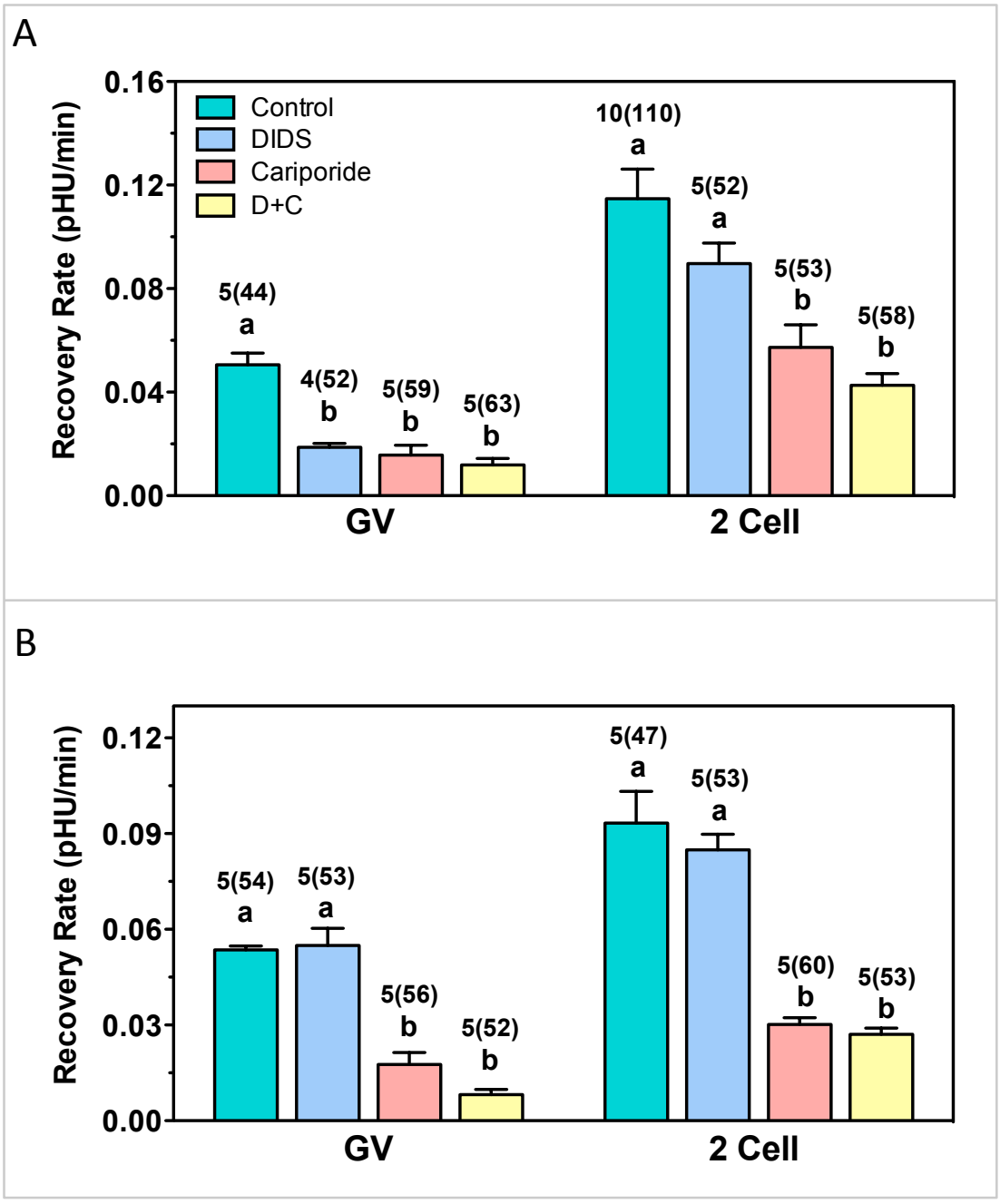
A
Recovery Rate (pHU/min)
0.16
0.12
0.08
0.04
0.00
Control
DIDS
Cariporide
D+C
5(44)
a
4(52)
b
5(59)
b
5(63)
b
10(110)
a
5(52)
a
5(53)
b
5(58)
b
GV
2 Cell
B
Recovery Rate (pHU/min)
0.12
0.09
0.06
0.03
0.00
5(54)
a
5(53)
a
5(56)
b
5(52)
b
5(47)
a
5(53)
a
5(60)
b
5(53)
b
GV
2 Cell

Figure 22

5. Effect of Chronic Acidosis and Various Inhibitors on Preimplantation Embryos in Culture

5.1. Embryo development in the presence of cariporide and DIDS at various DMO concentrations

While sodium dependent bicarbonate chloride exchanger does not appear to play a significant role in recovery from acidosis at the 2-cell stage, it was still possible that a minor component of NDBCE activity could exist in 2-cell stage and later embryos that contributes to maintenance of pH_i under chronic acidosis. This possibility is suggested by the trend for DIDS to reduce the rate of acute recovery from acidosis at the 2-cell stage embryos (Figure 22A), although this decrease was not significant. Therefore, 2-cell embryos were cultured for 3 days until they reached the blastocyst stage, in media containing 0, 15 or 20 mM DMO with 100 μM DIDS (NDBCE inhibitor) with or without cariporide (3 μM). Under normal conditions, at 5% CO_2 and 0 DMO, DIDS (84.7 ± 6.0% development to blastyocysts) and DIDS in combination with cariporide (98.0 ± 2.0%), had no effect on embryo development when compared to control (87.8 ± 5.0%) as shown in Figure 23A. DIDS had no effect on embryo development to the blastocyst stage at any external pH (Figure 23A). Cariporide (3 μM) alone also had no significant effect, as above, nor was development significantly affected by a combination of both inhibitors, although embryo development was impeded with increasing DMO concentrations (at 20 mM DMO: control – 60 ± 16.4%; cariporide – 32 ± 11.6%; DIDS – 52.4 ± 10% and DIDS plus cariporide 82.6 ± 5.6%). There was one observed anomaly at 20 mM DMO and 3 μM cariporide, where development was significantly decreased when compared to the DIDS + cariporide groups, but was not significantly different from the control (Figure 23A). The reason for this is unknown.

5.2. Measurement of blastocoel diameters in various treatment groups

To determine whether the decrease in external pH led to a more subtle impairment of embryo development that could affect growth and cell proliferation, the diameters of the blastocysts were measured from the experiments above. Embryos cultured from the two-cell stage for 3 days with either 3 μM cariporide, 100 μM DIDS both drugs in concert, or none (control) did not display any significant difference in blastocyst diameters as shown in Figure 23B.

Figure 23: Embryo development in the presence of DIDS and cariporide at various DMO concentrations.

(A) 2-cell embryos cultured for 72 hr until they reached the blastocyst stage. Control (black bar), 3 μM cariporide (blue bar), 100 μM DIDS (grey bar) and DIDS + cariporide (white bar). Each bar represents the mean ± SEM with the numbers above the bars indicating n(N), where n corresponds to the total number of embryos and N represents the number of experiments (ANOVA; Tukey-Kramer post hoc test, $P<0.05$). **(B)** The diameters of those cultured embryos that reached the blastocyst stage were measured by taking an average of two orthogonal diameter measurements. There was no significant effect of cariporide on development within each DMO concentration (NS; $P>0.05$ by ANOVA). Each bar represents the mean ± SEM with the numbers above the bars: N (n) where n corresponds to the total number of embryos and N represents the number of experiments.

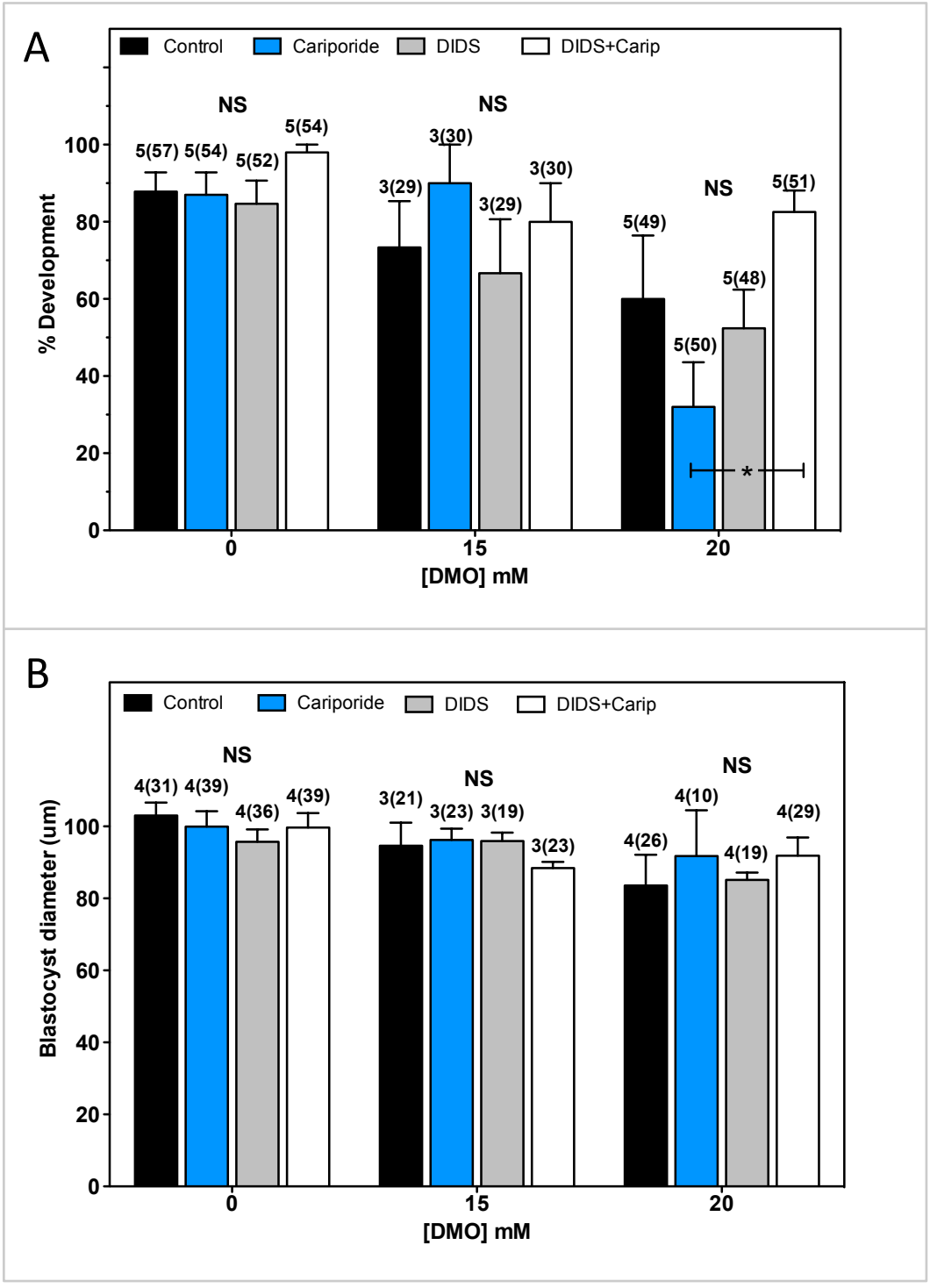
A
Control
Cariporide
DIDS
DIDS+Carip
NS
NS
NS
5(57)
5(54)
5(52)
5(54)
3(29)
3(30)
3(29)
3(30)
5(49)
5(50)
5(48)
5(51)
*
% Development
0
20
40
60
80
100
0
15
20
[DMO] mM
B
Control
Cariporide
DIDS
DIDS+Carip
NS
NS
NS
4(31)
4(39)
4(36)
4(39)
3(21)
3(23)
3(19)
3(23)
4(26)
4(10)
4(19)
4(29)
Blastocyst diameter (um)
0
20
40
60
80
100
0
15
20
[DMO] mM

Figure 23

5.3. Embryo development in the presence of cariporide and DIDS at various CO_2 concentrations

Two-cell embryos were cultured at different CO_2 levels with 10 μM cariporide, 100 μM H_2DIDS, both inhibitors (D+C), or control (0.1% DMSO) (Figure 24A). H_2DIDS was used, which has the same properties as DIDS but is not fluorescent when excited in the UV range, since the resulting blastocysts were subsequently fixed and used for cell counts (below – Figure 25B). As with our studies with DMO, these experiments showed that cariporide (10 μM) or H_2DIDS (100 μM) alone had no effect, nor was the development of embryos significantly affected by a combination of both inhibitors.

5.4. Effect of external pH on internal pH of embryos in the presence of cariporide and H_2DIDS

To determine whether prolonged exposure to lower external pH and a combination of inhibitors would alter the internal pH of 2-cell embryos, as in the NHE1 culture experiments, wherein only cariporide was utilized. Two-cell embryos were collected and loaded them with SNARF, and cultured them for 3 - 5 hours in various CO_2 levels and measured their internal pH right after incubation. No significant differences were observed between the various inhibitor treatments and the control, in CO_2 concentrations up to 15%. However, at the lowest external pH (6.7, 20% CO_2), pH_i was significantly lower in the group containing both 10 μM cariporide and 100 μM H_2DIDS compared to control (7.08 ± 0.04 versus 7.20 ± 0.02, respectively; Figure 24B), suggesting possible synergistic roles for NHE1 and NDBCE in maintaining pH_i in 2-cell embryos under extreme prolonged acidosis.

Figure 24: Development of 2-cell embryos to blastocysts in the presence of NDBCE and NHE1 inhibitors.

(A) Development of 2-cell embryos cultured for 72 hr in KSOM to the expanded blastocyst stage in the absence or presence of NHE1- and NDBCE-selective inhibitors. Embryos were cultured at different CO_2 levels with 10 μM cariporide, 100 μM H_2DIDS, both inhibitors (D+C), or control (0.1% DMSO). The CO_2 concentration (lower axis) was increased to decrease pH of the medium (upper axis). Each point represents a mean ± SEM, N=4-11. **(B)** pH_i of 2-cell embryos was measured after they were cultured for 3-5 hours under the various CO_2 concentrations. At the two lowest CO_2 levels, there was a small effect of the combination of both inhibitors on development, while there was a significant effect on pH_i only at 20% CO_2 (*P<0.05). Each point represents a mean ± SEM, N=5-6. Modified from a figure originally published in Siyanov and Baltz (2013).

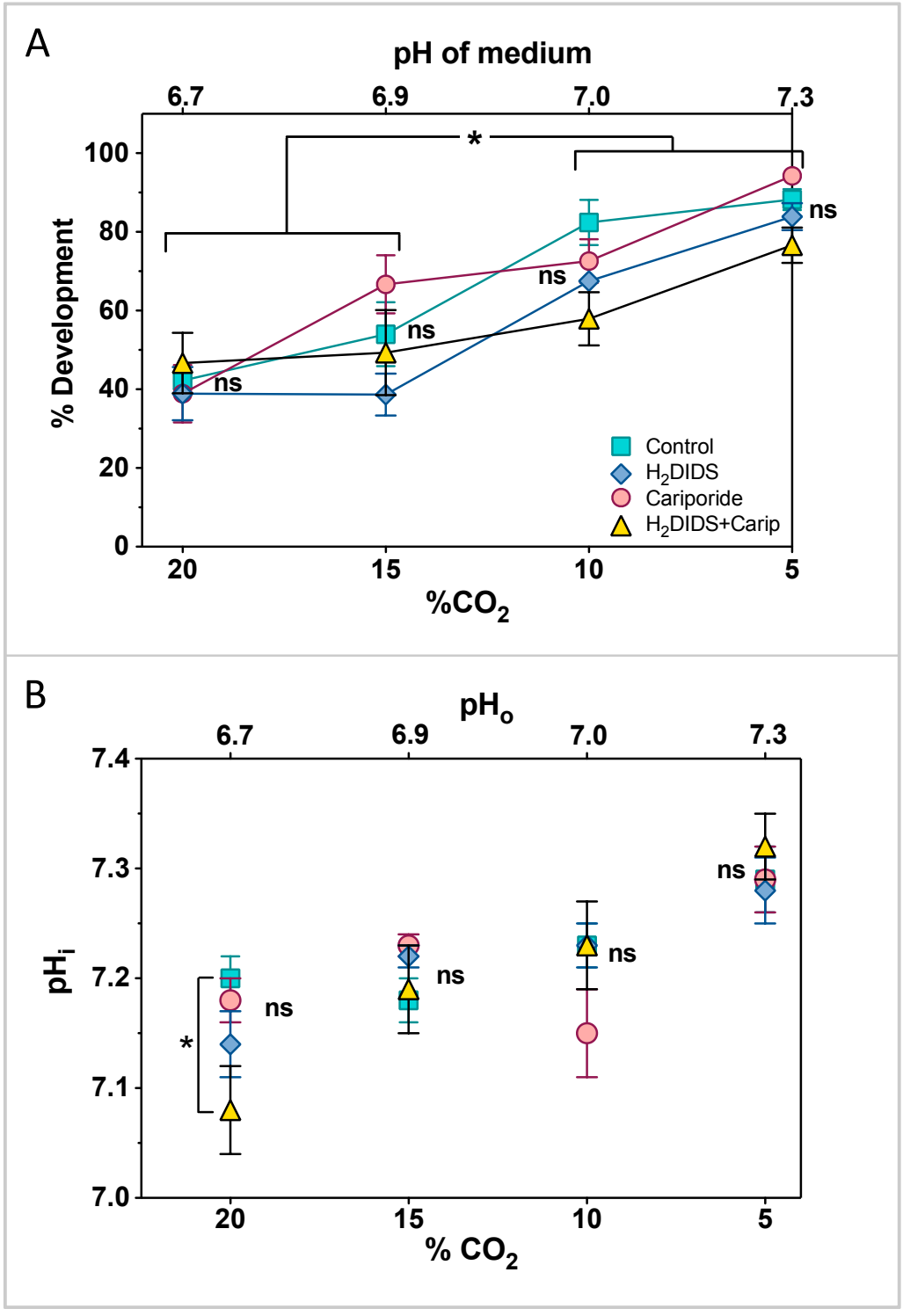
A
pH of medium
6.7
6.9
7.0
7.3
*
100
80
60
40
20
0
% Development
ns
ns
ns
ns
Control
H2DIDS
Cariporide
H2DIDS+Carip
20
15
10
5
%CO2
B
pHo
6.7
6.9
7.0
7.3
7.4
7.3
7.2
7.1
7.0
pHi
*
ns
ns
ns
ns
20
15
10
5
% CO2

Figure 24

5.5. Cell allocation in cultured blastocysts during prolonged exposures to acidic environments.

Zander-Fox et al. (2010) showed that both acute and chronic exposure to suboptimal pH do not perturb the fraction of embryos that form blastocysts (consistent with the results here), but significantly affected embryo physiology and implantation capability. They also found that even moderately acidotic culture medium can decrease blastocyst cell number and perturb cell allocation between the inner cell mass and trophectoderm (Zander-Fox et al., 2010). However, they did not address which pH-regulatory mechanisms might be implicated. In this study, we set out to determine whether inhibiting the two possible pH regulatory mechanisms found within the developing preimplantation embryo will lead to a more pronounced alteration in blastocyst cell numbers and cell lineage allocations. External pH was decreased by increasing CO_2 levels and addition of an NDBCE inhibitor H_2DIDS (Figure 24A).

Embryos cultured from the 2-cell stage that reached the blastocyst stage were fixed and the number of cells counted in the ICM and trophectoderm (Figure 25A). Decreasing external pH using increased CO_2 reduced the total number of cells in the blastocysts and in each of the ICM and TE lineages (Figure 25A). At normal external pH (7.3, 5% CO_2), the presence of either cariporide or H_2DIDS significantly reduced the number of ICM cells, while the presence of both cariporide and H_2DIDS caused a significant further reduction in ICM cell number and also affected TE. A similar effect on ICM was seen at 10% CO_2 (pH 7.0), but any effect of the inhibitors appeared to be largely lost within the general reduction of cell numbers at lower pH. These results suggest, as in the Zander-Fox findings, that decreasing external pH alone leads to a significant decrease in blastocyst cell numbers, however the inhibition of NDBCE or NHE1 alone had a detrimental effect on embryo

development, while a combination of both had the most pronounced effect. Though embryos seem to be very resilient when cultured under the various harsh pH conditions that were employed here and reach the blastocyst stages, in this study it was shown that those blastocysts are not the best specimens, and have decreased cell numbers.

Figure 25: The effect of culture in presence of NHE1 and NDBCE inhibitors on blastocyst cell numbers.

(A) Blastocyst obtained from 2-cell embryos cultured for ~72 hr to blastocysts at various CO_2 concentrations in the presence or absence of inhibitors (control (Ctrl), 10 μM cariporide (Carip), 100 μM H_2DIDS, or both (D+C)) shown in Figure 24 were differentially labeled for inner cell mass cells (ICM) and trophectoderm cells (TE). TOTAL represents the number of ICM+TE cells. Each bar represents the mean ± SEM of at least 4 independent replicates. Bars not sharing letters are significantly different ($P<0.01$ by ANOVA). **(B)** Example images of differentially stained expanded mouse blastocysts after 3 days of *in vitro* culture under various CO_2 concentrations. Note that the pink colour represents the chromatin in nuclei of permeablized TE stained red (propidium iodide) and blue (bisbenzimide). While ICM nuclei are a distinct blue colour, since they are stained only with bisbenzimide. Modified from a figure originally published in Siyanov and Baltz (2013).

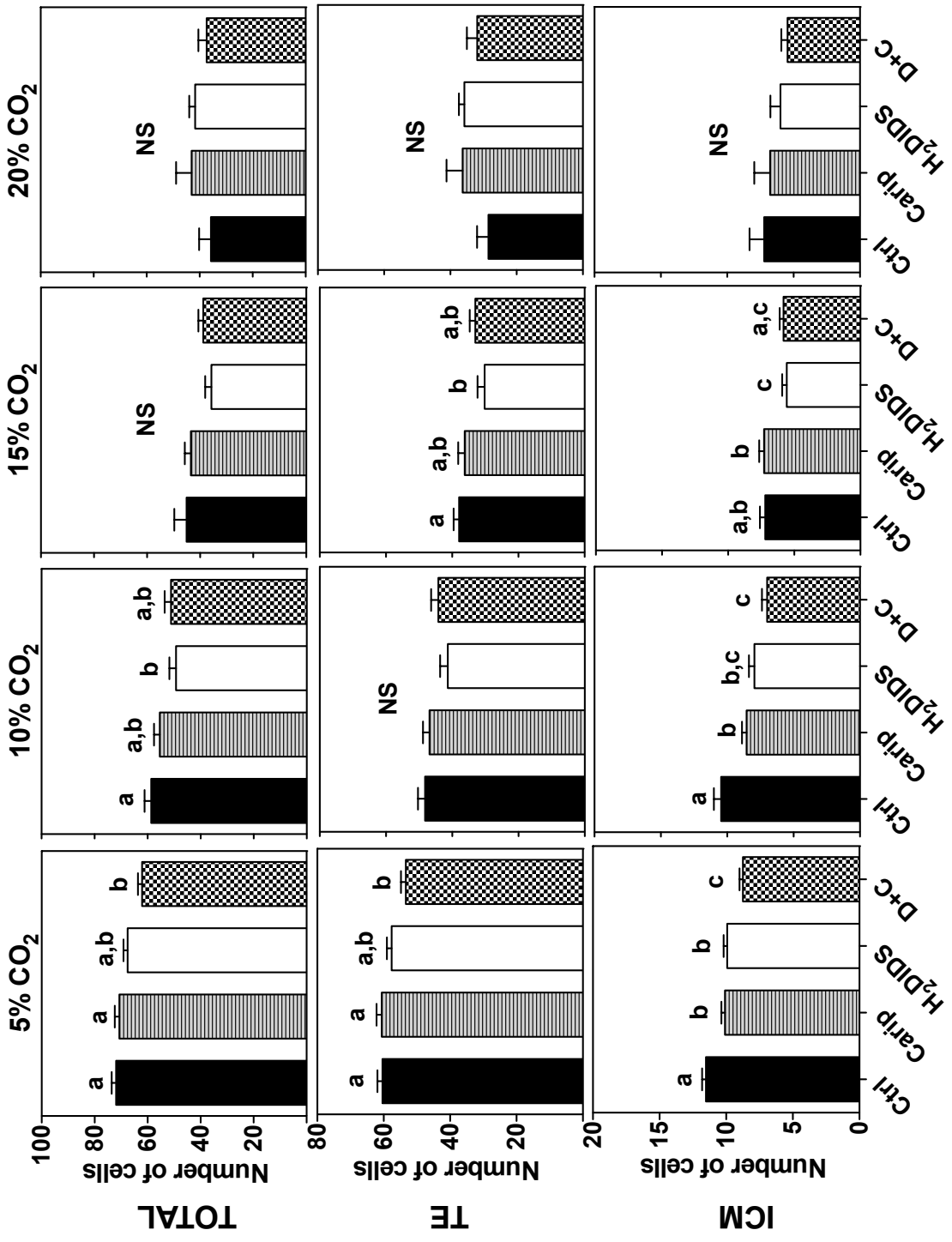
5% CO2
10% CO2
15% CO2
20% CO2
TOTAL
TE
ICM
Number of cells
Ctrl
Carip
H2DIDS
D+C
NS
a
a,b
b
a,c
c
b,c

Figure 25A

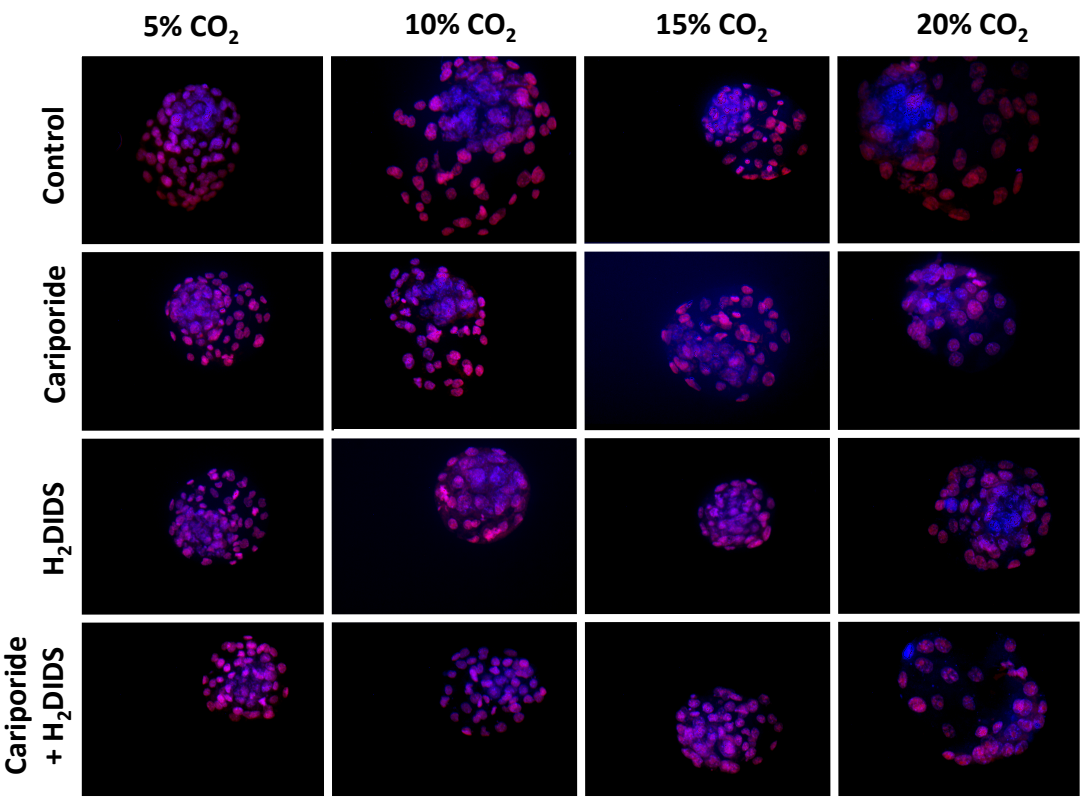
5% CO_2
10% CO_2
15% CO_2
20% CO_2
Control
Cariporide
H_2DIDS
Cariporide + H_2DIDS

Figure 25B

Discussion

1. Na^+/H^+ Exchanger Expression in Preimplantation Embryos

1.1. Transcripts encoding SLC9A1, SLC9A3 and SLC9A4 Na^+/H^+ exchanger isoforms were detected in oocytes and PI stage embryos.

Changes in cytosolic pH have been linked to a myriad of vital cellular mechanisms and functions, and found to play an important role in early embryonic development. In most mammalian cells, the membrane proteins that regulate intracellular recovery from acidosis are the Na^+/H^+ exchangers (isoforms NHE1-4) (Barr et al., 1998; Bidani et al., 1989; Gibb et al., 1997; Gillespie and Greenwell, 1988; Orlowski and Grinstein, 2004). Moreover, these transporters play a role in cell volume regulation, where NHE1, NHE2 and NHE4 are stimulated by increased osmolarity (Bookstein et al., 1994a; Kapus et al., 1994) and aid in the restoration of cell volume following acute cell shrinkage (Bookstein et al., 1994b; Counillon et al., 1993; Ritter et al., 2001; Zhou and Baltz, 2012), while NHE3 is stimulated by cell swelling (Alexander and Grinstein, 2006; Good et al., 2000; Watts and Good, 1999).

Previous molecular studies of mouse oocytes and embryos (Barr et al., 1998; FitzHarris et al., 2007; Gibb et al., 1997; Harding, 2002) showed the presence of several mRNA transcripts of plasma membrane NHE isoforms. NHE1, a ubiquitously expressed isoform, was found to be present within oocytes and preimplantation stages by several studies (Barr et al., 1998; Harding et al., 2002). Our study of growing oocytes and follicles has shown a clear presence of NHE1 and NHE3 isoforms in GV oocytes and granulosa cells (FitzHarris et al., 2007). These results confirmed previous observations by Barr et al. of mouse oocytes where they found transcripts that encode for the protein isoform SLC9A1 and SLC9A3 (Barr et al., 1998). Another study of mouse oocytes has also reported the presence

of mRNA encoding NHE4 (Harding, 2002), which was also confirmed by our study of GV oocytes (FitzHarris et al., 2007). Thus, our studies of GV oocytes have shown the presence of mRNA encoding for three NHE isoforms, NHE1, NHE3, and NHE4, while the surrounding granulosa cells only had mRNA for NHE1 and NHE3 present. In functional studies of granulosa cells we determined both NHE1 and NHE3 to be active in regulating the COC internal pH during induced acidosis (FitzHarris et al., 2007). Figure 26 summarizes the gene transcripts of pH regulatory mechanisms found within the mouse granulosa cells, oocytes and PI stage embryos.

Barr et al. performed molecular studies on various mouse preimplantation embryo stages, reporting the presence of NHE1 within all PI stages (Barr et al., 1998). In this study however, we detected transcripts not only encoding SLC9A1, but also SLC9A3, and SLC9A4 Na^+/H^+ exchanger isoforms in oocytes, eggs and early PI stage embryos, but not those for SLC9A2 or SLC9A5. NHE-related *Slc9* transcripts in PI embryos were likely maternal, since transcript numbers decreased to near undetectable levels by the 2- to 4-cell stages, and there was no subsequent increase in mRNA from the 2-cell stage, when global transcription from the embryonic genome begins (Schultz, 2002), at least through the morula stage. As in Barr et al.'s study, we found that NHE1 transcripts were present within all PI stages when visualized on an electrophoresis gel. Quantitative analysis of the transcripts showed that NHE1 might begin to be re-expressed in the blastocyst after the degradation of the maternal transcripts, which can be assessed from the small increase in transcript numbers at this stage (Figure 12B). These findings suggest that there are three possible candidates for pH_i regulators in preimplantation stage embryos, NHE1, NHE3 and/or NHE4 (Barr et al., 1998; Erdogan et al., 2011; FitzHarris et al., 2007; Harding, 2002).

A second mechanism has been implicated in acidosis relief within mouse oocytes, eggs and early PI embryos, the Na^+-dependent HCO_3^-/Cl^- exchanger. Although in my study, we did not perform RT-PCR studies for NDBCE exchanger, Erdogan et al. previously showed mRNA transcripts encoding *Slc4a8* (NDBCE mRNA) within GV oocytes, MII eggs and 1-cell embryos, with transcript numbers increasing from the GV to zygote stage (Erdogan et al., 2011). Functional studies described here and by Erdogan et al. have also confirmed NDBCE activity within all these stages (Results section and Erdogan et al., 2011).

1.2. NHE protein expression within COCs and blastocysts

To date, studies of the five plasma membrane NHE isoforms have determined that SLC9A1 and SLC9A4 are localized to the basolateral membrane of epithelia and SLC9A2 and SLC9A3 in the apical membrane, and all are capable of relieving intracellular acidosis (Counillon et al., 1993; Pizzonia et al., 1998; Ritter et al., 2001), while SLC9A5 is found principally within brain neurons (Attaphitaya et al., 1999; Baird et al., 1999). Studies of preimplantation mouse embryos have suggested the presence of at least one NHE isoform within the blastocyst stage. According to a study by Barr et al., the blastocyst contains two NHE plasma membrane protein isoforms, NHE1 and NHE3. They concluded that, although no embryonic mRNA transcripts for NHE3 were present in PI stage embryos, the protein found within the blastocyst was of oogenetic origin and persisted to the blastocyst stage (Barr et al., 1998). According to their immunocytochemistry studies, NHE3 was localized to the apical surface of TE cells, while NHE1 localized to the basolateral surface of these polarized cells. One-cell and 8-cell embryos were also stained for NHE3 and showed its localization to the cell surface (Barr et al., 1998). A second study, by Kawagishi et al. also

found that NHE3 protein was found within the blastocysts, localized to the apical surface (Kawagishi et al., 2004).

In my study we have attempted to assess SLC9A1 and SLC9A3 protein expression and localization using a number of available antibodies (refer to Materials and Methods section). However, we were not able to show consistent or distinct plasma membrane localization within oocytes or blastocyst embryos for either isoforms by immunofluorescence (Figure 13B). In contrast, considerable SLC9A1 and SLC9A3 immunofluorescence was clearly evident in cumulus cells surrounding the GV oocyte (Figure 13A), consistent with Fitzharris et al.'s finding of activity of both these isoforms within cumulus cells (FitzHarris et al., 2007). This discrepancy could be a result of Barr et al. utilizing a different immunocytochemical staining technique, with embedded and sectioned blastocysts, although the conclusion that there is clear membrane localization seems not to be convincingly shown by the weak staining in their examples (Barr et al., 1998). The images in Kawagishi et al. resemble the images we obtained in our study for NHE3 isoforms, with no clear membrane localization within blastocysts (Kawagishi et al., 2004). The reason the staining within embryos was so spotty and inconsistent is perhaps due to a low protein density in blastomere cell membranes, while cumulus cells may have a higher density of NHE1 and NHE3 in their membranes, which is made evident here by the immunofluorescence results with cumulus-oocyte complexes (Figure 13A).

Similarly, Western blots were unsuccessful in detecting SLC9A1 or SLC9A3 protein in oocytes and embryos. These negative results might again be due to a low expression level of NHE protein in PI embryos that nonetheless is sufficient for Na^+/H^+ exchanger activity in PI embryos, which could have been attributed to any of NHE1, NHE3 or NHE4. However,

this could not be further narrowed down by our protein expression data, and we therefore turned to alternatives for identifying the functional NHE isoforms in embryos.

It may be possible to probe which NHE isoforms are active in PI embryos by specifically interfering with expression using antisense techniques. However, the mRNA expression patterns indicated that translation likely occurs in oocytes and ends very early in PI embryo development, implying that the NHE proteins are of maternal origin and stable (Figure 12 and Barr et al., 1998), and thus techniques such as siRNA or antisense morpholinos are unlikely to be effective if employed in embryos. Supporting this, an attempt to decrease NHE activity using a specific antisense morpholino against NHE1 introduced into embryos from the 1-cell to 8-cell stages was not successful (not shown), although the lack of reliable antibody staining prevented the direct assessment of SLC9A1 knockdown.

Figure 26: Summary of gene transcripts for Na^+/H^+ isoforms (*Slc9*), HCO_3^-/Cl^- exchanger (*Slc4a2*) and Na^+-HCO_3^-/Cl^- (*Slc4a8*) within mouse granulosa cells, oocytes, MII eggs and preimplantation embryos.

In cumulus/granulosa cells of the oocyte two transcripts were expressed representing the NHE1 and NHE3 isoforms (as described by FitzHarris et al., 2007). In oocytes and preimplantation embryos expressed mRNA for three NHE isoforms, representing maternal gene transcripts, *Slc9a1, Slc9a3 and Slc9a4,* however no transcripts for *Slc9a2 or Slc9a4* were present in any of the PI stages. NHE1 exhibits an expression pattern typical for a constitutively expressed message in PI embryos, with a decrease during the maternal-to-zygotic transition followed by reactivation of expression at the blastocyst stage. NHE3 and NHE4 appeared to be exclusively of maternal origin, with essentially no mRNA detected after the degradation of the maternal genome (Siyanov and Baltz, 2013)

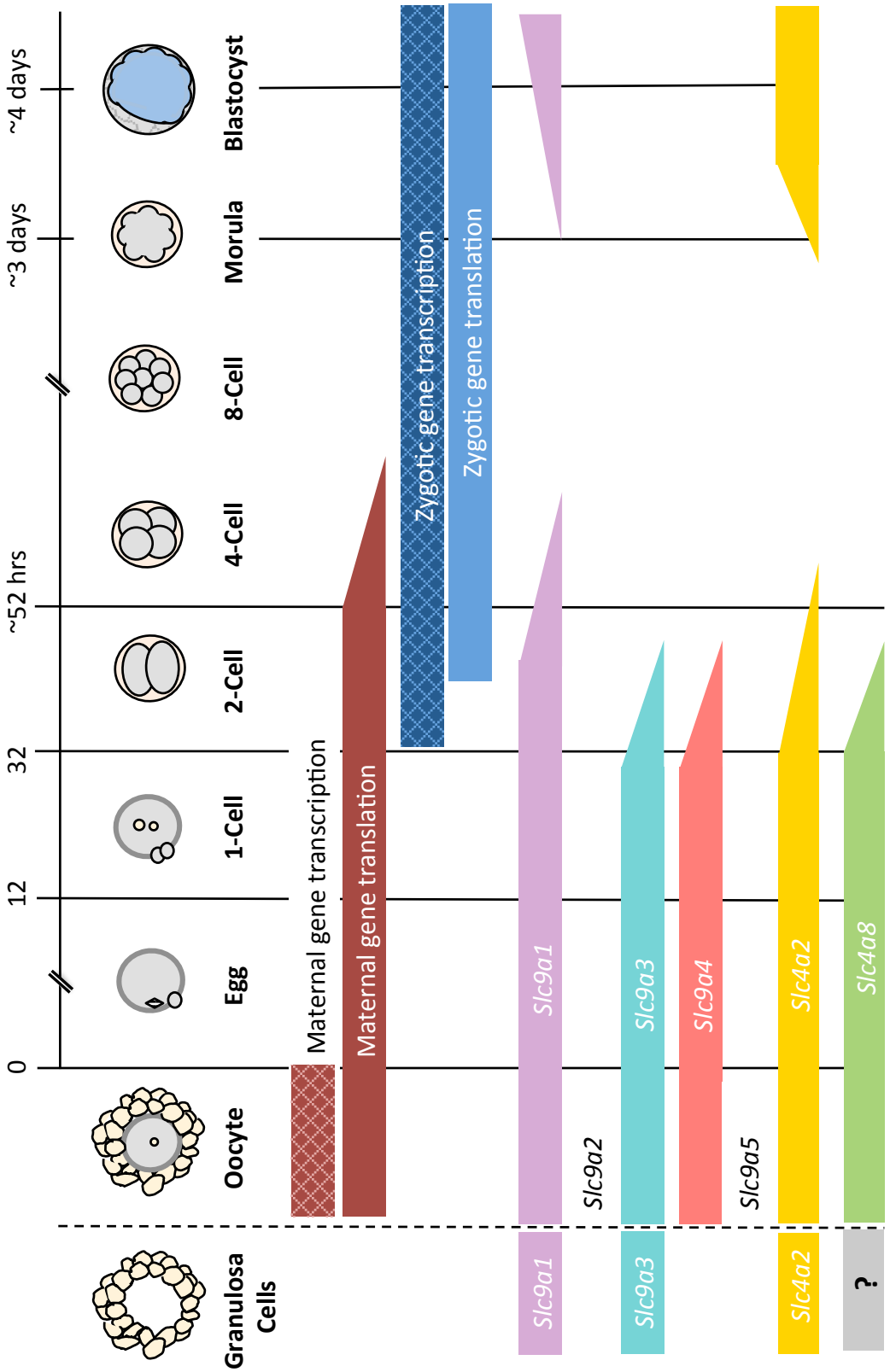
0
12
32
~52 hrs
~3 days
~4 days
Oocyte
Egg
1-Cell
2-Cell
4-Cell
8-Cell
Morula
Blastocyst
Granulosa Cells
Maternal gene transcription
Maternal gene translation
Zygotic gene transcription
Zygotic gene translation
Slc9a1
Slc9a2
Slc9a3
Slc9a4
Slc9a5
Slc4a2
Slc4a8
Slc9a1
Slc9a3
Slc4a2
?

Figure 26

2. NHE1 is the primary pH_i regulatory mechanism in PI mouse embryos

Although the expression data suggested that there are three candidates for mediating pH_i recovery within PI embryos, the functional studies established that NHE1 was the primary pH_i regulatory mechanism mediating recovery from acute intracellular acidosis. This was determined by use of several isoform-selective inhibitors: cariporide that very selectively inhibits NHE1 and S3226, an inhibitor that is more effective against NHE3 than NHE1. Inhibiting pH recovery from acidosis with the general NHE inhibitor amiloride (1 mM) significantly decreased pH_i recovery at all PI stages, leaving only a slight residual recovery. To ensure that the amiloride insensitive recovery was not due to NHE4, an amiloride-insensitive isoform (with IC_{50} ~800) μM (Chambrey et al., 1997a), amiloride concentration was increased to 5 mM to confirm that no additional decreases in recovery rates were observed. Hence it was concluded that the residual recovery most likely was due to passive diffusion out of the cell of acid equivalents such as intracellular lactate and/or pyruvate via monocarboxylate transporters as previously described (Gibb et al., 1997). Further studies with S3226 did not reveal any NHE3 activity in preimplantation embryos, since inhibiting both isoforms, NHE1 and NHE3, with cariporide and S3226 simultaneously did not have an additive inhibitory effect on pH_i recovery from acidosis (Figure 18).

The results reported here clearly differ from those of initial studies in which Baltz et al. (1990, 1991) claimed an absence of Na^+/H^+ antiporter mediated recovery from acidosis in 2-cell embryos derived from CF1 and BDF strain female mice. There are several possible explanations as to why those studies were not able to detect NHE activity. Firstly, the studies by Baltz et al. used a pH sensitive fluorophore BCECF, which is now known to produce free radicals during the photo-bleaching process under UV light exposure that are toxic to cells

(Nett and Deitmer, 1996), and led to embryos stalling development at the 4-cell stage (Baltz et al., 1990). We have also found that enzymatic isolation of oocytes from follicles or exposure to certain chemicals (such as octanol, used to block gap junctions) rendered the NHE antiporter inactive (FitzHarris et al., 2007), showing that it is very sensitive to environmental perturbations in embryos and oocytes. However, the main limitation of those earlier studies was the lack of knowledge of how media osmolarity and composition affect embryo development *in vitro*. The M2 media used by Baltz et al. had a higher osmolarity (290 – 310 mOsM) than the media used today, since then it was subsequently shown that embryos tend to do better in media with lower osmolarity (~250 mOsM) *in vitro*. Having to contend with a high external osmolarity activates the RVI mechanism in embryos to rapidly restore internal osmotic homeostasis. After RVI, NHE is inactivated and responds poorly even to decreased intracellular pH in embryos (Baltz and Tartia, 2010; Baltz and Zhou, 2012).

A subsequent study by Gibb et al. demonstrated that 2-cell mouse embryos (derived from QS female mice) do possess a functional NHE antiporter that actively restores internal pH from induced acidosis to basal pH (Gibb et al., 1997). They also proposed a secondary pH_i regulatory mechanism, a lactate/pyruvate transporter MCT1, which remains active even in the absence of sodium. During induced acidosis, in media lacking Na^+, the MCT1 antiporter allows the diffusion of weak acids lactate and pyruvate out of the cell, thus extruding excess internal H^+ until equilibrium is reached. However, pH_i would not return to a specific physiological setpoint value, since this mechanism produces only passive, unregulated efflux. They postulated that the presence of lactate and pyruvate in Baltz et al.'s media masked the activity of Na^+/H^+ antiporter. However, this is not supported by results obtained by Baltz et al. in experiments where lactate was eliminated. A more likely

explanation is that they used a different strain of mice that has a more robust NHE activity than those in CF1 mice used in the earlier studies (Baltz et al., 1990; Gibb et al., 1997), as was revealed in a later report by Steeves et al. (Steeves et al., 2001). In Steeves et al.'s study, ammonium pulse assay experiments performed on 2-cell stage embryos from three mouse strains (CF1, BDF and Balb C), with low lactate, bicarbonate-free media to reduce the H^+-lactate and NDBCE transport interference during pH_i recovery, confirmed the presence of Na^+/H^+ exchanger activity in all tested strains (Steeves et al., 2001). However, recovery from acidosis varied considerably between strains, with the most pronounced recovery observed in BalbC strain, confirming Gibb et al.'s finding of active amiloride and Na^+-dependent mechanism within the 2-cell mouse embryo but also revealing marked differences in activity between strains (Steeves et al., 2001).

A later study by Harding and colleagues tried to provide a functional description of NHE antiporter activity in eggs and various preimplantation stages in mouse embryos, using an amiloride analog HOE694, reporting two inhibition plateaus, one at 0.015 μM (which they proposed was caused by action on NHE1) and a second one at 1 μM proposed to be caused by NHE3 inhibition (Harding et al., 2002). Furthermore, they have stated that they could not exceed 50 μM HOE694 concentrations during their experiment, because at this drug concentration the embryos lysed. However, their reported half-maximal inhibition concentrations as shown in the figures are inconsistent with IC_{50} values established previously, where HOE694 has an IC_{50} of 0.016 μM for NHE1 and 630 μM for NHE3, considerably higher than that reported by Harding et al. (Counillon et al., 1993; Harding et al., 2002). These results are more consistent with NHE1 being active, regulating pH_i within the 2-cell mouse embryo and consistent with the simple explanation that NHE1 is the only

NHE isoform actively regulating pH_i recovery from acutely induced acidosis in the mouse preimplantation stages.

Under physiological conditions where bicarbonate is present in the environment of the embryo, another mechanism, the NDBCE antiporter, may play an active role in acidosis recovery. Erdogan et al. showed that mouse GV oocytes, MII eggs and 1-cell embryos had a robust NDBCE activity during induced acute acidosis (Erdogan et al., 2011). They found that Na^+-dependent recovery occurred both in the presence and absence of bicarbonate/CO_2 at all stages tested, with observed recovery rates that were on average two times faster in bicarbonate-containing media than those in bicarbonate-depleted media. Inhibition of Na^+/H^+ exchangers with either EIPA (a broad spectrum NHE inhibitor) or cariporide (NHE1 inhibitor) inhibited recovery to the same rate as observed in Na^+-free medium, suggesting that NHE1 is the primary pH regulatory mechanism in bicarbonate free conditions (Erdogan et al., 2011). In bicarbonate/CO_2-containing media, inhibition with either 1 μM cariporide or 100 μM DIDS resulted in approximately 50% reduction in recovery of the control groups, suggesting that both NHE1 and NDBCE played a role in pH_i recovery during acute acidification in GV oocytes and MII eggs. After egg activation, the 1-cell embryo displayed a more robust recovery from acidosis; however the fraction of the total recovery contributed by NDBCE in bicarbonate-containing media decreased at this stage relative to oocytes (Erdogan et al., 2011).

This study confirmed results obtained earlier by Erdrogan et al. (2011) in the GV oocytes (Figure 22A, B), and extended them to the 2-cell stage, showing that NDBCE played an even smaller role in pH recovery at that stage, while NHE1 mediated the majority of recovery from intracellular acidosis even in the presence of bicarbonate (Figure 22A, B).

Thus, we conclude that pH_i in PI embryos is regulated against acidosis mainly by NHE1 with possible smaller contributions by NDBCE, at least at the earliest PI stages.

3. NHE's do not regulate against prolonged acidosis in *in-vitro* cultured embryos

Next, we set out to ascertain whether Na^+/H^+ exchanger (NHE1) activity was required for embryo development, particularly under conditions of chronic acidosis. Under normal culture conditions, inhibition of Na^+/H^+ exchange activity by the NHE1 inhibitor cariporide did not inhibit the proportion of either 1-cell or 2-cell embryos that reached the expanded blastocyst stage (Figure 20A, B), indicating that cariporide was not nonspecifically toxic to embryos. However, simply lowering pH to 7.0 (with CO_2 increased to 10%) reduced 1-cell embryo development from 80% under normal conditions to ~40%. The added stress of decreasing external pH caused 1-cell embryos to block at the 2-cell stage and fail to develop to the expanded blastocyst stage. Addition of cariporide under the various culture conditions did not add to the inhibitory effect the decrease in external pH had on embryo development as can be observed in Figure 19A. Therefore, to bypass the 2-cell block observed with the 1-cell cultures, 2-cell embryos were utilized instead to carry out the same set of experiments. Decreasing external pH did not significantly decrease embryo development from 2-cell to blastocyst stage until CO_2 levels reached 25% (with measured media pH ~6.6) where only approximately 40% of embryos developed to the blastocyst stage (Figure20B). However, decrease of external pH in the presence cariporide did not lead to a dramatic decrease in embryo percentage reaching the blastocyst stage at any CO_2 level. Instead, development was practically identical as is indicated in Figure 19B. Incubating 2-

cell embryos for 3 to 5 hours in media equilibrated under increasing CO_2 concentrations revealed that the internal pH of embryos decreased as the pH dropped below 7.0 (Figure 20C). Addition of cariporide to the culture media and decreased pH_o did not lead to an additional decrease in internal pH. The fall in embryo internal pH was most likely the reason for the decreased embryo development in elevated [CO_2] alone since adding the NHE1 inhibitor cariporide did not lead to additional decrease in embryo development.

Culturing 2-cell embryos at increasing DMO concentrations both in the presence or absence of cariporide did not prevent embryo development. Embryos cultured in media with increasing DMO concentration did not lead to a significant internal pH decrease until pH_o was decreased to 6.3 (Figure 20A). As with the CO_2 experiment, addition of cariporide to the culture media did not lead to a significant decrease in the internal pH (Figure 20B). The observed decrease in internal pH at lower external pH media could be as a result of NHE inactivation by extracellular H^+, as was suggested by Aronson et al. (1983). In their study of microvillus membrane vesicles from rabbit renal cortex, they found that lowering external pH to 6.9 or below led to a complete protonation of the external transport site and loss of Na^+/H^+ exchange activity (Aronson et al., 1983).

Considering that culture media contain bicarbonate, NDBCE could be considered as a candidate exchanger that acts as a compensating mechanism when NHE1 was inhibited and aids in restoring internal pH during prolonged exposure to acidic environments. However, internal pH of 2-cell embryos cultured in the presence of both cariporide and DIDS did not significantly decrease pH_i of embryos, until 20% CO_2, where the control group maintained pH_i around 7.2, while embryos in the DIDS plus cariporide (D+C) group displayed a pH_i drop to ~7.0 (Figure 23B). This result suggested that perhaps NDBCE acts as a compensatory mechanism during NHE1 inactivity or is much more active in the range

near physiological pH_i. Consequently, culture experiments with 2-cell embryos were conducted, in media in which external pH was decreased by increasing CO_2 concentrations (Figure 23A). Inhibiting NDBCE alone or both NHE1 and NDBCE together did not significantly decrease embryo development. This suggested that, surprisingly, there is no requirement for either NHE1 or NDBCE in maintaining baseline pH_i under conditions where pH_i is chronically acidic.

This study explored the role of Na^+/H^+ exchangers as pH regulators in the acidic range both during acute and prolonged perturbations of embryo pH_i. NHE1, the active isoform in the mouse embryo, vigorously reacted to acute drop in pH_i, restoring the embryo to its optimal base pH, while failing to regulate pH_i when faced with lengthy acidosis. These were unexpected results, since the HCO_3^-/Cl^- anion exchangers that regulate pH on the alkaline spectrum were shown to be vital not only for internal pH recovery during acute increases in pH_i, but also extremely important for pH_i regulation during mouse PI embryo development. A study conducted by Zhao et al. found the HCO_3^-/Cl^- exchangers functional in all PI stages of mouse embryo, regulating internal pH after acute perturbations in pH, and their inactivation with DIDS significantly disrupted pH recovery in embryos (Zhao et al., 1995). Zhao et al. have also shown that increasing external pH (by lowering $[CO_2]$ from 5.0 to 0.4%; pH 7.4−8.3) did not have a significant effect on internal pH of embryos, which were able to maintain their internal pH within a normal physiological range of pH 7.2−7.3. Addition of 100 μM DIDS to culture media with elevated pH led to increased internal pH of embryos, showing that internal pH in the alkaline range is regulated by HCO_3^-/Cl^- exchangers. Moreover, increasing media pH did not impede embryo development from 2-cell stage to expanded blastocyst stage. However, elevating external pH in combination with

DIDS led to a significant decrease in embryo development, whereby at pH 8.3 only ~40% of 2-cell embryos reached the expanded blastocyst stage compared to 80% in the control group (Zhao et al., 1995). Since the mammalian oviduct where the PI embryo develops is alkaline, the requirement for HCO_3^-/Cl^- exchangers activity may be vital for maintaining pH_i within the acceptable range to ensure embryo development and proliferation (Leese, 1988; Maas et al., 1977; Iritani et al., 1971; Nichol et al., 1997; (Ben-Yosef et al., 1996). On the other hand, the embryo does not normally encounter such prolonged exposure to acidic environments *in vivo*, hence the NHE exchanger may be required only for short term activity to alleviate internal acidosis that occurs due to normal intracellular metabolic activities within the developing embryo (Shrode et al., 1997; Webb et al., 2011).

The only other study that attempted to determine the identity of NHE isoforms, through the use of pharmacological inhibitors, that aid in embryo development were performed by Kawagishi et al. (2004). Culturing embryos under normal conditions with increasing concentrations of cariporide from 1 μM to 50 μM had no effect on embryo development whether cultured from 2-cell or morula to the blastocyst stage. While 1 μM S3226 had no effect on 2-cell embryo development, increasing its concentration to 5 μM decreased embryo development to ~30% and stopped embryo development completely at 10 μM. Morula stage embryos cultured in various concentrations of S3226 have also failed to develop to the blastocyst stage at concentrations above 5 μM, thus they concluded that NHE3 was the primary pH_i regulatory mechanism in PI embryos. However, the concentrations of S3226 used in their study were high enough to inhibit both NHE1 and NHE3 isoforms, since the reported IC_{50} near 3.6 μM has been shown to be sufficient to inhibit both NHE1 and NHE3 (FitzHarris et al., 2007; Schwark et al., 1998), thus the effect on development is more likely attributable to NHE1 and not NHE3 as suggested by the

authors (Kawagishi et al., 2004; Schwark et al., 1998). As shown in the functional studies, the presence of both cariporide and S3226 during acute acidification did not have an additive effect at decreasing the rates of recovery from acidosis. The effect observed with higher concentrations of S3226 can be attributed to drug toxicity rather than inhibition of NHEs, for when we have tried to perform similar experiments we found that elevating S3226 concentration above 1 μM was detrimental to embryo development even under standard culture conditions (data not shown).

Although the *in vitro* developing embryos appear to be normal, it was shown by Zander Fox et al. that slight perturbation in pH (a drop of <0.2 pH units), whether brief or prolonged, produced blastocysts that appeared morphologically normal, but contained a significantly lower number of cells and decreased number of cells allocated to the ICM (Zander-Fox et al., 2010). Furthermore, embryos that developed under chronic acidosis resulted in lower implantation rates and fetuses with decreased birth weights and sizes (Zander-Fox et al., 2010). In this study, Zander-Fox et al.'s findings were substantiated and also demonstrated that inhibition of either NHE1 or NDBCE significantly reduced ICM cell numbers when compared to controls, with the most detrimental effect observed in the treatment group where both antiporters were inactivated (Figure 25). The dominant effect on development, however, was clearly due to decreased external pH, and not the addition of inhibitors, with both ICM and TE cell numbers decreasing substantially at higher CO_2 concentrations (Figure 25). The results showing that development and cell lineage allocation were not perturbed more substantially at lower pH than at normal culture pH may indicate that the effects of chronic NHE1 inhibition are due to interference with cell volume regulation rather than pH_i homeostasis (Zhou and Baltz, 2012).

4. NHE antiporters as pH_i regulatory mechanisms in other mammalian species

Intracellular pH regulation is an important component of mammalian cell homeostasis and is vital during preimplantation embryo development. Although no data are currently available on the expression of NHE genes or proteins within other mammalian embryos, several studies (with hamster, bovine and human embryos) did attempt to determine the mechanisms responsible for embryo pH_i regulation.

As in the mouse studies, hamster cleavage stage embryos demonstrated robust Na^+/H^+ and HCO_3^-/Cl^- antiporter activity (Lane et al., 1998, 1999). Incubating embryos in either Na^+-free medium or the presence of general NHE inhibitors in bicarbonate-free medium thwarted hamster embryo pH_i recovery from acidosis. Washing out these inhibitors or adding Na^+ back to the media led to a robust recovery of embryos to their initial resting pH_i. When embryo recovery was assessed in media containing bicarbonate/CO_2, the rates of recovery were not significantly different from those observed in the absence of bicarbonate, and could not be inhibited by DIDS, apparently excluding the presence of NDBCE exchangers in hamster embryos (Lane et al., 1998). Recovery from alkalosis was shown to be regulated by anion exchangers alone, and was shown to be Cl^- dependent, which was inhibited by DIDS (Lane et al., 1999). Also, culturing hamster embryos in media with elevated pH (in the presence of a weak base 5-10mM TMA - trimethylamine), led to a decrease in embryo development, while addition of DIDS completely abolished blastocyst formation (Lane et al., 1999).

Lane et al. (1998) has also tested the effect of NHE inhibition on embryo development in culture. They determined that incubating 2-cell hamster embryos in 10 mM

DMO led to an immediate intracellular acidification from a resting level of 7.23±0.15 to 6.91±0.03. However, after 4 hours in media containing the weak acid, intracellular pH of embryos had recovered back to the initial resting pH levels. Addition of a general NHE inhibitor EIPA (6.25 μM) did not affect pH_i under normal culture conditions, but addition of EIPA to the acidified culture media prevented embryo recovery from pH_i acidification, even after 4 hours in culture. When embryos were cultured for several days in media containing either DMO or 16% CO_2, no significant decreases in embryo development were observed when compared to the control media. However, addition of EIPA impaired hamster embryo development to the morula/blastocyst stage. From dose-response experiments conducted on hamster 2-cell embryos, it was concluded that those embryos have sensitivity to EIPA similar to that of NHE1 isoform (IC_{50} 1-10 μM) (Lane et al., 1998). These results differ from our results in mice, where inhibiting NHE1 with cariporide did not impair embryo pH_i recovery to the resting pH after 4-5 hour incubation with weak acid or high CO_2, nor did it reduce embryo development under chronic acidosis (Siyanov and Baltz, 2013). One marked difference between the 2-cell embryos of hamster and those of CF1 mice used here is that the NHE activity in hamster embryos is much more robust. This may explain the disparate results between species.

A study of preimplantation embryos in a larger mammalian species, the cow, showed that these also possess robust pH_i regulatory mechanisms. Bovine embryos displayed a vigorous NHE activity, but unlike mouse and hamster embryos exhibited a much less vigorous AE activity (Lane and Bavister, 1999). The presence of Na^+/H^+ and HCO_3^-/Cl^- exchangers in bovine oocytes and embryos, was confirmed by the removal of either sodium or chloride from the culture media, which resulted in an immediate decrease or increase in

pH_i, respectively (Lane and Bavister, 1999). The magnitude of the pH_i increase/decrease was significantly larger in embryos than oocytes, very similar to the results observed in studies with mouse oocytes (FitzHarris et al., 2007; Lane and Bavister, 1999). After intracellular acidosis induced by NH_4^+-pulse, bovine embryos also showed a strong recovery to the initial baseline pH_i. Addition of EIPA prevented recovery from acidosis, confirming that NHE exchangers mediate recovery from acidosis. On the other hand, recovery from alkalosis induced by incubation with NH_4^+ was very slow and incomplete in bovine embryos at all stages of development. Recovery from alkalization was observed for only 1-2 minutes with the pH_i leveling off well above the initial baseline pH levels, suggesting that although AE antiporters are present within these cells, their activity was very low and could not be considered to be a regulatory mechanism for pH_i by bovine embryos at physiological pH_i (Lane and Bavister, 1999).

Development of bovine embryos under chronic acidic or alkaline conditions was assessed by adding 10 mM DMO (weak acid) or 10 mM TMA (weak base) to the culture media, respectively. When two-cell embryos were cultured, 72% of control group embryos developed to expanded blastocysts. Culture with both EIPA and DMO significantly reduced embryo development compared to the control or either treatment with EIPA or DMO alone (Lane and Bavister, 1999). While culturing embryos in media containing only DIDS reduced embryo development, addition of TMA with DIDS led to embryo arrest in development between 4- to 16-cell stages. This inability of bovine embryos to regulate against alkaline loads might be due to the fact that the bovine AE antiporter setpoint was found to be set higher than pH 7.9 and thus is inactive near physiological pH (Lane and Bavister, 1999).

As with mouse embryos, the two studies of intracellular pH regulation in human embryos chronicled different results. The initial study with human embryos determined that

intracellular pH of embryos was not significantly different between stages, with each stage assessed having a pH_i around 7.4±0.1 (Dale et al., 1998). Dale et al. examined the response of embryos to challenges in the extracellular pH by buffering the media either to an acidic or basic pH. After introduction of human embryos into an alkaline medium, their internal pH rose sharply to that of the external media (pH 8.0), then it gradually recovered to the initial physiological value in ~5 minutes. When testing embryo response to mild acidosis (pH 7.0), it was observed that although the pH_i in all stages dropped when placed in mildly acidic medium, only blastocyst stage embryos were able to subsequently recover to their initial physiological pH. Since human embryos failed to buffer against acidosis, they tested the pH of human follicular fluid and determined it to be between pH 7.5 – 7.7, suggesting that the ability to regulate against acidosis during PI development is not required under normal physiological conditions (Dale et al., 1998). No attempt at the identifying mechanisms responsible for pH regulation within human PI embryos was reported in that study.

A later study by Phillips et al. found that the human embryo was capable of recovering from transient alkalosis as well as acidosis by means of AE antiporter and NHE plus NDBCE exchangers, respectively (Phillips et al., 2000). The mean baseline pH_i of cleavage stage embryos were much lower than that reported by Dale et al., at about pH 7.12 (Dale et al., 1998; Phillips et al., 2000). As with the previous study, cleavage stage embryos (2- to 8-cell) were shown to have a robust mechanism for pH_i recovery from alkaline loads. Phillips et al. extended their study to show that this regulation is carried out by HCO_3^-/Cl^- antiporters, for embryo pH_i recovery was dependent on external Cl^- and it was inhibited by the anion exchanger inhibitor DIDS (Phillips et al., 2000). They also determined that HCO_3^-/Cl^- antiporter is activated in the alkaline range, above pH ~7.2-7.3 (Phillips et al., 2000).

Unlike in Dale et al.'s study where only blastocyst stage embryos were able to recover from induced acidosis, Phillips et al. found that all stages of PI human embryos assessed in their study were able to recover from acidosis. However, these results are nonetheless consistent, since as Phillips et al. have shown in their study, Na^+-dependent recovery from acidosis is fairly low until pH_i falls below 6.9, and thus would not have been detected by the protocol used by Dale et al, where pH was lowered only to ~7.0, thus not activating the NHE antiporter (Phillips et al., 2000). Another drawback in Dale et al.'s paper is that it does not clearly state the composition of their media. If their media had low or no bicarbonate media it might have contributed to their difficulty at observing recovery from induced acidosis. As was demonstrated by Phillips et al., recovery from acidosis is dependent on HCO_3^-/CO_2 between pH_i 6.8 and 7.1 (via Na^+-dependent HCO_3^-/Cl^- exchanger) in cleavage stage embryos, however they did not investigate pH regulation in blastocyst stage human embryos (Phillips et al., 2000).

5. What is the role of NHEs in embryos?

In this study, it was determined that all cleavage stage mouse embryos possess an active sodium hydrogen exchanger, and identified this activity is due to NHE1. This exchanger alleviates acute, transient drops in internal pH of mouse embryos, working in tandem with an anion exchanger that regulate against unwanted pH_i increases to maintain pH_i within a desired range. However, unlike the HCO_3^-/Cl^- exchanger examined in earlier studies, the NHE1 exchanger was shown in this study to be active during transient pH decreases but not able to counter long-term, chronic pH shifts (Figure 27B). As noted above,

this difference in their functions can possibly be explained by the fact that, *in vivo*, embryos may only need to be able to regulate against high external pH, since the oviductal fluid of various mammalian species is alkaline, with measured values between pH 7.5-8.2 (Leese, 1988; Maas et al., 1977; Iritani et al., 1971; Nichol et al., 1997; (Ben-Yosef et al., 1996).

If, under physiological conditions, NHE activity is not required for long term pH_i regulation, what is the role of NHE exchangers in preimplantation mouse embryos? One possible role would be to only counter any sharp transient pH_i drops due to intracellular metabolic activities. Such a drop in intracellular pH would activate NHE1, which would then mediate a rapid recovery, analogous to the recovery seen in my experiments after acute ammonium pulse-induced acidosis.

However, a more important role for NHE activity in mouse PI embryos may be cell volume regulation. Early mouse PI embryos are highly sensitive to cell volume decreases and require a mechanism that can rapidly restore embryo to its normal osmolarity. Anion exchangers coupled with NHE1 in mouse embryos constitute a RVI volume regulatory mechanism, in which NHE1 is stimulated by an acute volume decrease, thus increasing internal pH_i, that in turn stimulates the secondary activation of HCO_3^-/Cl^- exchanger to ensure the influx of NaCl and water into the embryo to counteract the decrease in cell volume (Zhou and Baltz, 2012). As shown by previous work, the excess inorganic ions accumulated during this type of acute cell volume regulation are detrimental to embryo development, leading to a developmental block (at the 2-cell stage in mouse) (Wang et al., 2011). Thus after the osmolarity is acutely restored, embryos import an organic osmolyte glycine via the GLYT1 transporter, to replace the ions and restore the internal ionic strength. Thus, the initial recovery from any decrease in cell volume in embryos requires NHE activity, and since perturbed cell volume is so detrimental to embryo development, the main

physiological role for NHE in early PI mouse embryos may be volume regulation rather than pH regulation.

Figure 27: Model summarizing pH regulation in (a) oocytes and (b) preimplantation embryos.

(A) The growing oocyte is incapable of regulating its own internal pH, thus it relies on the gap junctions, which connect the oocyte with its surrounding granulosa cells to maintain its pH_i within a normal physiological range. Granulosa cell exchangers that participate in regulation against acidosis are Na^+/H^+ exchanger isoform 1 (open circle), and isoform 3 (green). The molecular identity of the HCO_3^-/Cl^- exchangers that regulate against alkalosis is unknown (blue circle). The blue arrows show diffusion of ions between oocyte and granulosa cells. A mature GV oocyte gains the ability to regulate its own pH_i and no longer relies on GC for pH regulation. However, upon resumption of meiosis the pH_i regulatory mechanism becomes dormant until the egg is fertilized. Figure replicated from FitzHarris et al. (2007). **(B)** The preimplantation embryo regains the ability to regulate its internal pH after the second pronuclear extrusion. However, NHE1 and NDBCE exchangers are only capable of correcting for acute deviations in pH_i (in the acidic range), and are inactive during prolonged exposures to acidic environments. The HCO_3^-/Cl^- exchangers not only regulate against short term pH_i perturbations in PI embryos, but are also vital for embryo development. Inhibition of anion exchangers during embryo cultures in high pH media led to embryo death and inability to maintain baseline pH_i. Taking into account the PI embryos are exposed to alkaline oviductal fluid it only makes sense that this exchanger will be active throughout embryo development, whereas NHE1 (a housekeeping membrane protein) is required for short bursts of activity, to remove excess protons from the embryo cytoplasm that has collected there during normal cellular metabolic activity. However, another role for NHE1 in PI embryos has been proposed by Zhou et al., where its primary role is volume regulation. It was shown that NHE1 is activated by cell shrinkage through a tyrosine kinase

Jak2 (which serves as a cell volume sensor in embryos). Upon activation the embryo [Na^+] increases leading to elevated internal pH, which in turn activates the AE exchanger to import Cl^-, thus restoring internal pH. The accumulation of NaCl in the cell leads to water influx into the cell, thus restoring the embryo's cell volume (Zhou and Baltz, 2012).

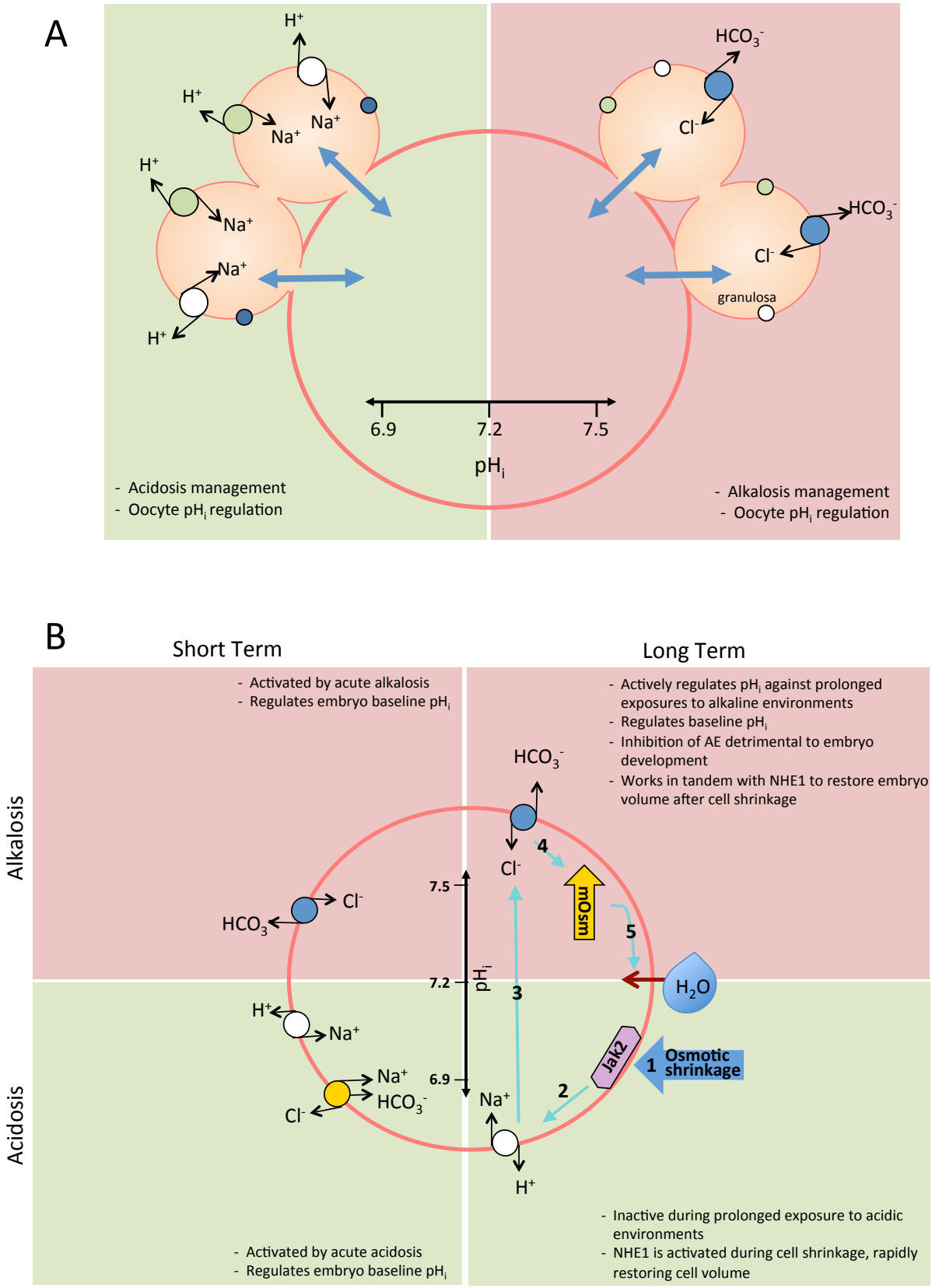
A
H+
Na+
HCO3-
Cl-
granulosa
6.9
7.2
7.5
pHi
- Acidosis management
- Oocyte pHi regulation
- Alkalosis management
- Oocyte pHi regulation
B
Short Term
Long Term
- Activated by acute alkalosis
- Regulates embryo baseline pHi
- Actively regulates pHi against prolonged exposures to alkaline environments
- Regulates baseline pHi
- Inhibition of AE detrimental to embryo development
- Works in tandem with NHE1 to restore embryo volume after cell shrinkage
Alkalosis
Acidosis
mOsm
Jak2
Osmotic shrinkage
H2O
1
2
3
4
5
- Activated by acute acidosis
- Regulates embryo baseline pHi
- Inactive during prolonged exposure to acidic environments
- NHE1 is activated during cell shrinkage, rapidly restoring cell volume

Figure 27

6. Health relevance

The preimplantation embryo is extremely vulnerable to *in vitro* stresses, and the long-term effects of culture has on the offspring are yet to be thoroughly studied and understood. Since 1978, infertility treatments in humans through assisted reproductive technologies (ART) have contributed to the birth of over 5 million individuals worldwide, and now account for over 60,000 births annually in United States alone (CDC, 2014; ICMART, 2012). This technology has been around for over 30 years, and many improvements to culture media, conditions and protocols have been implemented. However, the overall success rate of these technologies is still below 20% (CDC, 2014). This low success rate is due in part to our gap in knowledge of what makes a healthy embryo and understanding of the *in vivo* environment that surrounds it.

Understanding the physiological mechanisms that regulate key homeostatic functions in embryos such as internal pH (and cell volume regulation) is critical for the health of future IVF babies. pH is a powerful modulator of intracellular metabolic activity and alterations of pH_i may lead to changes in cellular proliferation, transcriptional activity, protein localization and synthesis (Shrode et al., 1997; Webb et al., 2011). Analysis of embryos produced under most culture conditions have shown that, although these blastocysts may appear normal, their physiology and ability to form a viable pregnancy can be significantly impaired (Feuer et al., 2014). Mouse pups produced from cultured PI embryos were shown to have alterations in postnatal growth trajectory, fat accumulation and glucose metabolism in adult mice (Feuer et al., 2014). As shown by Zander-Fox et al. and this study, even slight alterations in the pH_i of embryos, be they short-term or long-term, led to the formation of blastocysts with decreased cell numbers even if their gross morphology appeared to be

unaffected (Siyanov and Baltz, 2013; Zander-Fox et al., 2010). Although short-term exposure to acidic environments did not have an effect on implantation rates, it did significantly reduce fetal weight and length, while chronic exposure to acidic environments led to a decrease in implantation rates (Zander-Fox et al., 2010). Cryopreservation, another part of many IVF cycles, was also shown to impair the activity of both NHE and AE exchangers in 2-cell hamster embryos, thus reducing the embryos' ability to regulate its internal pH (Lane et al., 2000), which may be a factor in reduced developmental potential of embryos after cryopreservation and thawing.

All the evidence found in rodents and other animal models suggests that our current methods for ART could be improved, which in turn could improve the success rates of these procedures and the long term effect on the individuals that are born via these methods. We should reconsider the pH of the media the embryos are cultured in. Unlike the current *in vitro* system, where the media pH is kept around pH 7.2-7.4 (Pool, 2004; Swain, 2010, 2012), it should be matched up to the mammalian reproductive tract pH, where the gamete and cleavage stage embryos are exposed to alkaline conditions in the oviduct and the blastocyst faces an acidic environment within the uterus, prior to implantation (Figure 3). These fluctuations were shown to be optimal for egg fertilization and embryo implantation, respectively. Hence, any perturbation in embryo pH regulatory mechanisms may prove detrimental to proper embryo development/survival (Maas et al., 1976; Macdonald and Lumley, 1970; Pommerenke and Breckenridge, 1952).

Embryos tend to change pH of media due to accumulation of metabolic substances released by the embryo (Edwards et al., 1998; Lane and Gardner, 2003). These perturbations in media pH, as was shown in this study (Siyanov and Baltz, 2013) and several others (Siyanov and Baltz, 2013; Zander-Fox et al., 2010; Zhao et al., 1995), may lead to metabolic

perturbations, prevent/stimulate induction of specific molecular pathways and initiate potentially detrimental metabolic changes within the PI embryo (Feuer et al., 2014). A direct effect seen in this study was the reallocation of TE and ICM cells and a great decrease in general cell numbers in blastocyst embryos. Even slight external pH perturbations can lead to disastrous outcomes for the zygote, be it complete failure to implant after *in vitro* maturation, or smaller neonates that struggle with various health issues throughout their lives (Zander-Fox et al., 2010).

All these animal model studies need to be taken under consideration and new sets of culture media/conditions could be developed to encourage more *in vivo*-like environments for IVF practices so as to ensure that future offspring do not become another group of individuals with increased risk of chronic, debilitating diseases, that might put a strain on society and the health care system in the future decades.

7. Future work

As the use of pharmacological agents have their limitations, none of the NHE inhibitors are absolutely specific to one particular isoform, but rather have a concentration dependent inhibition. Although cariporide is considered to be highly selective for the NHE1 isoform, at much higher concentrations it has been shown to inhibit other plasma membrane NHE isoforms as well (Table 1). The second inhibitor S3226, has a close IC_{50} between being able to inhibit NHE3 and NHE1, and the drug also appears to be toxic to embryos at concentrations above 1 μM. To overcome these limitations and confirm my findings, it would be appropriate to develop embryo-specific knockout mice for each of the five plasma

membrane NHE isoforms. The effect of each individual isoform knockdown has on pH regulation during PI embryo development could then be assessed. Given that transcripts for NHE1 and NHE3 were already expressed in the growing oocyte, specific knock-downs in the developing oocyte would ensure that no residual maternal proteins remain within the PI embryo, while assessing their ability to recover from acute, induced acidosis (using, for example, the NH_4Cl-pulse assay). Culturing knockout embryos at various pH_o would determine internal pH of embryos and how embryo development is affected when embryos lack this vital pH regulatory mechanism.

The next logical step is to extend this study into the blastocyst stage (and its different cell lineages) and post-implantation stages, in order to determine the long term effects of NHE inhibition and pH perturbation have on embryo past implantation and past birth. These studies are relevant for our understanding of how slight pH perturbations or protein malfunctions may lead to health issues.

8. Conclusions

Suppressing pH_i regulation against acidosis during PI embryo development had only a surprisingly small effect on their viability, and functional regulatory mechanisms did not appear to provide much protection against even moderately lowered external pH. In contrast, the anion exchanger, HCO_3^-/Cl^- antiporter, which is responsible for pH regulation in the alkaline range, had previously been determined to be vital not only during acute pH_i elevations but also under conditions of chronic alkalosis where embryo development was severely impeded when AE activity was suppressed (Zhao et al., 1995). PI mouse embryos

were able to develop to blastocysts at nearly normal proportions even in very alkaline media (at least up to pH 8.3) while in contrast embryo development was severely decreased when AE activity was suppressed only in alkaline media (Zhao et al., 1995). The reasons for the contrasting poor ability of PI embryos to develop under mild acidosis and the lack of significant effect of inhibiting pH_i regulation against acidosis are not known. Human embryos before the blastocyst stage also apparently do not regulate against mild acidosis (pH 7.0) but can regulate against alkalosis (Dale et al., 1998), indicating that this may not be restricted to the mouse. It may be that such capacity is not normally required, since the normal *in vivo* environment of the PI embryo, oviductal fluid, is reported to be quite alkaline in a number of species (Iritani et al., 1971; Maas et al., 1984; Nichol et al., 1997). External acidosis may also itself decrease the effectiveness of pH_i regulation, since Na^+/H^+ exchange can be inhibited by external H^+ concentrations that are sufficiently high to compete with Na^+ transport (Aronson et al., 1983). Since NHE1 is strongly activated by decreased cell volume in PI mouse embryos, and its activity is required to maintain normal cell volume (Zhou and Baltz, 2012), a more vital physiological function of NHE1 in embryos may be cell volume homeostasis rather than protection against chronic acidosis.

References

Aharonovitz, O., Zaun, H.C., Balla, T., York, J.D., Orlowski, J., Grinstein, S., 2000. Intracellular pH regulation by Na(+)/H(+) exchange requires phosphatidylinositol 4,5-bisphosphate. The Journal of cell biology 150, 213-224.

Ajduk, A., Malagocki, A., Maleszewski, M., 2008. Cytoplasmic maturation of mammalian oocytes: development of a mechanism responsible for sperm-induced Ca2+ oscillations. Reproductive biology 8, 3-22.

Alexander, R.T., Grinstein, S., 2006. Na+/H+ exchangers and the regulation of volume. Acta physiologica 187, 159-167.

Alper, S.L., Chernova, M.N., Stewart, A.K., 2002. How pH regulates a pH regulator: a regulatory hot spot in the N-terminal cytoplasmic domain of the AE2 anion exchanger. Cell biochemistry and biophysics 36, 123-136.

Aronson, P.S., Nee, J., Suhm, M.A., 1982. Modifier role of internal H+ in activating the Na+-H+ exchanger in renal microvillus membrane vesicles. Nature 299, 161-163.

Aronson, P.S., Suhm, M.A., Nee, J., 1983. Interaction of external H+ with the Na+-H+ exchanger in renal microvillus membrane vesicles. J Biol Chem 258, 6767-6771.

Attaphitaya, S., Park, K., Melvin, J.E., 1999. Molecular cloning and functional expression of a rat Na+/H+ exchanger (NHE5) highly expressed in brain. J Biol Chem 274, 4383-4388.

Bachvarova, R., 1985. Gene expression during oogenesis and oocyte development in mammals. Dev Biol (N Y 1985) 1, 453-524.

Baird, N.R., Orlowski, J., Szabo, E.Z., Zaun, H.C., Schultheis, P.J., Menon, A.G., Shull, G.E., 1999. Molecular cloning, genomic organization, and functional expression of Na+/H+ exchanger isoform 5 (NHE5) from human brain. J Biol Chem 274, 4377-4382.

Baltz, J.M., Biggers, J.D., Lechene, C., 1990. Apparent absence of Na+/H+ antiport activity in the two-cell mouse embryo. Developmental biology 138, 421-429.

Baltz, J.M., Biggers, J.D., Lechene, C., 1991a. Relief from alkaline load in two-cell stage mouse embryos by bicarbonate/chloride exchange. J Biol Chem 266, 17212-17217.

Baltz, J.M., Biggers, J.D., Lechene, C., 1991b. Two-cell stage mouse embryos appear to lack mechanisms for alleviating intracellular acid loads. J Biol Chem 266, 6052-6057.

Baltz, J.M., Phillips, K.P., 1999. Chapter 4: Intracellular ion measurements in single eggs and embryos using ion-sensitive fluorophores., in: Richter, J.D. (Ed.), A comparative methods approach to the study of oocytes and embryos. Oxford University Press, New York, pp. xv, 520 p.

Baltz, J.M., Tartia, A.P., 2010. Cell volume regulation in oocytes and early embryos: connecting physiology to successful culture media. Hum Reprod Update 16, 166-176.

Baltz, J.M., Zhou, C., 2012. Cell volume regulation in mammalian oocytes and preimplantation embryos. Molecular reproduction and development.

Barcroft, L.C., Offenberg, H., Thomsen, P., Watson, A.J., 2003. Aquaporin proteins in murine trophectoderm mediate transepithelial water movements during cavitation. Developmental biology 256, 342-354.

Barr, K.J., Garrill, A., Hostead Jones, D., Orlowski, J., 1998. Contributions of Na+/H+ exchanger isofroms to preimplantation development of the mouse. . Molecular reproduction and development 50, 146-153.

Batten, B.E., Albertini, D.F., Ducibella, T., 1987. Patterns of organelle distribution in mouse embryos during preimplantation development. The American journal of anatomy 178, 204-213.

Bell, S.M., Schreiner, C.M., Schultheis, P.J., Miller, M.L., Evans, R.L., Vorhees, C.V., Shull, G.E., Scott, W.J., 1999. Targeted disruption of the murine Nhe1 locus induces ataxia, growth retardation, and seizures. Am J Physiol 276, C788-795.

Bellier, S., Chastant, S., Adenot, P., Vincent, M., Renard, J.P., Bensaude, O., 1997. Nuclear translocation and carboxyl-terminal domain phosphorylation of RNA polymerase II delineate the two phases of zygotic gene activation in mammalian embryos. The EMBO journal 16, 6250-6262.

Ben-Yosef, D., Oron, Y., Shalgi, R., 1996. Intracellular pH of rat eggs is not affected by fertilization and the resulting calcium oscillations. Biol Reprod 55, 461-468.

Benos, D.J., 1982. Amiloride: a molecular probe of sodium transport in tissues and cells. Am J Physiol 242, C131-145.

Bidani, A., Brown, S.E., Heming, T.A., Gurich, R., Dubose, T.D., Jr., 1989. Cytoplasmic pH in pulmonary macrophages: recovery from acid load is Na+ independent and NEM sensitive. Am J Physiol 257, C65-76.

Biggers, J.D., 1998. Reflections on the culture of the preimplantation embryo. The International journal of developmental biology 42, 879-884.

Biggers, J.D., Lawitts, J.A., Lechene, C.P., 1993. The protective action of betaine on the deleterious effects of NaCl on preimplantation mouse embryos in vitro. Molecular reproduction and development 34, 380-390.

Bjersing, L., Cajander, S., 1975. Ovulation and the role of the ovarian surface epithelium. Experientia 31, 605-608.

Boatman, D.E., 1997. Responses of gametes to the oviductal environment. Hum Reprod 12, 133-149.

Bolton, V.N., Oades, P.J., Johnson, M.H., 1984. The relationship between cleavage, DNA replication, and gene expression in the mouse 2-cell embryo. Journal of embryology and experimental morphology 79, 139-163.

Bookstein, C., DePaoli, A.M., Xie, Y., Niu, P., Musch, M.W., Rao, M.C., Chang, E.B., 1994a. Na+/H+ exchangers, NHE-1 and NHE-3, of rat intestine. Expression and localization. The Journal of clinical investigation 93, 106-113.

Bookstein, C., Musch, M.W., DePaoli, A., Xie, Y., Rabenau, K., Villereal, M., Rao, M.C., Chang, E.B., 1996. Characterization of the rat Na+/H+ exchanger isoform NHE4 and localization in rat hippocampus. Am J Physiol 271, C1629-1638.

Bookstein, C., Musch, M.W., DePaoli, A., Xie, Y., Villereal, M., Rao, M.C., Chang, E.B., 1994b. A unique sodium-hydrogen exchange isoform (NHE-4) of the inner medulla of the rat kidney is induced by hyperosmolarity. J Biol Chem 269, 29704-29709.

Bookstein, C., Xie, Y., Rabenau, K., Musch, M.W., McSwine, R.L., Rao, M.C., Chang, E.B., 1997. Tissue distribution of Na+/H+ exchanger isoforms NHE2 and NHE4 in rat intestine and kidney. Am J Physiol 273, C1496-1505.

Borland, R.M., Biggers, J.D., Lechene, C.P., Taymor, M.L., 1980. Elemental composition of fluid in the human Fallopian tube. Journal of reproduction and fertility 58, 479-482.

Borland, R.M., Hazra, S., Biggers, J.D., Lechene, C.P., 1977. The elemental composition of the environments of the gametes and preimplantation embryo during the initiation of pregnancy. Biol Reprod 16, 147-157.

Boron, W.F., De Weer, P., 1976. Active proton transport stimulated by CO2/HCO3-, blocked by cyanide. Nature 259, 240-241.

Buccione, R., Schroeder, A.C., Eppig, J.J., 1990. Interactions between somatic cells and germ cells throughout mammalian oogenesis. Biol Reprod 43, 543-547.

Cala, P.M., 1980. Volume regulation by Amphiuma red blood cells. The membrane potential and its implications regarding the nature of the ion-flux pathways. The Journal of general physiology 76, 683-708.

Camous, S., Heyman, Y., Meziou, W., Menezo, Y., 1984. Cleavage beyond the block stage and survival after transfer of early bovine embryos cultured with trophoblastic vesicles. Journal of reproduction and fertility 72, 479-485.

CDC, 2014. Assisted Reproductive Technology (ART), in: Prevention, C.f.D.C.a. (Ed.), ART Reports and Resources. CDC, http://www.cdc.gov/art/ARTReports.htm.

Chambrey, R., Achard, J.M., St John, P.L., Abrahamson, D.R., Warnock, D.G., 1997a. Evidence for an amiloride-insensitive Na+/H+ exchanger in rat renal cortical tubules. Am J Physiol 273, C1064-1074.

Chambrey, R., Achard, J.M., Warnock, D.G., 1997b. Heterologous expression of rat NHE4: a highly amiloride-resistant Na+/H+ exchanger isoform. Am J Physiol 272, C90-98.

Chambrey, R., St John, P.L., Eladari, D., Quentin, F., Warnock, D.G., Abrahamson, D.R., Podevin, R.A., Paillard, M., 2001. Localization and functional characterization of Na+/H+ exchanger isoform NHE4 in rat thick ascending limbs. American journal of physiology. Renal physiology 281, F707-717.

Cho, W.K., Stern, S., Biggers, J.D., 1974. Inhibitory effect of dibutyryl cAMP on mouse oocyte maturation in vitro. J Exp Zool 187, 383-386.

Cockburn, K., Rossant, J., 2010. Making the blastocyst: lessons from the mouse. The Journal of clinical investigation 120, 995-1003.

Collins, J.L., Baltz, J.M., 1999. Estimates of mouse oviductal fluid tonicity based on osmotic responses of embryos. Biol Reprod 60, 1188-1193.

Cooper, G., 1999. The cell cycle, The cell. A molecular approach. ASM Press, Washington, pp. 571-607.

Counillon, L., Pouyssegur, J., 2000. The expanding family of eucaryotic Na(+)/H(+) exchangers. J Biol Chem 275, 1-4.

Counillon, L., Scholz, W., Lang, H.J., Pouyssegur, J., 1993. Pharmacological characterization of stably transfected Na+/H+ antiporter isoforms using amiloride analogs

and a new inhibitor exhibiting anti-ischemic properties. Molecular pharmacology 44, 1041-1045.

Coupaye-Gerard, B., Bookstein, C., Duncan, P., Chen, X.Y., Smith, P.R., Musch, M., Ernst, S.A., Chang, E.B., Kleyman, T.R., 1996. Biosynthesis and cell surface delivery of the NHE1 isoform of Na+/H+ exchanger in A6 cells. Am J Physiol 271, C1639-1645.

Cox, G.A., Lutz, C.M., Yang, C.L., Biemesderfer, D., Bronson, R.T., Fu, A., Aronson, P.S., Noebels, J.L., Frankel, W.N., 1997. Sodium/hydrogen exchanger gene defect in slow-wave epilepsy mutant mice. Cell 91, 139-148.

Coy, P., Garcia-Vazquez, F.A., Visconti, P.E., Aviles, M., 2012. Roles of the oviduct in mammalian fertilization. Reproduction 144, 649-660.

Crow, J., Amso, N.N., Lewin, J., Shaw, R.W., 1994. Morphology and ultrastructure of fallopian tube epithelium at different stages of the menstrual cycle and menopause. Hum Reprod 9, 2224-2233.

Dale, B., Menezo, Y., Cohen, J., DiMatteo, L., Wilding, M., 1998. Intracellular pH regulation in the human oocyte. Hum Reprod 13, 964-970.

Dawson, K.M., Baltz, J.M., 1997. Organic osmolytes and embryos: substrates of the Gly and beta transport systems protect mouse zygotes against the effects of raised osmolarity. Biol Reprod 56, 1550-1558.

Denker, S.P., Huang, D.C., Orlowski, J., Furthmayr, H., Barber, D.L., 2000. Direct binding of the Na--H exchanger NHE1 to ERM proteins regulates the cortical cytoskeleton and cell shape independently of H(+) translocation. Molecular cell 6, 1425-1436.

Dickens, C.J., Leese, H.J., 1994. The regulation of rabbit oviduct fluid formation. Journal of reproduction and fertility 100, 577-581.

Ducibella, T., Huneau, D., Angelichio, E., Xu, Z., Schultz, R.M., Kopf, G.S., Fissore, R., Madoux, S., Ozil, J.P., 2002. Egg-to-embryo transition is driven by differential responses to Ca(2+) oscillation number. Developmental biology 250, 280-291.

Ducibella, T., Schultz, R.M., Ozil, J.P., 2006. Role of calcium signals in early development. Seminars in cell & developmental biology 17, 324-332.

Ducibella, T., Ukena, T., Karnovsky, M., Anderson, E., 1977. Changes in cell surface and cortical cytoplasmic organization during early embryogenesis in the preimplantation mouse embryo. The Journal of cell biology 74, 153-167.

Dudeja, P.K., Rao, D.D., Syed, I., Joshi, V., Dahdal, R.Y., Gardner, C., Risk, M.C., Schmidt, L., Bavishi, D., Kim, K.E., Harig, J.M., Goldstein, J.L., Layden, T.J., Ramaswamy, K., 1996. Intestinal distribution of human Na+/H+ exchanger isoforms NHE-1, NHE-2, and NHE-3 mRNA. Am J Physiol 271, G483-493.

Edwards, L.J., Williams, D.A., Gardner, D.K., 1998. Intracellular pH of the preimplantation mouse embryo: effects of extracellular pH and weak acids. Molecular reproduction and development 50, 434-442.

Edwards, R.G., 1965. Maturation in vitro of mouse, sheep, cow, pig, rhesus monkey and human ovarian oocytes. Nature 208, 349-351.

Eppig, J.J., 2001. Oocyte control of ovarian follicular development and function in mammals. Reproduction 122, 829-838.

Eppig, J.J., 2004. Regulation of mammalian oocyte maturation, The Ovary, 2nd ed. Elsevier, Amsterdam ; Boston, pp. xviii, 664 p.

Eppig, J.J., O'Brien, M., Wigglesworth, K., 1996. Mammalian oocyte growth and development in vitro. Molecular reproduction and development 44, 260-273.

Eppig, J.J., O'Brien, M.J., 1996. Development in vitro of mouse oocytes from primordial follicles. Biol Reprod 54, 197-207.

Erdogan, S., Cetinkaya, A., Tuli, A., Yilmaz, E.D., Dogan, A., 2011. Changes in the activity of defense mechanisms against induced acidosis during meiotic maturation in mouse oocytes. Theriogenology 75, 1057-1066.

Erdogan, S., FitzHarris, G., Tartia, A.P., Baltz, J.M., 2005. Mechanisms regulating intracellular pH are activated during growth of the mouse oocyte coincident with acquisition of meiotic competence. Developmental biology 286, 352-360.

Erickson, G.F., 1983. Primary cultures of ovarian cells in serum-free medium as models of hormone-dependent differentiation. Molecular and cellular endocrinology 29, 21-49.

Erickson, G.F., Sorensen, R.A., 1974. In vitro maturation of mouse oocytes isolated from late, middle, and pre-antral graafian follicles. J Exp Zool 190, 123-127.

Fafournoux, P., Noel, J., Pouyssegur, J., 1994. Evidence that Na+/H+ exchanger isoforms NHE1 and NHE3 exist as stable dimers in membranes with a high degree of specificity for homodimers. J Biol Chem 269, 2589-2596.

Falconer, D.S., Avery, P.J., 1978. Variability of chimaeras and mosaics. Journal of embryology and experimental morphology 43, 195-219.

Fan, H.Y., Sun, Q.Y., 2004. Involvement of mitogen-activated protein kinase cascade during oocyte maturation and fertilization in mammals. Biol Reprod 70, 535-547.

Fanger, G.R., Widmann, C., Porter, A.C., Sather, S., Johnson, G.L., Vaillancourt, R.R., 1998. 14-3-3 proteins interact with specific MEK kinases. J Biol Chem 273, 3476-3483.

Feuer, S.K., Liu, X., Donjacour, A., Lin, W., Simbulan, R.K., Giritharan, G., Piane, L.D., Kolahi, K., Ameri, K., Maltepe, E., Rinaudo, P.F., 2014. Use of a mouse in vitro fertilization model to understand the developmental origins of health and disease hypothesis. Endocrinology 155, 1956-1969.

Fiorenza, M.T., Bevilacqua, A., Canterini, S., Torcia, S., Pontecorvi, M., Mangia, F., 2004. Early transcriptional activation of the hsp70.1 gene by osmotic stress in one-cell embryos of the mouse. Biol Reprod 70, 1606-1613.

Fisher, R.S., Spring, K.R., 1984. Intracellular activities during volume regulation by Necturus gallbladder. The Journal of membrane biology 78, 187-199.

FitzHarris, G., Siyanov, V., Baltz, J.M., 2007. Granulosa cells regulate oocyte intracellular pH against acidosis in preantral follicles by multiple mechanisms. Development 134, 4283-4295.

Fliegel, L., Frohlich, O., 1993. The Na+/H+ exchanger: an update on structure, regulation and cardiac physiology. The Biochemical journal 296 (Pt 2), 273-285.

Fuster, D., Moe, O.W., Hilgemann, D.W., 2008. Steady-state function of the ubiquitous mammalian Na/H exchanger (NHE1) in relation to dimer coupling models with 2Na/2H stoichiometry. The Journal of general physiology 132, 465-480.

Gandolfi, T.A., Gandolfi, F., 2001. The maternal legacy to the embryo: cytoplasmic components and their effects on early development. Theriogenology 55, 1255-1276.

Garcia-Perez, A., Burg, M.B., 1991. Renal medullary organic osmolytes. Physiological reviews 71, 1081-1115.

Gardner, R.L., 1982. Investigation of cell lineage and differentiation in the extraembryonic endoderm of the mouse embryo. Journal of embryology and experimental morphology 68, 175-198.

Gawenis, L.R., Stien, X., Shull, G.E., Schultheis, P.J., Woo, A.L., Walker, N.M., Clarke, L.L., 2002. Intestinal NaCl transport in NHE2 and NHE3 knockout mice. American journal of physiology. Gastrointestinal and liver physiology 282, G776-784.

Gibb, C.A., Poronnik, P., Day, M.L., Cook, D.I., 1997. Control of cytosolic pH in 2cell mouse embryos:roles of H+-lactate cotransport and Na+/H+ exchange. . Am J Physiol 42, c404-c419.

Gillespie, J.I., Greenwell, J.R., 1988. Changes in intracellular pH and pH regulating mechanisms in somitic cells of the early chick embryo: a study using fluorescent pH-sensitive dye. The Journal of physiology 405, 385-395.

Ginsburg, M., Snow, M.H., McLaren, A., 1990. Primordial germ cells in the mouse embryo during gastrulation. Development 110, 521-528.

Goddard, M.J., Pratt, H.P., 1983. Control of events during early cleavage of the mouse embryo: an analysis of the '2-cell block'. Journal of embryology and experimental morphology 73, 111-133.

Golbus, M.S., Calarco, P.G., Epstein, C.J., 1973. The effects of inhibitors of RNA synthesis (alpha-amanitin and actinomycin D) on preimplantation mouse embryogenesis. J Exp Zool 186, 207-216.

Good, D.W., Di Mari, J.F., Watts, B.A., 3rd, 2000. Hyposmolality stimulates Na(+)/H(+) exchange and HCO(3)(-) absorption in thick ascending limb via PI 3-kinase. American journal of physiology. Cell physiology 279, C1443-1454.

Grinstein, S., 1988. Na^+/H^+ exchange. CRC Press, Boca Raton, Fla.

Grinstein, S., Foskett, J.K., 1990. Ionic mechanisms of cell volume regulation in leukocytes. Annual review of physiology 52, 399-414.

Grinstein, S., Goetz, J.D., Rothstein, A., 1984. 22Na+ fluxes in thymic lymphocytes. II. Amiloride-sensitive Na+/H+ exchange pathway; reversibility of transport and asymmetry of the modifier site. The Journal of general physiology 84, 585-600.

Grinstein, S., Woodside, M., Goss, G.G., Kapus, A., 1994. Osmotic activation of the Na+/H+ antiporter during volume regulation. Biochemical Society transactions 22, 512-516.

Guérin, P., Gallois, E., Croteau, S., 1995. Techniques de récolte et aminogrammes des liquides tubaire et folliculaire chez les femelles domestiques. Revue Méd. Vét. 146, 805-814.

Han, J., Burgess, K., 2010. Fluorescent indicators for intracellular pH. Chemical reviews 110, 2709-2728.

Harding, E.A., 2002. Developmental Changes in the Management of Acid Loads During Preimplantation Mouse Development. Biology of Reproduction 67, 1419-1429.

Harding, E.A., Gibb, C.A., Johnson, M.H., Cook, D.I., Day, M.L., 2002. Developmental changes in the management of acid loads during preimplantation mouse development. Biol Reprod 67, 1419-1429.

Harris, S.E., Gopichandran, N., Picton, H.M., Leese, H.J., Orsi, N.M., 2005. Nutrient concentrations in murine follicular fluid and the female reproductive tract. Theriogenology 64, 992-1006.

Haugland, R.P., Spence, M.T.Z., Johnson, I.D., 1996. Handbook of fluorescent probes and research chemicals, 6th ed. Molecular Probes, Eugene, OR, USA (4849 Pitchford Ave., Eugene 97402).

Hisamitsu, T., Ben Ammar, Y., Nakamura, T.Y., Wakabayashi, S., 2006. Dimerization is crucial for the function of the Na+/H+ exchanger NHE1. Biochemistry 45, 13346-13355.

Hisamitsu, T., Pang, T., Shigekawa, M., Wakabayashi, S., 2004. Dimeric interaction between the cytoplasmic domains of the Na+/H+ exchanger NHE1 revealed by symmetrical intermolecular cross-linking and selective co-immunoprecipitation. Biochemistry 43, 11135-11143.

Hoffmann, E.K., Lambert, I.H., Pedersen, S.F., 2009. Physiology of cell volume regulation in vertabrates. Phys Rev 89, 193-277.

Hogan, B., 1994. Manipulating the mouse embryo : a laboratory manual, 2nd ed. Cold Spring Harbor Laboratory Press, Plainview, N.Y.

Hoogerwerf, W.A., Tsao, S.C., Devuyst, O., Levine, S.A., Yun, C.H., Yip, J.W., Cohen, M.E., Wilson, P.D., Lazenby, A.J., Tse, C.M., Donowitz, M., 1996. NHE2 and NHE3 are human and rabbit intestinal brush-border proteins. Am J Physiol 270, G29-41.

Houliston, E., Maro, B., 1989. Posttranslational modification of distinct microtubule subpopulations during cell polarization and differentiation in the mouse preimplantation embryo. The Journal of cell biology 108, 543-551.

Houliston, E., Pickering, S.J., Maro, B., 1987. Redistribution of microtubules and pericentriolar material during the development of polarity in mouse blastomeres. The Journal of cell biology 104, 1299-1308.

Howlett, S.K., Bolton, V.N., 1985. Sequence and regulation of morphological and molecular events during the first cell cycle of mouse embryogenesis. Journal of embryology and experimental morphology 87, 175-206.

Humphreys, B.D., Jiang, L., Chernova, M.N., Alper, S.L., 1995. Hypertonic activation of AE2 anion exchanger in Xenopus oocytes via NHE-mediated intracellular alkalinization. Am J Physiol 268, C201-209.

ICMART, 2012. Monitoring Assisted Reproductive Technology (ICMART) World Report: Prelimenary 2008 Data., in: Committee, I.I. (Ed.). ESHRE, http://www.eshre.eu/eshre/English/press-room/pressreleases/press-releases-2012/5-million-babies/page.aspx/1606.

Iritani, A., Nishikawa, Y., Gomes, W.R., VanDemark, N.L., 1971. Secretion rates and chemical composition of oviduct and uterine fluids in rabbits. Journal of animal science 33, 829-835.

Jeong, Y.J., Choi, H.W., Shin, H.S., Cui, X.S., Kim, N.H., Gerton, G.L., Jun, J.H., 2005. Optimization of real time RT-PCR methods for the analysis of gene expression in mouse eggs and preimplantation embryos. Molecular reproduction and development 71, 284-289.

Jiang, L., Chernova, M.N., Alper, S.L., 1997. Secondary regulatory volume increase conferred on Xenopus oocytes by expression of AE2 anion exchanger. Am J Physiol 272, C191-202.

Johnson, J.D., Epel, D., 1976. Intracellular pH and activation of sea urchin eggs after fertilisation. Nature 262, 661-664.

Johnson, M.H., Maro, B., 1984. The distribution of cytoplasmic actin in mouse 8-cell blastomeres. Journal of embryology and experimental morphology 82, 97-117.

Kapus, A., Grinstein, S., Wasan, S., Kandasamy, R., Orlowski, J., 1994. Functional characterization of three isoforms of the Na+/H+ exchanger stably expressed in Chinese hamster ovary cells. ATP dependence, osmotic sensitivity, and role in cell proliferation. J Biol Chem 269, 23544-23552.

Karmazyn, M., Avkiran, M., Fliegel, L., 2003. The sodium-hydrogen exchanger : from molecule to its role in disease. Kluwer Academic Publishers, Boston.

Kawagishi, R., Tahara, M., Sawada, K., Morishige, K., Sakata, M., Tasaka, K., Murata, Y., 2004. Na+ / H+ exchanger-3 is involved in mouse blastocyst formation. Journal of experimental zoology. Part A, Comparative experimental biology 301, 767-775.

Kemp, B.E., Pearson, R.B., 1990. Protein kinase recognition sequence motifs. Trends in biochemical sciences 15, 342-346.

Kidder, G.M., Watson, A.J., 2005. Roles of Na,K-ATPase in early development and trophectoderm differentiation. Seminars in nephrology 25, 352-355.

Kishi, J., Noda, Y., Narimoto, K., Umaoka, Y., Mori, T., 1991. Block to development in cultured rat 1-cell embryos is overcome using medium HECM-1. Hum Reprod 6, 1445-1448.

Klanke, C.A., Su, Y.R., Callen, D.F., Wang, Z., Meneton, P., Baird, N., Kandasamy, R.A., Orlowski, J., Otterud, B.E., Leppert, M., et al., 1995. Molecular cloning and physical and genetic mapping of a novel human Na+/H+ exchanger (NHE5/SLC9A5) to chromosome 16q22.1. Genomics 25, 615-622.

Kleyman, T.R., Cragoe, E.J., Jr., 1988a. Amiloride and its analogs as tools in the study of ion transport. The Journal of membrane biology 105, 1-21.

Kleyman, T.R., Cragoe, E.J., Jr., 1988b. The mechanism of action of amiloride. Seminars in nephrology 8, 242-248.

Knudsen, J.F., Litkowski, L.J., Wilson, T.L., Guthrie, H.D., Batta, S.K., 1979. follicular fluid electrolytes and osmolality in cyclic pigs. Journal of reproduction and fertility 57, 419-422.

Lane, M., 2001. Mechanisms for managing cellular and homeostatic stress in vitro. Theriogenology 55, 225-236.

Lane, M., Baltz, J.M., Bavister, B.D., 1998. Regulation of intracellular pH in hamster preimplantation embryos by the sodium hydrogen (Na+/H+) antiporter. Biol Reprod 59, 1483-1490.

Lane, M., Baltz, J.M., Bavister, B.D., 1999. Bicarbonate/chloride exchange regulates intracellular pH of embryos but not oocytes of the hamster. Biol Reprod 61, 452-457.

Lane, M., Bavister, B.D., 1999. Regulation of intracellular pH in bovine oocytes and cleavage stage embryos. Molecular reproduction and development 54, 396-401.

Lane, M., Gardner, D.K., 2003. Ammonium induces aberrant blastocyst differentiation, metabolism, pH regulation, gene expression and subsequently alters fetal development in the mouse. Biol Reprod 69, 1109-1117.

Lane, M., Lyons, E.A., Bavister, B.D., 2000. Cryopreservation reduces the ability of hamster 2-cell embryos to regulate intracellular pH. Hum Reprod 15, 389-394.

Lang, F., Busch, G.L., Ritter, M., Volkl, H., Waldegger, S., Gulbins, E., Haussinger, D., 1998. Functional significance of cell volume regulatory mechanisms. Physiological reviews 78, 247-306.

Latham, K.E., Garrels, J.I., Chang, C., Solter, D., 1991. Quantitative analysis of protein synthesis in mouse embryos. I. Extensive reprogramming at the one- and two-cell stages. Development 112, 921-932.

Lawitts, J.A., Biggers, J.D., 1993. Culture of preimplantation embryos. Methods Enzymol 225, 153-164.

Ledoussal, C., Lorenz, J.N., Nieman, M.L., Soleimani, M., Schultheis, P.J., Shull, G.E., 2001. Renal salt wasting in mice lacking NHE3 Na+/H+ exchanger but not in mice lacking NHE2. American journal of physiology. Renal physiology 281, F718-727.

Leese, H.J., 1988. The formation and function of oviduct fluid. Journal of reproduction and fertility 82, 843-856.

Lehoux, S., Abe, J., Florian, J.A., Berk, B.C., 2001. 14-3-3 Binding to Na+/H+ exchanger isoform-1 is associated with serum-dependent activation of Na+/H+ exchange. J Biol Chem 276, 15794-15800.

Li, X., Alvarez, B., Casey, J.R., Reithmeier, R.A., Fliegel, L., 2002. Carbonic anhydrase II binds to and enhances activity of the Na+/H+ exchanger. J Biol Chem 277, 36085-36091.

Maas, D.H., Stein, B., Metzger, H., 1984. PO2 and pH measurements within the rabbit oviduct following tubal microsurgery: reanastomosis of previously dissected tubes. Advances in experimental medicine and biology 169, 561-570.

Maas, D.H., Storey, B.T., Mastroianni, L., Jr., 1976. Oxygen tension in the oviduct of the rhesus monkey (Macaca mulatta). Fertility and sterility 27, 1312-1317.

Maas, D.H., Storey, B.T., Mastroianni, L., Jr., 1977. Hydrogen ion and carbon dioxide content of the oviductal fluid of the rhesus monkey (Macaca mulatta). Fertility and sterility 28, 981-985.

Macdonald, R.R., Lumley, I.B., 1970. Endocervical pH measured in vivo through the normal menstrual cycle. Obstetrics and gynecology 35, 202-206.

MacPhee, D.J., Jones, D.H., Barr, K.J., Betts, D.H., Watson, A.J., Kidder, G.M., 2000. Differential involvement of Na(+),K(+)-ATPase isozymes in preimplantation development of the mouse. Developmental biology 222, 486-498.

Mamo, S., Gal, A.B., Bodo, S., Dinnyes, A., 2007. Quantitative evaluation and selection of reference genes in mouse oocytes and embryos cultured in vivo and in vitro. BMC developmental biology 7, 14.

Manejwala, F.M., Cragoe, E.J., Jr., Schultz, R.M., 1989. Blastocoel expansion in the preimplantation mouse embryo: role of extracellular sodium and chloride and possible apical routes of their entry. Developmental biology 133, 210-220.

Maro, B., Johnson, M.H., Pickering, S.J., Louvard, D., 1985. Changes in the distribution of membranous organelles during mouse early development. Journal of embryology and experimental morphology 90, 287-309.

Masereel, B., 2003. An overview of inhibitors of Na+/H+ exchanger. European Journal of Medicinal Chemistry 38, 547-554.

Masui, Y., Markert, C.L., 1971. Cytoplasmic control of nuclear behavior during meiotic maturation of frog oocytes. J Exp Zool 177, 129-145.

McLaren, A., Southee, D., 1997. Entry of mouse embryonic germ cells into meiosis. Developmental biology 187, 107-113.

Mehlmann, L.M., 2005. Stops and starts in mammalian oocytes: recent advances in understanding the regulation of meiotic arrest and oocyte maturation. Reproduction 130, 791-799.

Mehlmann, L.M., Mikoshiba, K., Kline, D., 1996. Redistribution and increase in cortical inositol 1,4,5-trisphosphate receptors after meiotic maturation of the mouse oocyte. Developmental biology 180, 489-498.

Mehlmann, L.M., Terasaki, M., Jaffe, L.A., Kline, D., 1995. Reorganization of the endoplasmic reticulum during meiotic maturation of the mouse oocyte. Developmental biology 170, 607-615.

Minami, N., Suzuki, T., Tsukamoto, S., 2007. Zygotic gene activation and maternal factors in mammals. J Reprod Dev 53, 707-715.

Nett, W., Deitmer, J.W., 1996. Simultaneous measurements of intracellular pH in the leech giant glial cell using 2',7'-bis-(2-carboxyethyl)-5,6-carboxyfluorescein and ion-sensitive microelectrodes. Biophys J 71, 394-402.

Nichol, R., Hunter, R.H., Cooke, G.M., 1997. Oviduct fluid pH in intact and unilaterally ovariectomized pigs. Canadian journal of physiology and pharmacology 75, 1069-1074.

Nishiyama, T., Ohsumi, K., Kishimoto, T., 2007. Phosphorylation of Erp1 by p90rsk is required for cytostatic factor arrest in Xenopus laevis eggs. Nature 446, 1096-1099.

Noel, J., Roux, D., Pouyssegur, J., 1996. Differential localization of Na+/H+ exchanger isoforms (NHE1 and NHE3) in polarized epithelial cell lines. Journal of cell science 109 (Pt 5), 929-939.

Ohsugi, M., Ohsawa, T., Semba, R., 1993. Similar responses to pharmacological agents of 1,2-OAG-induced compaction-like adhesion of two-cell mouse embryo to physiological compaction. J Exp Zool 265, 604-608.

Okada, Y., 1997. Volume expansion-sensing outward-rectifier Cl- channel: fresh start to the molecular identity and volume sensor. Am J Physiol 273, C755-789.

Oktay, K., Briggs, D., Gosden, R.G., 1997. Ontogeny of follicle-stimulating hormone receptor gene expression in isolated human ovarian follicles. The Journal of clinical endocrinology and metabolism 82, 3748-3751.

Oktem, O., Urman, B., 2010. Understanding follicle growth in vivo. Hum Reprod 25, 2944-2954.

Orlowski, J., Grinstein, S., 2004. Diversity of the mammalian sodium/proton exchanger SLC9 gene family. Pflugers Archiv : European journal of physiology 447, 549-565.

Orlowski, J., Grinstein, S., 2011. Na(+)/H(+) exchangers. Comprehensive Physiology 1, 2083-2100.

Ozil, J.P., Banrezes, B., Toth, S., Pan, H., Schultz, R.M., 2006. Ca2+ oscillatory pattern in fertilized mouse eggs affects gene expression and development to term. Developmental biology 300, 534-544.

Pang, T., Su, X., Wakabayashi, S., Shigekawa, M., 2001. Calcineurin homologous protein as an essential cofactor for Na+/H+ exchangers. J Biol Chem 276, 17367-17372.

Paris, S., Pouyssegur, J., 1983. Biochemical characterization of the amiloride-sensitive Na+/H+ antiport in Chinese hamster lung fibroblasts. J Biol Chem 258, 3503-3508.

Parker, L., Schimmer, B., 2006. Chapter 8 - Embryology and genetics of the mammalian gonads and ducts in Knobil and Neill's physiology of reproduction, 3rd ed. Elsevier, Amsterdam ; Boston.

Pauken, C.M., Capco, D.G., 1999. Regulation of cell adhesion during embryonic compaction of mammalian embryos: roles for PKC and beta-catenin. Molecular reproduction and development 54, 135-144.

Pelech, S.L., Sanghera, J.S., 1992. MAP kinases: charting the regulatory pathways. Science 257, 1355-1356.

Peters, J.M., 2005. Cyclin degradation: don't mes(s) with meiosis. Current biology : CB 15, R461-463.

Phillips, K.P., Baltz, J.M., 1996. Intracellular pH change does not accompany egg activation in the mouse. Molecular reproduction and development 45, 52-60.

Phillips, K.P., Leveille, M.C., Claman, P., Baltz, J.M., 2000. Intracellular pH regulation in human preimplantation embryos. Hum Reprod 15, 896-904.

Phillips, K.P., Petrunewich, M.A., Collins, J.L., Baltz, J.M., 2002. The intracellular pH-regulatory HCO3-/Cl- exchanger in the mouse oocyte is inactivated during first meiotic metaphase and reactivated after egg activation via the MAP kinase pathway. Molecular biology of the cell 13, 3800-3810.

Phillips, K.P., Zhou, W.L., Baltz, J.M., 1998. Fluorophore toxicity in mouse eggs and zygotes. Zygote 6, 113-123.

Pizzonia, J.H., Biemesderfer, D., Abu-Alfa, A.K., Wu, M.S., Exner, M., Isenring, P., Igarashi, P., Aronson, P.S., 1998. Immunochemical characterization of Na+/H+ exchanger isoform NHE4. Am J Physiol 275, F510-517.

Pommerenke, W.T., Breckenridge, M.A., 1952. Biochemical studies of the female genital tract. Annals of the New York Academy of Sciences 54, 786-795.

Pool, T.B., 2004. Optimizing pH in Clinical Embryology. The Embryologists' Newsletter 7, 1-17.

Puceat, M., 1999. pHi regulatory ion transporters: an update on structure, regulation and cell function. Cellular and molecular life sciences : CMLS 55, 1216-1229.

Qiu, J.J., Zhang, W.W., Wu, Z.L., Wang, Y.H., Qian, M., Li, Y.P., 2003. Delay of ZGA initiation occurred in 2-cell blocked mouse embryos. Cell research 13, 179-185.

Rankin, T., Familari, M., Lee, E., Ginsberg, A., Dwyer, N., Blanchette-Mackie, J., Drago, J., Westphal, H., Dean, J., 1996. Mice homozygous for an insertional mutation in the Zp3 gene lack a zona pellucida and are infertile. Development 122, 2903-2910.

Reeve, W.J., Kelly, F.P., 1983. Nuclear position in the cells of the mouse early embryo. Journal of embryology and experimental morphology 75, 117-139.

Ritter, M., Fuerst, J., Woll, E., Chwatal, S., Gschwentner, M., Lang, F., Deetjen, P., Paulmichl, M., 2001. Na(+)/H(+)exchangers: linking osmotic dysequilibrium to modified cell function. Cellular physiology and biochemistry : international journal of experimental cellular physiology, biochemistry, and pharmacology 11, 1-18.

Roos, A., Boron, W.F., 1981. Intracellular pH. Physiological reviews 61, 296-434.

Sardet, C., Fafournoux, P., Pouyssegur, J., 1991. Alpha-thrombin, epidermal growth factor, and okadaic acid activate the Na+/H+ exchanger, NHE-1, by phosphorylating a set of common sites. J Biol Chem 266, 19166-19171.

Sardet, C., Franchi, A., Pouyssegur, J., 1989. Molecular cloning, primary structure, and expression of the human growth factor-activatable Na+/H+ antiporter. Cell 56, 271-280.

Saunders, C.M., Larman, M.G., Parrington, J., Cox, L.J., Royse, J., Blayney, L.M., Swann, K., Lai, F.A., 2002. PLC zeta: a sperm-specific trigger of Ca(2+) oscillations in eggs and embryo development. Development 129, 3533-3544.

Schini, S.A., Bavister, B.D., 1988. Development of golden hamster embryos through the two-cell block in chemically defined medium. J Exp Zool 245, 111-115.

Schneider, H., Scheiner-Bobis, G., 1997. Involvement of the M7/M8 extracellular loop of the sodium pump alpha subunit in ion transport. Structural and functional homology to P-loops of ion channels. J Biol Chem 272, 16158-16165.

Scholz, W., Albus, U., Counillon, L., Gogelein, H., Lang, H.J., Linz, W., Weichert, A., Scholkens, B.A., 1995. Protective effects of HOE642, a selective sodium-hydrogen exchange subtype 1 inhibitor, on cardiac ischaemia and reperfusion. Cardiovascular research 29, 260-268.

Schultheis, P.J., Clarke, L.L., Meneton, P., Miller, M.L., Soleimani, M., Gawenis, L.R., Riddle, T.M., Duffy, J.J., Doetschman, T., Wang, T., Giebisch, G., Aronson, P.S., Lorenz, J.N., Shull, G.E., 1998. Renal and intestinal absorptive defects in mice lacking the NHE3 Na+/H+ exchanger. Nature genetics 19, 282-285.

Schultz, R.M., 2002. The molecular foundations of the maternal to zygotic transition in the preimplantation embryo. Hum Reprod Update 8, 323-331.

Schwark, J.R., Jansen, H.W., Lang, H.J., Krick, W., Burckhardt, G., Hropot, M., 1998. S3226, a novel inhibitor of Na+/H+ exchanger subtype 3 in various cell types. Pflugers Archiv : European journal of physiology 436, 797-800.

Semplicini, A., Spalvins, A., Canessa, M., 1989. Kinetics and stoichiometry of the human red cell Na+/H+ exchanger. The Journal of membrane biology 107, 219-228.

Shrode, L.D., Tapper, H., Grinstein, S., 1997. Role of intracellular pH in proliferation, transformation, and apoptosis. Journal of bioenergetics and biomembranes 29, 393-399.

Sirard, M.A., Richard, F., Blondin, P., Robert, C., 2006. Contribution of the oocyte to embryo quality. Theriogenology 65, 126-136.

Siyanov, V., Baltz, J.M., 2013. NHE1 is the sodium-hydrogen exchanger active in acute intracellular pH regulation in preimplantation mouse embryos. Biol Reprod 88, 157.

Skinner, M.K., 2005. Regulation of primordial follicle assembly and development. Hum Reprod Update 11, 461-471.

Slepkov, E.R., Rainey, J.K., Sykes, B.D., Fliegel, L., 2007. Structural and functional analysis of the Na+/H+ exchanger. The Biochemical journal 401, 623-633.

Soleimani, M., Singh, G., Bizal, G.L., Gullans, S.R., McAteer, J.A., 1994. Na+/H+ exchanger isoforms NHE-2 and NHE-1 in inner medullary collecting duct cells. Expression, functional localization, and differential regulation. J Biol Chem 269, 27973-27978.

Sorensen, R.A., Wassarman, P.M., 1976. Relationship between growth and meiotic maturation of the mouse oocyte. Developmental biology 50, 531-536.

Speake, P.F., Mynett, K.J., Glazier, J.D., Greenwood, S.L., Sibley, C.P., 2005. Activity and expression of Na+/H+ exchanger isoforms in the syncytiotrophoblast of the human placenta. Pflugers Archiv : European journal of physiology 450, 123-130.

Steeves, C.L., Lane, M., Bavister, B.D., Phillips, K.P., Baltz, J.M., 2001. Differences in intracellular pH regulation by Na(+)/H(+) antiporter among two-cell mouse embryos derived from females of different strains. Biol Reprod 65, 14-22.

Sternlicht, A.L., Schultz, R.M., 1981. Biochemical studies of mammalian oogenesis: kinetics of accumulation of total and poly(A)-containing RNA during growth of the mouse oocyte. J Exp Zool 215, 191-200.

Strange, K., Emma, F., Jackson, P.S., 1996. Cellular and molecular physiology of volume-sensitive anion channels. Am J Physiol 270, C711-730.

Sun, A.M., Liu, Y., Dworkin, L.D., Tse, C.M., Donowitz, M., Yip, K.P., 1997. Na+/H+ exchanger isoform 2 (NHE2) is expressed in the apical membrane of the medullary thick ascending limb. The Journal of membrane biology 160, 85-90.

Swain, J.E., 2010. Optimizing the culture environment in the IVF laboratory: impact of pH and buffer capacity on gamete and embryo quality. Reproductive biomedicine online 21, 6-16.

Swain, J.E., 2012. Media composition: pH and buffers. Methods in molecular biology 912, 161-175.

Swann, K., Lai, F.A., 2013. PLCzeta and the initiation of Ca(2+) oscillations in fertilizing mammalian eggs. Cell calcium 53, 55-62.

Szabo, E.Z., Numata, M., Shull, G.E., Orlowski, J., 2000. Kinetic and pharmacological properties of human brain Na(+)/H(+) exchanger isoform 5 stably expressed in Chinese hamster ovary cells. J Biol Chem 275, 6302-6307.

Thomas, J.A., Buchsbaum, R.N., Zimniak, A., Racker, E., 1979. Intracellular pH measurements in Ehrlich ascites tumor cells utilizing spectroscopic probes generated in situ. Biochemistry 18, 2210-2218.

Thompson, E.M., Legouy, E., Renard, J.P., 1998. Mouse embryos do not wait for the MBT: chromatin and RNA polymerase remodeling in genome activation at the onset of development. Developmental genetics 22, 31-42.

Thouas, G.A., Korfiatis, N.A., French, A.J., Jones, G.M., Trounson, A.O., 2001. Simplified technique for differential staining of inner cell mass and trophectoderm cells of mouse and bovine blastocysts. Reproductive biomedicine online 3, 25-29.

Tominaga, T., Ishizaki, T., Narumiya, S., Barber, D.L., 1998. p160ROCK mediates RhoA activation of Na-H exchange. The EMBO journal 17, 4712-4722.

Toth, S., Huneau, D., Banrezes, B., Ozil, J.P., 2006. Egg activation is the result of calcium signal summation in the mouse. Reproduction 131, 27-34.

Tse, C.M., Brant, S.R., Walker, M.S., Pouyssegur, J., Donowitz, M., 1992. Cloning and sequencing of a rabbit cDNA encoding an intestinal and kidney-specific Na+/H+ exchanger isoform (NHE-3). J Biol Chem 267, 9340-9346.

Tunquist, B.J., Maller, J.L., 2003. Under arrest: cytostatic factor (CSF)-mediated metaphase arrest in vertebrate eggs. Genes & development 17, 683-710.

Van Winkle, L.J., 1999. Transport Kinetics., in: Van Winkle, L.J. (Ed.), Biomembrane Transport. Academic Press, San Diego, pp. 665-731.

Van Winkle, L.J., Campione, A.L., 1991. Ouabain-sensitive Rb+ uptake in mouse eggs and preimplantation conceptuses. Developmental biology 146, 158-166.

Van Winkle, L.J., Haghighat, N., Campione, A.L., 1990. Glycine protects preimplantation mouse conceptuses from a detrimental effect on development of the inorganic ions in oviductal fluid. J Exp Zool 253, 215-219.

Verbalis, J.G., Gullans, S.R., 1991. Hyponatremia causes large sustained reductions in brain content of multiple organic osmolytes in rats. Brain research 567, 274-282.

Vestweber, D., Gossler, A., Boller, K., Kemler, R., 1987. Expression and distribution of cell adhesion molecule uvomorulin in mouse preimplantation embryos. Developmental biology 124, 451-456.

Wakabayashi, S., Bertrand, B., Ikeda, T., Pouyssegur, J., Shigekawa, M., 1994. Mutation of calmodulin-binding site renders the Na+/H+ exchanger (NHE1) highly H(+)-sensitive and Ca2+ regulation-defective. J Biol Chem 269, 13710-13715.

Wakabayashi, S., Fafournoux, P., Sardet, C., Pouyssegur, J., 1992. The Na+/H+ antiporter cytoplasmic domain mediates growth factor signals and controls "H(+)-sensing". Proceedings of the National Academy of Sciences of the United States of America 89, 2424-2428.

Wakabayashi, S., Hisamitsu, T., Pang, T., Shigekawa, M., 2003a. Kinetic dissection of two distinct proton binding sites in Na+/H+ exchangers by measurement of reverse mode reaction. J Biol Chem 278, 43580-43585.

Wakabayashi, S., Hisamitsu, T., Pang, T., Shigekawa, M., 2003b. Mutations of Arg440 and Gly455/Gly456 oppositely change pH sensing of Na+/H+ exchanger 1. J Biol Chem 278, 11828-11835.

Wakabayashi, S., Ikeda, T., Iwamoto, T., Pouyssegur, J., Shigekawa, M., 1997a. Calmodulin-binding autoinhibitory domain controls "pH-sensing" in the Na+/H+ exchanger NHE1 through sequence-specific interaction. Biochemistry 36, 12854-12861.

Wakabayashi, S., Ikeda, T., Noel, J., Schmitt, B., Orlowski, J., Pouyssegur, J., Shigekawa, M., 1995. Cytoplasmic domain of the ubiquitous Na+/H+ exchanger NHE1 can confer Ca2+ responsiveness to the apical isoform NHE3. J Biol Chem 270, 26460-26465.

Wakabayashi, S., Shigekawa, M., Pouyssegur, J., 1997b. Molecular physiology of vertebrate Na+/H+ exchangers. Physiological reviews 77, 51-74.

Wang, F., Kooistra, M., Lee, M., Liu, L., Baltz, J.M., 2011. Mouse Embryos Stressed by Physiological Levels of Osmolarity Become Arrested in the Late Two-Cell Stage Before Entry into M-Phase. Biol Reprod.

Wang, H., Dey, S.K., 2006. Roadmap to embryo implantation: clues from mouse models. Nature reviews. Genetics 7, 185-199.

Warner, C.M., Versteegh, L.R., 1974. In vivo and in vitro effect of alpha-amanitin on preimplantation mouse embryo RNA polymerase. Nature 248, 678-680.

Wassarman, P.M., Schultz, R.M., Letourneau, G.E., LaMarca, M.J., Josefowicz, W.J., Bleil, J.D., 1979. Meiotic maturation of the mouse oocytes *in vitro*. Adv. Exp. Med. Biol. 112, 251-268.

Watson, A.J., 2007. Oocyte cytoplasmic maturation: a key mediator of oocyte and embryo developmental competence. Journal of animal science 85, E1-3.

Watts, B.A., 3rd, Good, D.W., 1999. Hyposmolality stimulates apical membrane Na(+)/H(+) exchange and HCO(3)(-) absorption in renal thick ascending limb. The Journal of clinical investigation 104, 1593-1602.

Waymouth, C., 1970. Osmolality of mammalian blood and of media for culture of mammalian cells. In vitro 6, 109-127.

Webb, B.A., Chimenti, M., Jacobson, M.P., Barber, D.L., 2011. Dysregulated pH: a perfect storm for cancer progression. Nature reviews. Cancer 11, 671-677.

Williams, N., Kraft, N., Shortman, K., 1972. The separation of different cell classes from lymphoid organs. VI. The effect of osmolarity of gradient media on the density distribution of cells. Immunology 22, 885-899.

Winkel, G.K., Ferguson, J.E., Takeichi, M., Nuccitelli, R., 1990. Activation of protein kinase C triggers premature compaction in the four-cell stage mouse embryo. Developmental biology 138, 1-15.

Xu, Z., Kopf, G.S., Schultz, R.M., 1994. Involvement of inositol 1,4,5-trisphosphate-mediated Ca2+ release in early and late events of mouse egg activation. Development 120, 1851-1859.

Yan, W., Nehrke, K., Choi, J., Barber, D.L., 2001. The Nck-interacting kinase (NIK) phosphorylates the Na+-H+ exchanger NHE1 and regulates NHE1 activation by platelet-derived growth factor. J Biol Chem 276, 31349-31356.

Yanagimachi, R., Bhattacharyya, A., 1988. Acrosome-reacted guinea pig spermatozoa become fusion competent in the presence of extracellular potassium ions. J Exp Zool 248, 354-360.

Yancey, P.H., Clark, M.E., Hand, S.C., Bowlus, R.D., Somero, G.N., 1982. Living with water stress: evolution of osmolyte systems. Science 217, 1214-1222.

Yoshida, T., Sunamori, M., Miyamoto, H., Suzuki, A., 1993. Comparison of intermittent injection with single-flush UW solution for donor heart preservation. Transplantation proceedings 25, 3201-3204.

Zander-Fox, D.L., Mitchell, M., Thompson, J.G., Lane, M., 2010. Alterations in mouse embryo intracellular pH by DMO during culture impair implantation and fetal growth. Reproductive biomedicine online 21, 219-229.

Zhao, Y., Baltz, J.M., 1996. Bicarbonate/chloride exchange and intracellular pH throughout preimplantation mouse embryo development. Am J Physiol 271, C1512-1520.

Zhao, Y., Chauvet, P.J., Alper, S.L., Baltz, J.M., 1995. Expression and function of bicarbonate/chloride exchangers in the preimplantation mouse embryo. J Biol Chem 270, 24428-24434.

Zhao, Y., Doroshenko, P.A., Alper, S.L., Baltz, J.M., 1997. Routes of Cl- transport across the trophectoderm of the mouse blastocyst. Developmental biology 189, 148-160.

Zhou, C., Baltz, J.M., 2012. Janus kinase 2 mediates the acute response to a cell volume decrease in mouse preimplantation embryos by activating Na(+) /H(+) exchanger isoform 1. Journal of cellular physiology.

Appendix

Cariporide data was fit (by nonlinear least squares) to:

$$\text{Rate} = r_\infty + r_o * IC_{50}/(IC_{50} + [\text{cariporide}])$$

r_∞ is the residual rate at infinite cariporide

r_o is the additional rate with no cariporide (the total rate is $r_\infty + r_o$ when [cariporide] = 0, or the residual rate)

IC_{50} is the concentration of cariporide that is half-maximally effective

The last term of this equation is derived from the Michaelis-Menten equation:

$$\text{Rate} = V_{max} * [S]/([S] + K_m).$$

To obtain the value of this term in the presence of a competitive inhibitor, K_m is replaced with the apparent K_m in the presence of the inhibitor, which is given by: $K_m * (1 + [I]/K_i)$ where K_i is the inhibition constant for the inhibitor (Van Winkle, 1999). The ratio of the rate in the presence of inhibitor to the uninhibited rate is: $\text{rate}/r_0 = (K_m + [S])/(K_m + [S] + [I] * K_m/K_i)$. Since, at $[I] = IC_{50}$ the rate is, by definition, $r_0/2$, $K_m + [S]$ must equal $IC_{50} * (K_m/K_i)$. Solving for K_i yields $K_i = K_m * IC_{50}/(K_m + [S])$. Substituting for K_i in the expression for rate/r_0 and rearranging then gives $\text{rate} = r_0 * IC_{50}/(IC_{50} + [I])$, where [I] is the concentration of cariporide, to which we have added the residual rate, r_∞, which is the rate in the presence of maximal inhibition by cariporide.